POLSKIE TOWARZYSTWO MINERALOGICZNE

MINERALOGICAL SOCIETY OF POLAND

MINERALOGIA POLONICA

Vol. 35, No 2, 2004

KRAKÓW 2004

EDITORIAL BOARD
Komitet Redakcyjny

Prof. M. Banaś, Poland
Prof. R.C. Ewing, USA
Prof. Wł. Kowalski, Poland
Prof. B. Kwiecińska, Poland
Prof. A. Majerowicz, Poland
Prof. A. Manecki, Poland
Prof. M. Michalik, Poland
Prof. W. Narębski, Poland
Prof. A.N. Platonov, Ukraine
Dr. A. Skowroński, Poland (Assistant Editor)
Prof. J. Staněk, Czech Republic
Dr. T. Szydłak, Poland (Assistant Editor)
Prof. J. Zussman, U.K.
Prof. W. Żabiński, Poland (Editor)

ADDRESS
Adres Redakcji

Mineralogical Society of Poland
Polskie Towarzystwo Mineralogiczne
30-059 Kraków, al. Mickiewicza 30, AGH
Fax (48-12) 633 43 30

Edited with the financial support of the
Ministry of Scientific Research and Information Technology
and the Faculty of Geology, Geophysics and Environment Protection
of the AGH University of Science and Technology in Cracow

Wydano z pomocą finansową Ministerstwa Nauki i Informatyzacji
oraz Wydziału Geologii, Geofizyki i Ochrony Środowiska AGH

© Copyright by Mineralogical Society of Poland, Kraków 2004

Printed in Poland

MINERALOGIA POLONICA
Vol. 35, No 2, 2004
PL ISSN 0032-6267

Adam PIECZKA[1], *Krzysztof ŁOBOS*[2], *Michał SACHANBIŃSKI*[3]

THE FIRST OCCURRENCE OF ELBAITE IN POLAND

A b s t r a c t . An amphibolite-hosted quartzo-feldspar-mica pegmatite with schorl, green elbaite, spessartine, andalusite, spinel, hyalophane, zircon, columbite and beryl was found near Gilów in the E part of the Góry Sowie gneissic block (Lower Silesia, Poland). The black tourmaline crystals are chracterized by the change of their composition from Mg- and Al-enriched schorl, typical of the Góry Sowie block, to Al- and, Al- and Li-enriched schorl, and to Fe-bearing elbaite. Light green tourmaline corresponds to (Fe,Mn)--bearing elbaite. The crystallization sequence of the tourmaline varieties results from progressive change of composition of pegmatite melts in the last metamorphic stage of a parent sedimentary protolith around 370–380 Ma ago. The stage of Li-bearing tourmaline formation corresponds to crystallization of a phosphate assemblage with ferrisicklerite-sarcopside-graftonite lamellar intergrowths known from other pegmatites of the Góry Sowie block.

Key-words: tourmaline, elbaite, the Góry Sowie gneissic block, Lower Silesia, Poland

INTRODUCTION

Tourmaline is a relatively common mineral in igneous and metamorphic rocks in some geological units of the Polish part of the Sudety Mts. Except green-grey dravite from the pass between Czoło and Wołowa Góra hills near Kowary (the Karkonosze Mts), in all other occurrences it is represented by black, (Al,Mg)-bearing varieties of schorl or less frequent, Al-depleted, Fe-rich tourmaline. The latter is usually enriched in Fe^{3+} as a result of the $(NaFe^{2+})_{-1}\square Fe^{3+}$ and the $(Fe^{2+}OH)_{-1}Fe^{3+}O$ substitutions, both typical of the tourmaline group minerals (Foit, Rosenberg 1977). Such tourmaline varieties are common in pegmatoidal secretions within the Izera granitogneisses, some pegmatites of the Karkonosze, Strzegom and Strzelin granite massifs, pegmatites of the Góry Sowie gneissic block, and in some parts of the Śnieżnik metamorphic unit (Pieczka 1996). The coloured varieties of elbaite in the Polish part of the Sudety Mts have not been mentioned in the older, German-language literature.

[1] AGH, University of Science and Technology, Faculty of Geology, Geophysics and Environment Protection, al. Mickiewicza 30, 30-059 Kraków, Poland; e-mail: pieczka@uci.agh.edu.pl

[2] ul. Kwiatowa 15, 55-075 Bielany Wrocławskie, Poland.

[3] University of Wrocław, Institute of Geological Sciences, ul. Cybulskiego 30, 50-205 Wrocław, Poland; e-mail: msach@ing.uni.wroc.pl

As late as the autumn of 2001, one of the authors (K.Ł.) found in the NE part of the Góry Sowie block fragments of a pegmatite with few prismatic crystals of green tourmaline.

The Góry Sowie block is a geological unit of the triangular shape, situated in the central part of the Sudety Mts among Ząbkowice Śląskie, Nowa Ruda and Świdnica, east of Wałbrzych (Fig. 1). The Sudetic Marginal Fault separates the block into an elevated, mountainous, SW part of the Góry Sowie Mts proper, and the down-thrown, NE part, developed as a hilly foreland. The borders with the surrounding units (the metamorphic rocks of the Niemcza dislocation zone to E, the metamorphic envelope of the Upper Carboniferous Strzegom-Sobótka granite massif and Upper Devonian-Lower Carboniferous sedimentary sequence of the Świebodzice depression to N, the Carboniferous--Permian rocks of the Intrasudetic depression and Ordovician-Lower Carboniferous sedimentary sequence of the Bardo basin to SW) are tectonic, while to NE the Góry Sowie block borders on ultrabasic and basic rocks of the Mt. Ślęża ophiolite.

The major rocks of the Góry Sowie block represent oligoclase-biotite paragneisses and migmatites, dated at around 384–370 MA (van Breemen et al. 1988; Bröcker et al. 1998; Timmermann et al. 2000; Aftalion, Bowes 2002). They are accompanied by much less frequent and locally occurring granulites, metamorphosed around 402 ± 1 MA

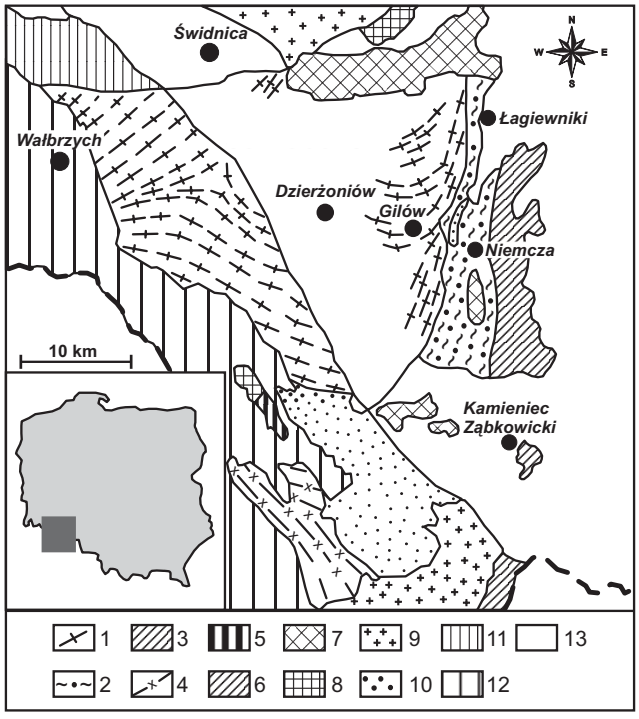


Fig. 1. Geological sketch of the Góry Sowie gneissic block with adjacent units
1 — the Góry Sowie gneisses; 2 — mylonites of the Niemcza Zone; 3 — schists of the Niemcza-Kamieniec Metamorphic Unit; 4 — rocks of the Kłodzko Metamorphic Unit; 5 — diabases of the Nowa Ruda massif; 6 — gneisses and schists of the Złote Mts; 7 — serpentinites; 8 — gabbros; 9 — granitoids; 10 — sedimentary rocks of the Bardo Basin; 11 — sedimentary rocks of the Świebodzice Depression; 12 — sedimentary and volcanic rocks of the Intrasudetic Depresion; 13 — Cenozoic sediments

(light-coloured variety; O'Brien et al. 1997), two-stage metamorphosed amphibolites (402 ± 3 MA and around 380 MA; Brueckner et al. 1996), and serpentinites. In these rocks, particularly in the gneisses and migmatites, can be locally found pegmatite veins or vein-nest bodies, reaching a length of even some tens of metres. More common are fine pegmatoidal secretions, concordant with the textures of the enclosing gneisses and migmatites. The age of the pegmatites was established at 370 ± 4 MA by van Breemen et al. (1988), using Rb-Sr dating of muscovite from the Lutomia pegmatite.

In the Góry Sowie Mts pegmatites predominate such typical minerals as quartz, feldspars (albite-oligoclase, orthoclase, microcline), muscovite, biotite, schorl, garnet transitional members from the almandine-spessartine series, apatite, less frequent are zircon, disthene, sillimanite, rutile, beryl, columbite, cordierite, monacite, xenotime, sarcopside, triplite, hureaulite, magnetite, pyrite, sphalerite, uraninite and goethite (*fide* Lis and Sylwestrzak 1986). Pieczka (2002) found in the Góry Sowie block area a rich assemblage of phosphate minerals with graftonite, ferrisicklerite, sarkopside, beusite, stanekite, alluaudite, hagendorfite, whitlockite, fairfieldite, whitmoreite, earlshannonite, jahnsite, phosphoferrite-kryzhanovskite and apatite, containing small inclusions of monacite, xenotime, uraninite, hematite, pyrite, sphalerite, cuprite, chalcocite, oligonite and, probably, native copper.

A pegmatite with green tourmaline described in this paper was found in an old trenche localized in upper part of a hill in the E, down-thrown part of the Góry Sowie block near Gilów.

DESCRIPTION OF THE PEGMATITE

Fragments of the pegmatite were spotted in an old trench, mingled with soil and accompanied by numerous pieces of amphibolites, which most probably represent the host rock. The pegmatite vein itself is not directly exposed. The fragments of the pegmatite differ slightly in their mineral composition. Usually they represent a typical, medium-grained pegmatite, containing quartz with weak undulatory extinction, white feldspars, light-coloured mica sometimes with pale-greenish tint, numerous crystals of black tourmaline reaching the length of 10 cm, grains of Mn-bearing almandine up to 2–3 cm large, very seldom prisms of green tourmaline up to 4 cm long (Fig. 2), and yellowish beryl up to 2 cm long. Some of the pegmatite fragments are devoid of feldspars and composed mainly of intergrowing booklets of mica with flakes 1–3 cm in size, sporadical, some-millimetre-long black tourmaline crystals, equally fine, dark brownish garnets with composition close to spessartine, and pinkish-red grains of andalusite, reaching some millimetres.

METHODS

Microprobe analyses were carried out in the EDS mode at the Institute of Non-Ferrous Metals in Gliwice (Poland), using a Jeol JCXA-733 Superprobe. The conditions

were as follows: accelerating voltage 20 kV, current 20 nA, beam diameter around 2 μm, counting time 60 sec. The contents of Na, Mg, Al, Si, K, Ca, Ti, Mn, Fe, Co, Zn, Ba and F were measured from the Kα lines, while the Ba content from the Lα line. The data were first drift- and dead time-corrected, then ZAF-corrected. The standards included: albite (Na), periclase (Mg), corundum (Al), quartz (Si), MAD-10 (K), wollastonite (Ca), fluorite (F), BaF_2 (Ba) and metallic Ti, Mn, Fe, Co and Zn.

The formulae of the tourmaline varietes were calculated after normalization of atomic contents to 6 Si atoms per formula unit (apfu), and in the case when the amount of octahedral components was higher than 9 apfu to the Σ(Y+Z+Si) = 15 apfu, assuming the excess of Al above 9(Y+Z) apfu substituting for an Si deficiency. The B_2O_3 content was calculated stoichiometrically, assuming the presence of 3 B atoms pfu. The content of Fe^{3+} was accepted as 5% of the total Fe, as such an amount had been obtained earlier for other dark-coloured tourmaline species from the Góry Sowie area (Pieczka 1996). In the case of elbaite, the total Fe was assumed as Fe^{2+}, while the Li content was estimated as a supplement of octahedral cations to 9 pfu. The $H_2O(+)$ amount was calculated stoichiometrically after supplementing the composition of tourmaline with Fe^{3+}, B and Li.

The chemical composition of white mica was normalized to 12 oxygens, assuming the presence of OH groups in two (OH, F) sites, and applying a relation between the amount of tetrahedral cations $(Si+Ti+Al_T) = 4$ pfu and their charge, which together with the charge of alkalies should total 16 units. The deficiency of alkalies and some excess of Si were accepted as effects of the $\square Si(KAl_T)_{-1}$ substitution. The presence of Li in white mica was tested using AAS, but in the microprobe analyses the Li amount was estimated as supplementing to 6 the charge of the octahedral cations.

The chemical compositions of some other minerals found (Ba-rich feldspar, garnet, andalusite and (Zn-Fe)-bearing spinel) were recalculated after normalizaton to 4, 12, 5 and 4 oxygen atoms, respectively.

X-ray investigations of black and green tourmaline crystals, and also of accompanying garnet and beryl were carried out with a Philips X'pert diffractometer under the following conditions: CuK_α radiation, a graphite monochromator, the range recorded 3–71°(2Θ), the step 0.02°(2Θ)/s, quartz as an internal standard. Unit-cell parameters of tourmaline, garnet and beryl were refined with the PDS'94 computer program.

The Raman spectra of the green elbaite oriented $\parallel$ **c** were obtained from several points using a Jobin-Yvon T-64000 spectrometer equipped with an Argon laser beam (λ = 514.5 nm).

RESULTS

Tourmaline

Black tourmaline crystals are heterogenous under the microscope. They consist of two colour varieties showing relatively distinct pleochroism in the shades: ω — an intensively blue core and a blue-grey mantle; the latter with grey, blue and pale blue

zones parallel to crystal elongation, and also with irregular, intensively blue patches, ε — a colourless core and light pinkish mantle. In some zones of these crystals oriented parallel to the *z* axis, and also in small veins cutting them across as well as in irregular patches, there appear a variety with somewhat lighter pleochroism: ω — light bluish (very delicate), ε — colourless. Within this zone are visible elongated, colourless (both ω and ε) domains arranged parallel to the length of the zone as well as relicts of the major, blue-grey variety (Fig. 3). In some fragments of the bluish-coloured crystals can be observed a very thin rim of colourless tourmaline. Birefringence assessed on the basis of interference colours in the crystals cut parallel to the *z* axis has been estimated at 0.029–0.028 in the strong coloured varieties, 0.021–0.020 in pale blue tourmaline, and 0.014–0.013 in the colourless domains. The heterogeneity of the black tourmaline crystals is also pronounced in BSE images. The crystals of green tourmaline seem to be wholly homogenous. Under the microscope they are colourless, with birefringence around 0.013–0.012.

The blue grey zones predominating in the black tourmaline show composition I presented in Table 1. Analysis II represents the composition of the pale bluish zone parallel to the crystal elongation, while analyses III and IV correspond to the very light-coloured and colourless, elongated patchy zones, visible within the turmaline II. The tourmaline I can be classified as an Mg- and Al-enriched schorl, a typical black tourmaline from the Góry Sowie gneissic block (Pieczka 1996). Its total iron exceeding 2 apfu is the highest of the recorded in this region so far, while the F content, usually low in the Góry Sowie tourmalines, is only 0.01–0.02 apfu in the sample analysed. The unit-cell parameters of the tourmaline I are: $a = 15.979(1)$ Å and $c = 7.171(1)$ Å, and correspond to an Al- and Mg-bearing schorl. The less frequent tourmaline II, although can be classified as the former, reveals a very high Al content, reaching almost one atom of possible three in the triad of the Y octahedra. The amount of Li reaching 0.03 apfu, estimated as a supplement of the Y cations up to the amount of 3 apfu, is negligible, but may be result from the accepted assumptions and/or possible errors in the microprobe analyses. On the other hand, this amount of lithium may be treated as a sign of progressing enrichment in Al and Li that is distinctly visible in tourmalines III and IV (Fig. 4). Both latter varieties forming patchy, elongated zones, despite their comparable Al contents are characterized by more pronounced deficiency of octahedral cations that may be explained by an increasing Li content, an element non-determinable in microprobe analyses. Therefore, the zones with the composition III may be identified as Li-enriched, Al-bearing schorl, while those of analysis IV as Fe-rich elbaite. In the dark tourmaline varieties (from I to IV), the contents of Fe total and Mg progressively decrease while those of Al, Li, traces of Mn and F increase, the process expressed by the change of the Mn/(Mn+Fe) ratio from around 0.03 to 0.07. The tourmaline I normalized to 6 Si pfu indicates the amount of octahedral cations higher than nine, allowed by structural constraints. Normalization of the same analysis to the amount of the octahedral cations and silicon equal to 15 apfu shows a small deficiency of Si (0.04 apfu) that is compensated by an equivalent excess of Al. It has not been possible to recognize fully a role of boron, whose amount particularly in the Li-bearing varieties of tourmaline may exceed 3 apfu, also partly entering

TABLE 1

Representative compositions of schorl and elbaite from the Gilów pegmatite

Component	Schorl				Elbaite		
	I	II	III	IV	V	VI	VII
Na_2O	2.49	2.38	2.62	2.64	2.09	2.62	2.49
CaO	0.09	0.18	0.26	0.27	0.21	0.21	0.15
K_2O	0.03	0.01	0.00	0.00	0.02	0.01	0.02
MgO	1.65	1.34	0.93	0.99	0.00	0.14	0.10
FeO	13.35	10.19	8.98	7.64	2.82	2.95	2.91
Fe_2O_3*	0.78	0.60	0.52	0.45	0.00	0.00	0.00
MnO	0.40	0.56	0.58	0.61	1.90	1.99	1.89
CoO	0.05	0.08	0.02	0.06	0.00	0.04	0.10
ZnO	0.16	0.20	0.10	0.12	0.04	0.05	0.00
TiO_2	0.18	0.19	0.13	0.02	0.09	0.07	0.04
Li_2O*	0.00	0.04	0.55	1.11	1.65	1.48	1.36
Al_2O_3	32.14	34.79	35.37	34.54	38.32	37.90	38.40
B_2O_3*	10.14	10.23	10.40	10.44	10.79	10.64	10.63
SiO_2	34.80	35.32	35.90	36.03	37.25	36.73	36.70
H_2O*	3.10	2.61	2.85	3.35	3.58	3.23	3.11
F	0.03	0.24	0.34	0.44	0.38	0.44	0.49
Total	***99.40***	***98.97***	***99.54***	***98.70***	***99.15***	***98.51***	***98.40***
	Number of ions						
Na	0.828	0.783	0.847	0.854	0.651	0.831	0.789
Ca	0.016	0.033	0.046	0.049	0.036	0.036	0.026
K	0.008	0.002	0.000	0.000	0.004	0.003	0.005
□	0.148	0.182	0.107	0.097	0.309	0.130	0.180
X	***1.000***	***1.000***	***1.000***	***1.000***	***1.000***	***1.000***	***1.000***
Mg	0.421	0.340	0.231	0.247	0.000	0.035	0.025
Fe^{2+}*	1.913	1.448	1.255	1.064	0.380	0.403	0.398
Fe^{3+}*	0.101	0.076	0.066	0.056	0.000	0.000	0.000
Mn	0.059	0.081	0.083	0.085	0.259	0.276	0.262
Co	0.006	0.011	0.003	0.008	0.000	0.005	0.014
Zn	0.021	0.026	0.012	0.015	0.005	0.006	0.000
Ti	0.024	0.025	0.016	0.002	0.011	0.009	0.005
Li*	0.000	0.028	0.367	0.743	1.069	0.970	0.897
Al.	0.456	0.966	0.968	0.780	1.275	1.297	1.399
Y	***3.000***	***3.000***	***3.000***	***3.000***	***3.000***	***3.000***	***3.000***
Al_Z	6.000	6.000	6.000	6.000	6.000	6.000	6.000
B	3.000	3.000	3.000	3.000	3.000	3.000	3.000
Si	5.964	6.000	6.000	6.000	6.000	6.000	6.000
^{IV}Al	0.036						
T	***6.000***	***6.000***	***6.000***	***6.000***	***6.000***	***6.000***	***6.000***
OH*	3.548	2.954	3.183	3.719	3.851	3.523	3.388
F	0.017	0.130	0.180	0.232	0.194	0.226	0.253
O	27.435	27.916	27.637	27.049	26.955	27.251	27.359
Mn/(Mn+Fe)	***0.028***	***0.051***	***0.056***	***0.070***	***0.405***	***0.407***	***0.397***

* Calculated from stoichiometry.

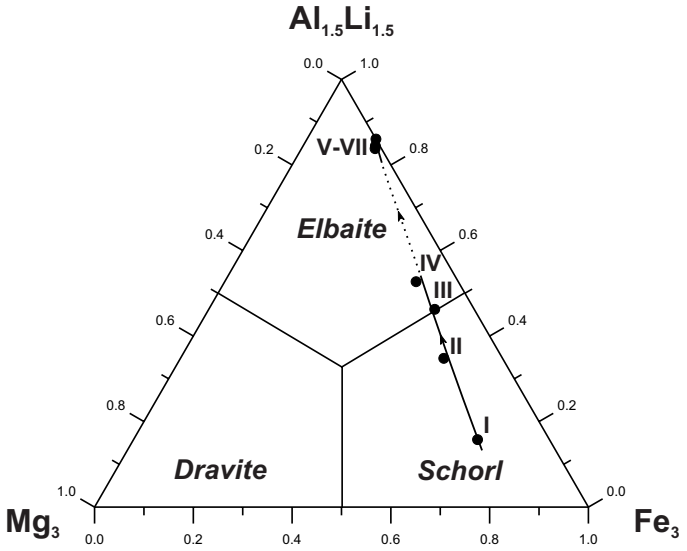


Fig. 4. Compositional trend in tourmaline crystals from the Gilów pegmatite in the Mg_3-Fe_3-$Al_{1.5}Li_{1.5}$ ternary plot: I — (Mg, Al)-enriched schorl, II — Al-bearing schorl, III — Al-bearing, Li-enriched schorl, IV — Fe-rich elbaite, V–VII — (Fe, Mn)-bearing elbaite

tetrahedral sites (Hawthorne 1996; Hughes et al. 2000; Hughes et al. 2001; Hawthorne 2002).

The green elbaite does not show changes in its chemical composition that may be revealed in its BSE images. Within the grain studied, there clearly dominates composition corresponding to analysis VI (Table 1), while the compositions corresponding to analyses V and VII (their differences from analyses VI are, in fact, small) are sporadic.

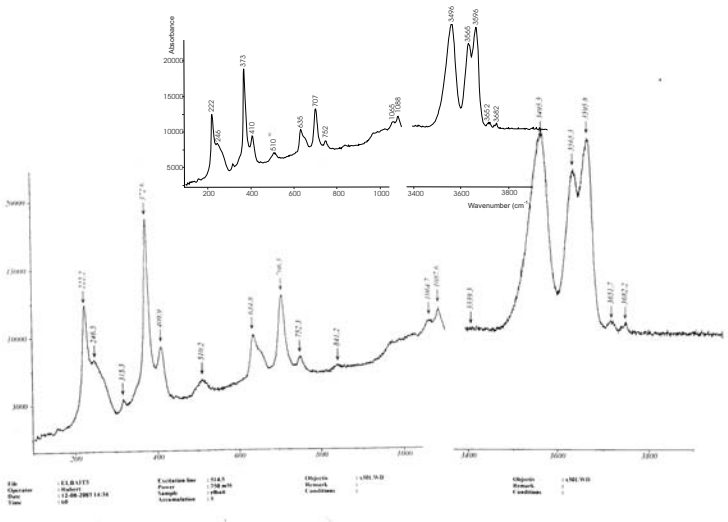


Fig. 5. Raman spectrum of the Góry Sowie Mts elbaite

The features characteristic of this elbaite include: practically constant amounts of Fe (0.38–0.40 apfu), Mn (0.26–0.28 apfu), and F (0.20–0.25 apfu), and as a consequence also the stable Mn/(Mn+Fe) ratio around 0.40–0.41, and additional oscillations of the Li amount around 1 apfu. More significant diversification of the elbaite composition has been noted at the X site occupancy, as in few analyses the amount of Na decreases from 0.85–0.78 apfu, typical Na concentrations not only in the green elbaite but also in the accompanying black tourmaline, to 0.65 apfu. The unit-cell parameters of the green elbaite (composition VI) are: a = 15.884(1) Å and c = 7.115(1) Å, being typical of (Fe,Mn)-bearing elbaites. The Raman spectrum of a prismatic green crystal recorded in the frequency range 100–3800 cm^{-1} (Fig. 5) shows strong similarities with the ones of an elbaite-type tourmaline (Gasharova et al. 1997). The tourmaline studied is characterized by sharp peaks at 222, 373, 707 cm^{-1}, and 3496, 3565 and 3596 cm^{-1}.

Other associated phases

Next to the black tourmaline, the major minerals of the pegmatite studied include white, coarse-tabular feldspar and plates or flakes of pale-coloured mica. Relatively common are fine crystals of garnet, light brownish to dark brownish-red, and equally fine crystals of raspberry-red to red-grey and pink andalusite. Only in BSE images have been observed small inclusions of a Ba-enriched K-feldspar, spinel, zircon, and columbite.

The feldspars are represented almost exclusively by chequered albite. In one case, within a polycrystalline aggregate of white mica and andalusite, a small grain of a Ba-enriched K-feldspar has been found; the grain reveals the composition transitional between orthoclase and celsian with an amount of around 34 mol.% of the $Ba[Al_2Si_2O_8]$ end-member (Table 2). This phase can be identified as hyalophane. An excess of Al above one atom in its composition corresponds well with the amount of bivalent alkali earth cations (Ca+Ba). Although Mn and Fe occur in traces, the Mn/(Mn+Fe) value around 0.25 points to formation of this feldspar in a later stage of pegmatite fractionation.

The white micas show typical features, including their birefringence around 0.035–0.032. Chemical analyses were done on two mica varieties: mica-A — platy, polycrystalline aggregates containing grains of andalusite and fine crystals of dark tourmaline; and mica-B — vein mica aggregates among garnet grains. Both types can be identified as Al-micas, but the B type contains distinctly higher admixtures, particularly of Fe, Mg and Mn, while the A variety is Na-enriched (Table 2). The amount of octahedral Li in the mica-A has been estimated at around 0.11 apfu, while in the mica-B as high as 0.50 apfu. The ratio Mn/(Mn+Fe) ≈ 0.015 and 0.085, respectively, reveals that the flaky mica-B is slightly later than the coarse-platy mica-A.

The garnets are represented by crystals some millimetres to 2–3 cm large, dark brownish red, and smaller ones, light brownish in colour. The darker crystals show the ($Al_{57}Spe_{40}Py_3Gro_{<0.01}$) composition, transitional between almandine and spessartine, with the Mn/(Mn+Fe) ratio of 0.390 (Table 2), and the unit-cell parameter a = 11.566(1) Å. The lighter variety has its unit-cell slightly larger (a = 11.589(1) Å), which

TABLE 2

Representative compositions of tourmaline-associated phases in the Gilów pegmatite

Component	Mica-A	Mica-B	Hyalophane	Garnet	Andalusite	Spinel
Na_2O	0.94	0.35	1.03	0.11	0.09	0.00
CaO	0.03	0.06	0.11	0.12	0.02	0.00
K_2O	9.76	10.35	7.37	0.00	0.04	0.00
BaO			16.68			
MgO	0.18	0.75	0.00	0.70	0.00	0.43
FeO	1.43	3.29	0.56	24.23	1.01	18.26
MnO	0.02	0.30	0.19	16.70	0.01	0.78
ZnO						22.63
TiO_2	0.06	0.07	0.32	0.21	0.02	0.00
Al_2O_3	36.34	32.68	22.67	20.78	62.43	58.09
SiO_2	45.59	45.40	49.83	36.28	36.12	0.00
Li_2O*	0.40	1.84				
H_2O*	4.50	4.46				
Total	***99.25***	***99.54***	***98.76***	***99.12***	***99.72***	***100.20***
	number of ions					
Na	0.122	0.046	0.104	0.017	0.005	0.000
Ca	0.003	0.004	0.006	0.010	0.001	0.000
K	0.830	0.888	0.491	0.000	0.001	0.000
Ba			0.341			
Mg	0.018	0.075	0.000	0.087	0.000	0.019
Fe	0.080	0.185	0.025	1.674	0.023	0.449
Mn	0.001	0.017	0.008	1.168	0.000	0.019
Zn						0.491
Ti	0.003	0.003	0.013	0.013	0.000	0.000
Al	2.856	2.591	1.395	2.023	2.004	2.014
Si	3.040	3.055	2.602	2.996	0.984	0.000
Li*	0.107	0.498				
OH*	2	2				
O	10	10	4	12	5	4
Mn/(Mn+Fe)	***0.015***	***0.086***	***0.253***	***0.390***	***0.009***	***0.028***

* Calculated from stoichiometry

points to a higher amount of Mn in its composition. From the size of the unit-cell it can be concluded that it represents a spessartine species with around 65 mol.% of the spessartine end-member, the highest noted for garnets from the Góry Sowie pegmatites to date (Pieczka et al. 1997).

The raspberry-red andalusite shows traces of admixtures that can be associated with microinclusions of foreign phases, especially of white mica (Table 2). Worth noticing is an amount of FeO around 1 wt.%, probably inducing the intensive reddish colour of this mineral.

Beryl forming short-prismatic crystals, occurs very seldom within basic pegmatite. Its unit-cell: a = 9.219(1) Å and c = 9.196 (2) Å indicates a low-alkali and low-hydrated variety.

In a single BSE image, intergrowths of several crystals of the Al-(Zn-Fe)-spinel with sizes reaching 100 μm were observed within the aggregate of white mica. This phase is practically homogenous, admixture-free, and relations among Zn, Fe, Mn and Mg (Table 2) allow classifying it as a transitional member between gahnite and hercynite with the composition $Gh_{50}He_{46}Ga_2Sp_2$.

CONCLUSIONS

A complex of mudstones and sandstones metamorphosed and migmatized 384–370 Ma ago under low- and medium-pressure conditions (600–770ºC/3–8 kbar; Żelaźniewicz 1995, 2003) was the protolith of the Góry Sowie gneisses (van Breemen et al. 1988; Bröcker et al. 1998; Timmermann et al. 2000; Aftalion and Bowes 2002). One of the effects of this progressive metamorphism, particularly in its last stage, included generation of low-temperature, mobile pegmatite melts, rich in SiO_2, Al_2O_3, alkalies (Na_2O, K_2O), volatiles, and some less frequent elements such as Fe, Mn, Be, B, P, F, and locally also Li. Crystallization of these melts gave rise to formation of sometimes extensive systems of veins and nests, composed of coarse-crystalline quartz, feldspars (mainly plagioclase), micas, and some other minerals in the study area: dark, Al- and Mg-enriched schorl, beryl, (Fe-Mn) bering garnets; in the last stages there crystallized an assemblage of Fe-Mn-phosphates with lamellar intergrowths of graftonite, sarcopside and ferrisicklerite (Pieczka 2002).

Quite typical of this pattern is the pegmatite described, occurring in amphibolites near Gilów. Local metamorphism of those amphibolites was determined by Dziedzicowa (1994) as low-pressure granulite facies (770–700ºC/3–4 kbar), while the metamorphism of neighbouring gneisses and migmatites at 650–730ºC/3–5 kbar (Żelaźniewicz 1995, 2003). The Al- and Mg-enriched schorl of the pegmatite indicates the stage of boron metasomatism and crystallization of dark tourmalines, typical of the Góry Sowie gneissic block. Chequered albite, some-centimetres-large crystals of muscovite, zircon, andalusite and spinel seem to be associated with earlier stages of the pegmatite formation. The two last minerals are without alkalies and manifest the peraluminous character of initial pegmatite melts. The zones with lighter pleochroism, extended lengthwise in some black tourmaline crystals, depleted of typical octahedral cations

point to gradually increasing activity first of Al, and then also of Li in later and latest stages of pegmatite fractionation. The outer rim of colourless lithium tourmaline on the Mg- and Al-enriched schorl, and also the crystals of light green (Fe-Mn)-bearing elbaite growing immediately next to the dark tourmaline indicate that the stage of crystallization of lithium phases took place at the final stage of pegmatite formation in the Góry Sowie area. This increasing role of Li and other accessory elements is also manifested by enrichment of the younger forms of light-coloured mica in lithium and the presence of accessory hyalophane. Considering the Mn/(Mn+Fe) ratio values, 0.27–0.28 for ferrisicklerite (Pieczka 2002), around 0.05–0.07 for Li-enriched schorl and micas, and even 0.39–0.40 for green tourmaline, it can be concluded that the Góry Sowie elbaite and Li-enriched white mica are almost simultaneous with ferrisicklerite.

Acknowledgements. The authors thank M. Olesch and an unknown reviewer for their comments. This work was supported by the AGH, University of Science and Technology (Cracow) grant No. 11.11.140.158.

REFERENES

AFTALION M., BOWES D.R., 2002: U-Pb zircon isotopic evidence for Mid-Devonian migmatite formation in the Góry Sowie domain of the Bohemian Massif, Sudeten Mountains, SW Poland. *N. Jb. Min. Mh.* 4, 182–192.

BRÖCKER M., ŻELAŹNIEWICZ A., ENDERS M., 1998: Rb-Sr and U-Pb geochronology of migmatic gneisses from the Góry Sowie (West Sudetes, Poland): the importance of Mid-Late Devonian metamorphism. *J. Geol. of London* 155, 1025–1036.

BRUECKNER H.K., BLUSZTAJN J., BAKUN-CZUBAROW N., 1996: Trace element and Sm-Nd "age" zoning in garnets from peridotites of the Caledonian and Variscan mountains and tectonic implications. *J. Metamorphic Geol.* 14/1, 61–73.

DZIEDZICOWA H., 1994: LP hornblende granulite facies within the Góry Sowie gneisses of the Fore-Sudetic Block. In: Kryza, R. (ed.) Igneous activity and metamorphic evolution of the Sudetes area, Abstracts, Wrocław, 43.

FOIT F.F., Jr., ROSENBERG P.E., 1977: Coupled substitutions in the tourmaline group. *Contrib. Mineral. Petrol.* 62, 109–127.

GASHAROVA B., MIHAILOVA B., KONSTANTINOV L., 1997: Raman spectra of various types of tourmalines. *Eur. J. Mineral.* 9, 935–940.

HAWTHORNE F.C., 1996: Structural mechanisms for light-element variations in tourmaline. *Can. Mineral.* 34, 123–132.

HAWTHORNE F.C., 2002: Bond-valence constraints on the chemical composition of tourmaline. *Can. Mineral.* 40, 789–797.

HUGHES J.M., ERTL A., DYAR M.D., GREW E.S., SHEARER Ch.K., YATES M.G., GUIDOTTI Ch.V., 2000: Tetrahedrally coordinated boron in a tourmaline: bron-rich olenite from Stoffhütte, Koralpe, Austria. *Can. Mineral.* 38, 861–868.

HUGHES K.A., HUGHES J.M., DYAR M.D., 2001: Chemical and structural evidence for $^{[4]}B \Leftrightarrow {}^{[4]}Si$ substitution in natural tourmalines. *Eur. J. Mineral.* 13, 743–747.

LIS J., SYLWESTRZAK H., 1986: Minerały Dolnego Śląska. Wyd. Geol. Warszawa.

O'BRIEN P.J., KRÖNER A., JAECKEL P., HEGNER E., ŻELAŹNIEWICZ A., KRYZA R., 1997: Petrological and isotope studies on Palaeozoic high-preasure granulites. Góry Sowie Mts, Polish Sudetes. *J. Petrol.* 38, 433–456.

PIECZKA A., 1996: Mineralogical study of Polish tourmalines. *Prace Min.* 85 (*in polish*).

PIECZKA A., 2002: New data on phosphate minerals from the Góry Sowie Mts. (SW Poland). In: Zbornik abstractov: Slovensko-česko-pol'ské mineralogicko-petrograficko-ložiskově dni, Herlany 2002, 29.
PIECZKA A., GOŁĘBIOWSKA B., KRACZKA J., 1997: Mn-garnets from the Sowie Mts metamorphic pegmatites. *Miner. Polon.* 28/2, 81–88.
TIMMERMANN H., PARRISH R.R., NOBLE S.R., KRYZA R., 2000: New U-Pb monazite and zircon data from the Sudetes Mountains in SW Poland; evidence for a single-cycle Variscan Orogeny. *J. Geol. Soc. of London* 157/2, 265–268.
VAN BREEMEN O., BOWES D.R., AFTALION M., ŻELAŹNIEWICZ A., 1988: Devonian tectonothermal activity in the Sowie Góry gneissic block, Sudetes, southwestern Poland: evidence from Rb-Sr and U-Pb isotopic studies. *An. Soc. Geol. Polon.* 58, 3–10.
ŻELAŹNIEWICZ A., 1995: Fore-Sudetic part of the Góry Sowie Block, SW Poland. *An. Soc. Geol. Polon.* 66, 85–109.
ŻELAŹNIEWICZ A., 2003: Developments in the geology of the crystalline basement of the West Sudetes in 1990–2003. In: Ciężkowskai, A., Wojewoda, J., Żelaźniewicz, A. (ed.): West Sudetes from Wend to Quaternary. WIND Wrocław, 7–16.

Adam PIECZKA, Krzysztof ŁOBOS, Michał SACHANBIŃSKI

PIERWSZE WYSTĄPIENIE ELBAITU W POLSCE

Streszczenie

We wschodniej części bloku sowiogórskiego, w okolicy Gilowa, zlokalizowano pośród amfibolitów wystąpienie pegmatytu kwarcowo-skaleniowo-muskowitowego zawierającego schorl, zielony elbait, spessartyn, andaluzyt, spinel, hialofan, cyrkon, columbit i beryl. Kryształy czarnego turmalinu charakteryzują się ewolucją składu chemicznego od typowego dla rejonu Gór Sowich schorlu magnezowo-glinowego, poprzez odmiany glinowe do schorli glinowo-litowych i bogatych w Fe^{2+} elbaitów. Zielony elbait jest ogniwem wzbogaconym w Fe i Mn. Sekwencja krystalizacji kolejnych odmian turmalinu wiąże się z frakcjonacją antektycznego medium pegmatytowego w późnym stadium metamorfozy pierwotnie osadowego protolitu około 370–380 Ma. Stadium tworzenia się wzbogaconych w Li odmian turmalinu odpowiada mniej więcej krystalizacji zespołu fosforanowego z przerostami ferrisicklerytu, sarkopsydu i graftonitu, poznanego z innych pegmatytów bloku sowiogórskiego.



Fig. 2. Green elbaite from the Gilów pegmatite

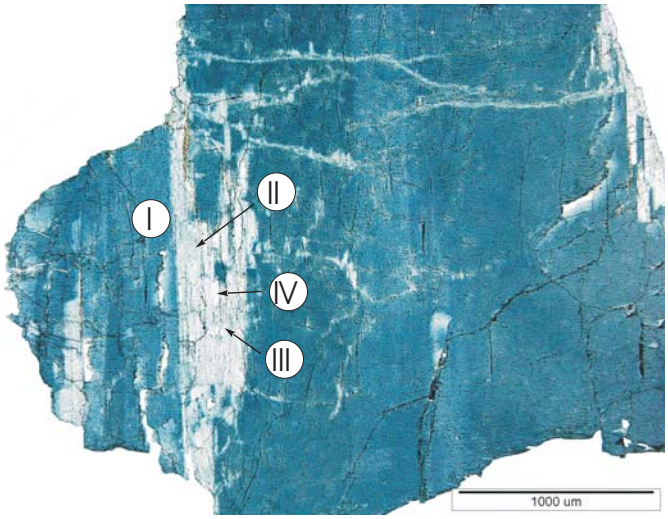


Fig. 3. Zones and veinlets of a late (Al,Li)-bearing tourmaline within schorl from the Gilów pegmatite (1 polar, transmitting light). I–IV denote number of analysis

MINERALOGIA POLONICA
Vol. 35, No 2, 2004
PL ISSN 0032-6267

Adam SZUSZKIEWICZ[1], *Krzysztof ŁOBOS*[1]

GAHNITE FROM SIEDLIMOWICE, STRZEGOM-SOBÓTKA GRANITIC MASSIF, SW POLAND

A b s t r a c t. Green spinel was found in a vein pegmatite in Siedlimowice (Strzegom-Sobótka massif, SW Poland). X-ray diffraction and electron microprobe analyses allowed defining the mineral as gahnite with the formula $(Zn_{6.1}Fe_{1.8}Mn_{0.1})(Al_{15.8}Fe_{0.2})O_{32}$ and unit cell parameters a = 8.1018 ± 0.008 Å, V = 531.787 ± 0.156 Å^3. Its chemical composition is typical of gahnites of igneous association. Formation of the zincian spinel was most probably controlled by local variations of crystallization conditions, e.g. the variations of a Zn/Fe ratio in a pegmatitic fluid or of oxygen fugacity.

Key-words: gahnite, zincian spinel, Siedlimowice, Strzegom pegmatite

INTRODUCTION

Gahnite belongs to the spinel group minerals with the general formula AB_2O_4, where A stands for Mg^{2+}, Mn^{2+},Fe^{2+}, Ni^{2+}, Zn^{2+} and B for Al^{3+}, Cr^{3+}, Fe^{3+}. It is an end member of the gahnite ($ZnAl_2O_4$) — hercynite ($FeAl_2O_4$) solid solution, occurring as an accessory mineral in rare-element pegmatites, peraluminous granites and certain metamorphic rocks as well as a heavy mineral in sedimentary rocks. Polish localities where gahnite has been reported are confined to the Sudety area (SW Poland) and comprise Przecznica and Kotlina near Mirsk, Szklarska Poręba, Jordanów Śląski and alluvia of the Izera Mts (Lis, Sylwestrzak 1986). The mineral has not been described from the Strzegom-Sobótka granite pegmatites yet.

The Siedlimowice granite quarry is located about 10 km north-east of Świdnica (SW Poland). The granite crops out in the eastern part of the Strzegom-Sobótka granite massif, a complex Variscan intrusion of the Fore-Sudetic Block whose petrography and mineralogy have been a matter of extensive research (e.g. Majerowicz 1972; Pin et al. 1989; Janeczek 1985; Puziewicz 1990). The rock quarried here is a two-mica granite crystallized from magma close to water saturation at a depth deeper than 15 km.

[1] University of Wrocław, Institute of Geological Sciences, pl. M. Borna 9, 50-204 Wrocław, Poland. e-mail: asz@ing.uni.wroc.pl

The locality is well known for its rare-element vein pegmatites, which were a subject of several mineralogical reports, either as a separate subject (Janeczek, Sachanbiński 1989) or a part of larger monographies (Janeczek 1985). The following phases were described from the Siedlimowice pegmatites by Janeczek and Sachanbiński (1989): feldspars (microcline, albite, oligoclase), quartz, muscovite, biotite, chlorite, Fe-Mn garnets, beryl, columbite, zircon, apatite. No zincian phase has been reported so far from the location. However, a few data presented by Janeczek and Sachanbiński (1989) indicate the presence of zinc as a trace element in some muscovites and garnets (550 and 1,750 g/t, respectively). The paper presents the results of the studies of the zincian spinel from this locality.

SAMPLE DESCRIPTION

Gahnite crystals were found in few boulders containing fragments of a vein pegmatite on the second exploitation level in the Siedlimowice quarry. Despite the abundance of pegmatite fragments, the gahnite-bearing rock is extremely rare and detailed observations did not result in finding the mineral *in situ*, i.e. in the quarry walls. The thickness of the gahnite-bearing veins may only be roughly estimated as not lower than 20 cm. They are built of a mineral assemblage typical of the Siedlimowice pegmatites, i.e. major K-feldspar, plagioclase, quartz and muscovite, minor chlorite and biotite, and accessory garnet, beryl, columbite and zircon. Comparing gahnite-devoid and gahnite-bearing pegmatite fragments, the latter contain noticeably lower amount of garnet which forms crystals smaller (up to 3 mm) than elsewhere in the quarry.

The grains of gahnite are dark green, translucent at edges. They occur in central parts of the pegmatite as idiomorphic octahedral crystals (rarely with subordinate dodecahedron faces) up to 5 mm large, embedded in grey quartz, more rarely in white K-feldspar, subordinately in muscovite and exceptionally in beryl (one sample). The crystals are generally not twinned although often intergrown. An intergrowth of gahnite and garnet was also noted. A single spinel crystal found within a mica aggregate was flattened in a similar way to garnets described by Janeczek and Sachanbiński (1989).

METHODS

Spinel grains were separated from the pegmatite mass by handpicking and inspected under a binocular microscope. About 20 mg of the material was used for XRD measurements which were carried out at room temperature on a powdered sample by means of a Siemens D500 X-ray diffractometre with Co-K_α Fe-filtered radiation, over the range: 20–145°2θ with a step 0.02°2θ. The results are shown in Table 1. Unit cell parameters were calculated using a WIN-METRIC programme and based on 13 lines with a tolerance of 0.01°2θ.

A thin section was prepared from a few grains and after observations under a standard E600-Pol polarizing microscope it was coated with graphite for microprobe

TABLE 1

Observed and calculated diffraction lines of gahnite from Siedlimowice

hkl	*d* (obs.)	*d* (calc.)	I/I_o
220	2.8628	2.8644	72
311	2.4417	2.4428	100
400	2.0249	2.0254	13
331	1.8583	1.8587	11
422	1.6535	1.6538	14
333	1.5591	1.5592	83
440	1.4317	1.4322	84
620	1.2808	1.2810	10
533	1.2356	1.2355	11
642	1.0826	1.0826	10
553	1.0549	1.0548	11
800	1.0127	1.0127	6
822	0.9549	0.9548	20

analyses. The WDS analyses were conducted by means of a Cameca SX100 electron microprobe with a beam current of 20 nA and acceleration voltage of 15 kV using the following standards: synthetic corundum (Al), sphalerite (Zn), rhodonite (Mn), rutile (Ti), diopside (Mg, Ca), haematite (Fe), chromite (Cr). The representative chemical analyses of five spinel crystals carried out in edge and/or central parts of separate crystals are presented in Table 2. They were recalculated basing on 32 oxygens and a part of Fe was assumed to be trivalent from overall stoichiometry.

RESULTS AND DISCUSSION

The X-ray diffraction pattern (Table 1) corresponds well with that of gahnite and allows calculation of the unit-cell parameter for 13 peaks indexed: $a = 8.1018 \pm 0.008$ Å, and the volume $V = 531.787 \pm 0.156$ Å^3. The a value is intermediate between those of gahnite and hercynite (8.086 and 8.149 Å, respectively), closer to the gahnite end member (Hill et al. 1979).

The spinel crystals investigated seem to be fairly homogenous and neither optical observations nor BSE image analysis have revealed any mineral inclusions or a clear zoning pattern. Chemical analyses (Table 2) do not show any important variations in the gahnite composition and give the spinel formula $(Zn_{6.1}Fe_{1.8}Mn_{0.1})(Al_{15.8}Fe_{0.2})O_{32}$ for the averaged values. A low MgO content (not exceeding 0.12% with an average of 0.09%) is typical of rare-element granite pegmatites (Batchelor, Kinnaird 1984;

TABLE 2

Representative compositions of gahnite from Siedlimowice

Component	Grain 1	Grain 2		Grain 3		Grain 4			Grain 5		Mean
		edge	centre	edge	centre	edge		centre	edge	centre	
Al_2O_3	55.68	55.88	55.11	55.65	54.83	55.17	55.36	55.40	54.88	54.78	55.27
Fe_2O_3	0.65	1.29	2.03	1.47	1.64	1.91	1.81	1.61	1.87	1.79	1.61
MgO	0.08	0.12	0.11	0.08	0.11	0.07	0.07	0.07	0.08	0.07	0.09
MnO	0.21	0.44	0.41	0.49	0.46	0.39	0.39	0.39	0.47	0.43	0.41
FeO	8.39	9.04	8.57	9.33	9.29	8.66	8.47	8.73	8.84	9.05	8.84
ZnO	34.88	34.28	34.65	33.92	33.34	34.62	34.91	34.58	34.05	33.74	34.30
Total	99.89	101.05	100.87	100.93	99.66	100.81	101.01	100.77	100.18	99.85	100.50
Cation proportions based on 32 oxygens											
Al	15.84	15.74	15.81	15.79	15.76	15.77	15.80	15.76	15.77	15.80	15.84
Fe^{3+}	0.14	0.22	0.16	0.18	0.20	0.19	0.17	0.20	0.19	0.17	0.14
Mg	0.04	0.04	0.03	0.04	0.02	0.03	0.02	0.03	0.03	0.03	0.04
Fe^{2+}	1.82	1.74	1.88	1.90	1.75	1.71	1.77	1.80	1.85	1.79	1.82
Mn	0.09	0.08	0.10	0.10	0.08	0.08	0.08	0.10	0.09	0.08	0.09
Zn	6.09	6.20	6.04	6.01	6.19	6.23	6.18	6.13	6.09	6.14	6.09
Selected molar proportions											
Zn/Fe	3.67	3.35	3.57	3.21	3.17	3.53	3.64	3.50	3.40	3.29	3.43
(Zn+Mn)/Al	0.79	0.78	0.80	0.78	0.77	0.80	0.80	0.79	0.79	0.78	0.79
(Fe+Mg)/Al	0.22	0.23	0.23	0.24	0.25	0.23	0.22	0.23	0.23	0.24	0.23

Morris at al. 1997; Tindle, Breaks 1998). The presence of Cr has not been detected with the microprobe. On the ternary plot showing molecular proportions of Zn, Fe_{tot} and Mg (Fig. 1), which was used by Batchelor and Kinnaird (1984) to differentiate between igneous and metamorphic gahnites, the zincian spinel from Siedlimowice falls into the first field.

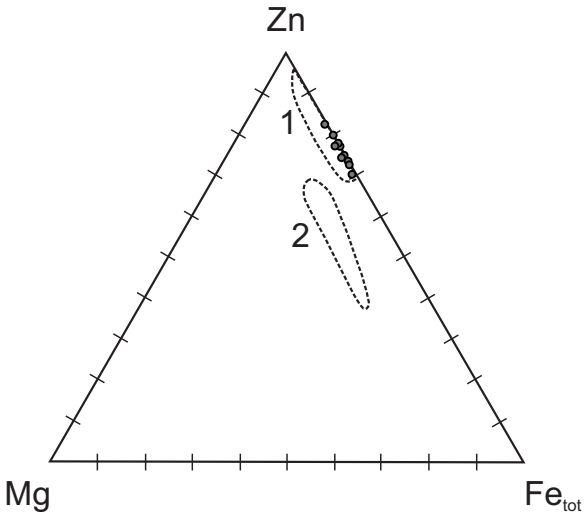


Fig. 1. Composition of gahnite from Siedlimowice in terms of Mg, Zn and total Fe molecular proportions. Fields for igneous (1) and metamorphic (2) associations are marked after Batchelor and Kinnaird (1984)

The molecular (Zn+Mn)/Al ratio was plotted against the molecular (Fe_{tot}+Mg)/Al ratio (Fig. 2); the plot depicts a complex diadochy between (Zn+Mn) and (Fe+Mg) in the mineral structure (Batchelor, Kinnaird 1984). In the gahnite from Siedlimowice the (Zn+Mn)/Al and (Fe+Mg)/Al ratios range from 0.77 to 0.80 and from 0.22 to 0.24, respectively, placing the analyses within the igneous association field on the line of almost perfect diadochy.

The possibility that earlier investigators and mineral collectors have overlooked the presence of gahnite in Siedlimowice seems highly improbable due to its distinctive appearance. This and the fact that the gahnite-bearing pegmatite fragments are very rare in the quarry suggest its local and spatially restricted occurrence in the pegmatite veins. This hypothesis has arisen from our failure of identifying the garnet-bearing pegmatite in the quarry walls. Most probably it was completely exploited during quarring.

Discussing the origin of the zincian spinel studied, our observations that fragments of the pegmatite containing gahnite are devoid of larger garnet crystals and the data of Janeczek and Sachanbiński (1989) showing elevated contents of Zn in some garnets must be considered. Combination of the two suggests that the formation of the zincian spinel was controlled by local changes in chemistry of the pegmatite fluid, such as variations of Zn/Fe ratio, variations of oxygen fugacity, etc., they may have resulted in the crystallisation of gahnite at the expense of garnet.

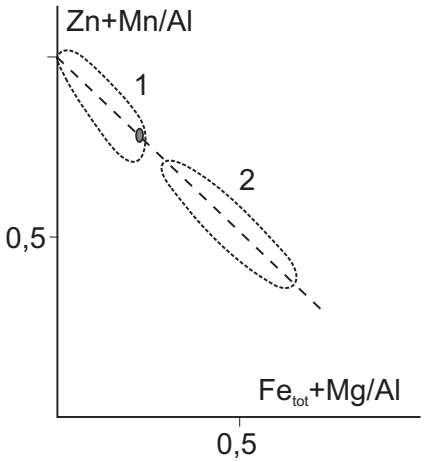


Fig. 2. Plot of the (Zn + Mn)/Al vs. (Fe_{tot} + Mg)/Al molecular ratios depicting a complex (Zn, Mn) – (Fe, Mg) substitution in gahnite from Siedlimowice (dark spot).
Fields for igneous (1) and metamorphic (2) associations are marked after Batchelor, Kinnaird (1984)

The presence of a tabular gahnite crystal within a muscovite aggregate may indicate that a part of the spinel was formed in the process of biotite muscovitization, which was described as taking part in the formation of some garnets (Janeczek, Sachanbiński 1989). Nonetheless, further research is needed to unravel the question of detailed geochemical conditions of the gahnite formation; finding the gahnite-bearing pegmatite *in situ* would be especially fruitful in drawing sound conclusions.

REFERENCES

BATCHELOR C.E., KINNAIRD J.A., 1984: Gahnite compositions compared. *Mineral. Mag*. 48, 425–429.

HILL R.J., CRAIG J.R., GIBBS G.V., 1979: Systematics of the spinel structure type. *Phys. Chem. Minerals* 4, 317–339.

JANECZEK J., 1985: Typomorficzne minerały pegmatytów masywu granitoidowego Strzegom–Sobótka. *Geol. Sudetica* 20, 2, 1–81.

JANECZEK J., SACHANBIŃSKI M., 1989: Pegmatyty berylowe w granicie dwułyszczykowym wschodniej części masywu Strzegom–Sobótka. *Arch. Miner*. 54, 1, 57–79.

LIS J., SYLWESTRZAK H., 1986: Minerały Dolnego Śląska. Wyd. Geolog., Warszawa, 791 pp.

MAJEROWICZ A., 1972: Masyw granitoidowy Strzegom-Sobótka. *Geol. Sudetica* 6, 7–96.

MORRIS T.F., BREAKS F.W., AVERILL S.A., CRABTREE D.C., MCDONALD A., 1997: Gahnite composition: implication for base metal and rare-element exploration. *Explor. Mining Geol*. 6, 3, 253–260.

PIN C., PUZIEWICZ J., DUTHOU J.-L., 1989: Ages and origins of a composite granitic massif in the Variscan belt: A Rb-Sr study of the Strzegom-Sobótka Massif, W Sudetes (Poland)., *N. Jb. Miner. Abh*. 160, 71–82.

PUZIEWICZ J., 1990: Masyw granitoidowy Strzegom-Sobótka. Aktualny stan badań. *Arch. Miner*. 45, 1–2, 135–151.

TINDLE G.A., BREAKS F., 1998: Oxide minerals of the Separation Rapids rare-element granitic pegmatite group, northwestern Ontario. *Can. Mineral*. 36, 609–635.

Adam SZUSZKIEWICZ, Krzysztof ŁOBOS

GAHNIT Z SIEDLIMOWIC (MASYW GRANITOWY STRZEGOM-SOBÓTKA, SW POLSKA)

Streszczenie

W czynnym łomie granitu dwułyszczykowego w Siedlimowicach, położonym około 10 km na północny-wschód od Świdnicy, natrafiono na fragmenty pegmatytu żyłowego zawierającego kryształy ciemnozielonego spinelu. Wykształcony w postaci oktaedrów spinel tkwił w środkowej części pegmatytu złożonego ze skalenia potasowego, plagioklazu, kwarcu i muskowitu z podrzędnymi ilościami chlorytu i biotytu oraz akcesorycznym granatem, berylem, kolumbitem i cyrkonem. Badania składu chemicznego oraz analizy rentgenowskie pozwoliły określić minerał jako gahnit o składzie $(Zn_{6.1}Fe_{1.8}Mn_{0.1})(Al_{15.8}Fe_{0.2})O_{32}$ oraz następujących parametrach komórki elementarnej: $a = 8.1018 \pm 0.008$ Å, $V = 531.787 \pm 0.156$ Å^3. Skład chemiczny badanego spinelu jest typowy dla gahnitu z granitoidowych pegmatytów ziem rzadkich. Powstanie gahnitu najprawdopodobniej związane było z lokalnymi zmianami warunków krystalizacji pegmatytu, takimi jak zmiany lotności tlenu lub zawartości Zn/Fe w stopie pegmatytowym.

MINERALOGIA POLONICA
Vol. 35, No 2, 2004
PL ISSN 0032-6267

Anna ŁATKIEWICZ[1], *Witold ŻABIŃSKI*[2]

GREENOCKITE CdS FROM THE SILESIA-CRACOW Zn-Pb ORE DEPOSITS

A b s t r a c t. The occurrence of greenockite CdS in the Silesia-Cracow Zn-Pb ore deposits, mentioned just in 19th century, has been most probably for the first time documented here by chemical analysis and morphological observation.

Key-words: greenockite, cadmium sulphide, Silesia-Cracow ore deposits

INTRODUCTION

The occurrence of cadmium sulphide (greenockite) in the Silesia-Cracow Zn- Pb ore deposits was first mentioned by Traube (1888). He observed its lemon yellow coatings on a red galmei in a deposit in the vicinity of Bytom (Beuthen, Apfelgrube), but gave no more detailed information. During the 20th century the yellow efflorescence on partly weathered Zn sulphide ores were sometimes observed (pers. commun.), however — according to the present authors knowledge — nobody published the results of their investigations (see e.g. Żabiński 1960; Harańczyk 1965).

In this note the results of SEM morphological and EDS chemical investigation of greenockite efflorescence coming from a Zn-Pb ore mine of the Olkusz region are presented.

EXPERIMENTAL

The morphology of the mineral and its chemical composition were examined using field emission scanning electron microscope (HITACHI S-4700) equipped with an energy dispersive spectrometer (NORAN Vantage), accelerating voltage being 20 kV.

[1] Jagiellonian University, Institute of Geological Sciences, ul. Oleandry 2a, 30-063 Kraków, Poland.
[2] AGH, University of Science and Technology, Faculty of Geology, Geophysics and Environment Protection, al. Mickiewicza 30, 30-059 Kraków, Poland.

The sample was coated with the carbon film. The content of cations was evaluated according to the "standardless" procedure of calculation (i.e. using standards from the software library supplied by the manufacturer).

RESULTS AND DISCUSSION

The cadmium sulphide examined occurs in the form of fine-grained (powder), yellow efflorescence on a partly oxidized zinc sulphide, hosted by the ore-bearing dolomite (Phot. 1).

EDS chemical analysis was performed in several spots of the yellow efflorescence, CdS being always the dominant phase. Figure 1 represents EDS spectrum of the "purest" CdS, with small admixture of other elements (Zn, Mg, Al, Si) coming mostly from the "background" minerals. Weight- and atomic contents of the elements mentioned, recalculated to 100%, are shown in Table 1.

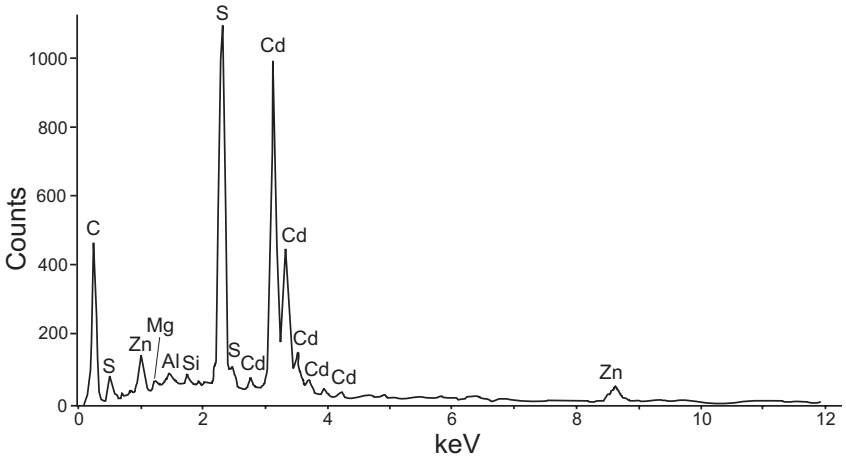


Fig. 1. EDS spectrum of the "purest" CdS

TABLE 1

Chemical composition of greenockite from the Olkusz region

Element	Wt.%	Atomic %
Cd	71.30	44.23
S	20.83	45.31
Zn	6.58	7.02
Mg	0.51	1.47
Al	0.33	0.85
Si	0.45	1.12
Total	100.00	100.00

The morphology of CdS crystals is presented on Phots. 2a and 2b. The aggregates of tiny crystals are clearly visible, the individual microliths displaying a tabular habit. This observation strongly confirms the supposition that it is the common hexagonal cadmium sulphide polymorph (β-CdS greenockite) rather than its rare cubic modification (α-CdS hawleyite) (Strunz 1978).

The origin of greenockite is most probably connected with its lower solubility in an acid solution in comparison with zinc sulphide, which initially hosted cadmium (Polański 1988). Greenockite can, therefore, precipitate from a sulphuric solution immediately after partial oxidation and dissolution of Zn ore.

REFERENCES

HARAŃCZYK Cz., 1965: Geochemia kruszców śląsko-krakowskich złóż rud cynku i ołowiu (in Polish). *Prace Geol. PAN* 30, Warszawa.

POLAŃSKI A., 1988: Podstawy geochemii (in Polish). Wyd. Geol., Warszawa.

STRUNZ H., 1978: Mineralogische Tabellen. 7. Auflage, Leipzig.

TRAUBE H., 1888: Die Minerale Schlesiens. Breslau.

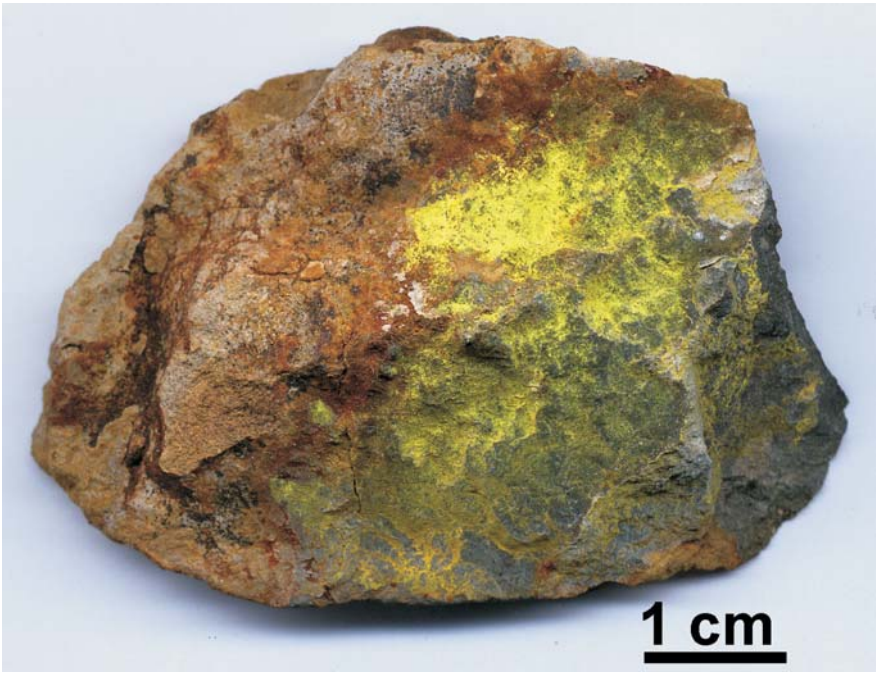
ŻABIŃSKI W., 1960: Geochemistry of cadmium in the oxidation zone of Silesia-Cracow zinc and lead ore deposits. *Bull. Acad. Pol. Sci., Sér. Sci. Géol. Géogr.*, VIII, 4.

Anna ŁATKIEWICZ, Witold ŻABIŃSKI

GREENOCKIT CdS ZE ŚLĄSKO-KRAKOWSKICH ZŁÓŻ RUD Zn-Pb

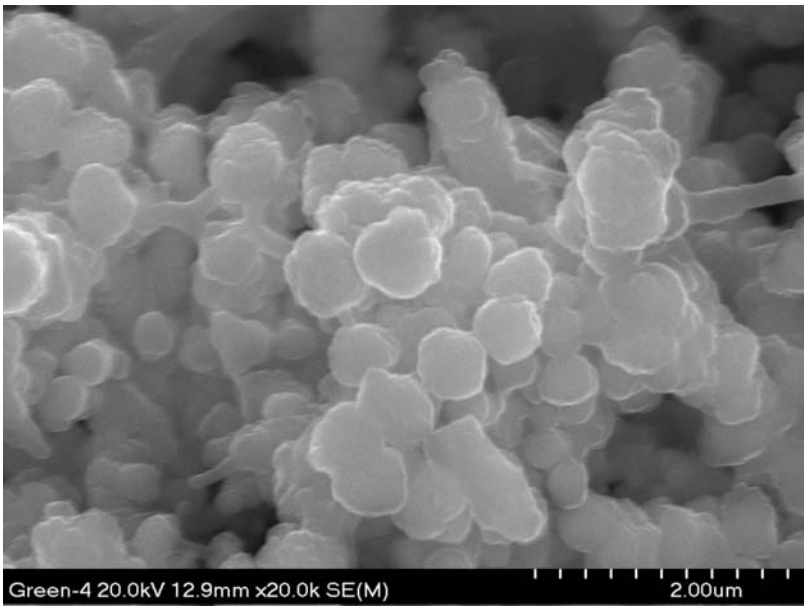
Streszczenie

Wzmianka o występowaniu greenockitu w jednej z kopalń rud Zn i Pb w rejonie Bytomia pochodzi jeszcze z XIX wieku (Traube 1888). W ciągu XX stulecia w ustnych przekazach wspominano o napotkaniu żółtych nalotów na wietrzejących siarczkowych rudach cynku, jednak nikt — według stanu wiedzy autorów tego komunikatu — nie opublikował wyników badań tych nalotów. Przedmiotem tej notatki są wyniki badań żółtych nalotów napotkanych na wietrzejących rudach Zn w jednej z kopalń rejonu Olkusza (Fot. 1). Za pomocą elektronowego mikroskopu skaningowego z przystawką EDS wykazano, że badany nalot jest niemal czystym siarczkiem kadmu, a tabliczkowata forma jego mikrokryształów (Fot. 2a, b) przemawia bardziej za heksagonalną modyfikacją siarczku (β-CdS greenockit) niż za jego rzadkim polimorfem regularnym (α-CdS hawleyit).

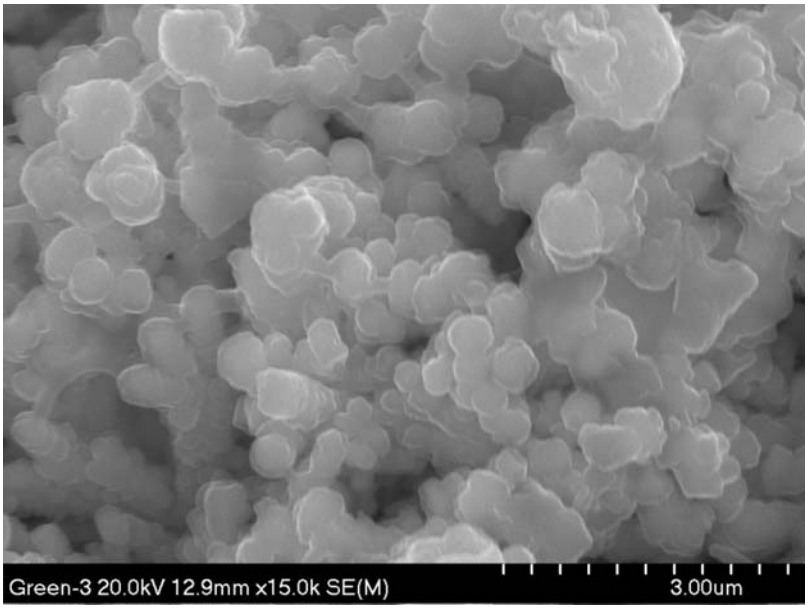


Phot. 1. Greenockite coating on partly oxidized zinc ore

a)



b)



Phot. 2. Aggregates of greenockite crystals.
Whole scale (bottom-right): a — 2 μm, b — 3 μm

MINERALOGIA POLONICA
Vol. 35, No 2, 2004
PL ISSN 0032-6267

Magdalena DUMAŃSKA-SŁOWIK[1]

MINERALOGICAL AND GEOCHEMICAL INVESTIGATION OF MICAS FROM THE GÓRY SOWIE MTS PEGMATITES

A b s t r a c t . Micas from pegmatites of the Góry Sowie Mts were characterized using: microscopic observations, X-ray diffractometry, IR-spectroscopy and chemical analyses. The main stress of this study was put on concentration of main and trace elements in these minerals. Micas are very sensitive indicators of petrogenetic processes. A depletion in F, Rb, Cs, Li, Sn and REE as well as an enrichment in Ba show the high-temperature, post-magmatic crystallization of these minerals. The biotites are enriched in Cr what can confirm metamorphic and metasomatic genesis of the pegmatites.

Key-words: muscovite, biotite, pegmatite, the Góry Sowie Mts, high-temperature crystallization

INTRODUCTION

Micas are the most common sheet silicates on Earth. Their specific structure enables to incorporate a large numbers of main and trace elements of different radii and charges. The concentration of some elements can be a sensitive indicator of physico-chemical environment in which a host rock crystallized. Hence, the composition of mica minerals usually bears an important imprint on petrogenetic processes.

The object of this study are dioctahedral and trioctahedral micas from the pegmatites of the Góry Sowie Mts. A special attention was paid to trace and main elements present in the structure of these minerals.

GEOLOGICAL SETTING

The Devonian gneiss formation of the Góry Sowie Mts (Van Breemen et al. 1988), extending among Łagiewniki, Srebrna Góra and Świdnica, is one of major structural elements of the Sudetes. This area was intersected in Tertiary by the Marginal Sudetic

[1] AGH, University of Science and Technology, Faculty of Geology, Geophysics and Environmental Protection, al. Mickiewicza 30, 30-059 Kraków, Poland.

fault into two fragments: the SW part of the Góry Sowie Mts range proper, and the NE, thrown down part comprising foreland of the Góry Sowie Mts. The region is almost entirely built of the oldest metamorphic formations represented by oligoclase-biotite paragneisses, migmatites (mixed gneisses) and orthogneisses occurring in the SE part of this area. Amphibolites, serpentinites, granulites, pegmatites and quartz veins are less frequent. The pegmatites occur as vein-, lens- or nest-shaped forms within the gneisses. It was suggested that numerous pegmatite small bodies occurring in gneisses and amphibolites are older than the nests and veins intersecting discordantly the structures of their country rocks (Smulikowski 1953). Probably, these pegmatites were formed as a result of partial melting (anatexis) of some rock components during migmatization processes (Kryza 1977; Pieczka 2000). The age of the Góry Sowie Mts pegmatites has been accepted as 370 ± 4 Ma (Van Breemen et al. 1988; *fide* Pieczka 2000).

For the identification and characterization of micas the pegmatites from Jedlinka Górna (GS/2M), Kolce-Walim (GS/3M), Osówka (GS/4M, GS/4B), Sokolec (GS/6M, GS/7M), an area next to Bystrzyckie lake (GS/10B, GS/10M, GS/13M, GS/13B), Zagórze Śląskie (GS/11B), Michałkowa (GS/14M, GS/14B) and Lutomia (GS/1M, GS/1B) were collected (Fig. 1).

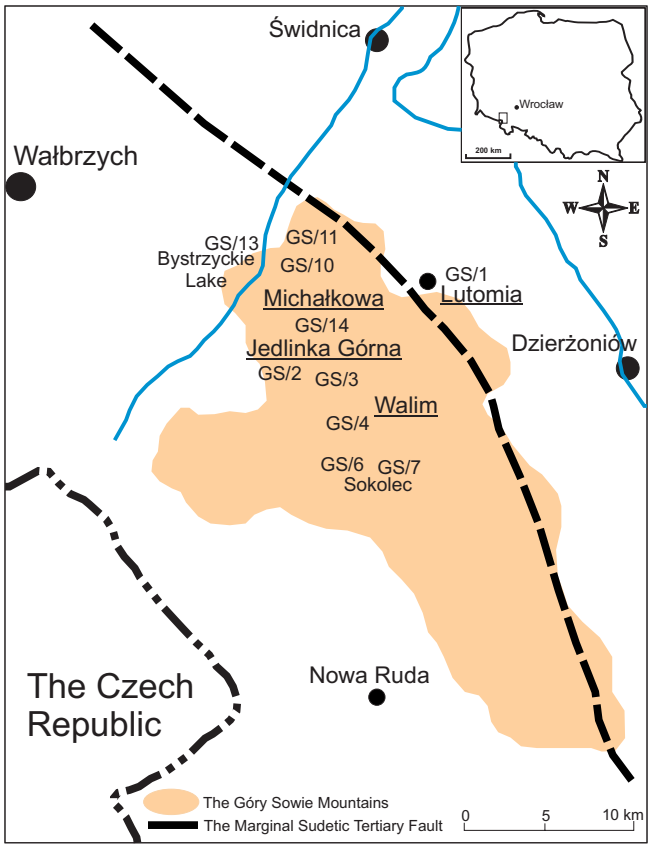


Fig. 1. The sketch map of the Góry Sowie Mts with sampling sites

EXPERIMENTAL METHODS

Micas were analysed using transmitting optical microscopy, chemical analyses, IR spectroscopy and X-ray diffractometry.

Chemical analyses were conducted at the Activation Laboratories Ltd in Ancaster, Ontario (Canada). Main components: SiO_2, TiO_2, Al_2O_3, Fe_2O_3, MnO, MgO, CaO, Na_2O, K_2O, P_2O_5, and some trace elements: Ba, Sr, Zr, Y, Be, V, Cu, Pb, Zn, Ag, Ni, Cd and Bi were analysed using ICP-AES. The analyses were made with ICP spectrometers (JARRELL ASH model Enviro and PERKIN ELMER model 6000). Over 20 other trace elements, including some REE, were determined using INAA. The irradiations were carried out in a 2 MW Pool Type reactor (neutron flux — 5×10^{11} ncm^{-2} s^{-1}) and further investigations with a Ge ORTEC and CANBERRA detector. Fluorine was analyzed with a Carl Zeiss Jena spectrophotometer. Absorbance was measured using a colorimeter (λ = 532 nm). The formula units of micas were calculated in relation to 22 oxygens.

Infrared spectra for the region 400–3700 cm^{-1} were recorded with a BIO-RAD model FTS-165 spectrophotometer. Monocrystals of mica flakes were pressed in the form of discs with KBr. The special attention was paid to the OH stretching region.

X-ray investigations were carried out on powdered, randomly oriented samples using a Philips X'PERT diffractometer with a graphite monochromator under the following operating conditions: CuKa radiation (λ = 1.53), scanning speed 0.02°(2θ)/1 sec., range 5–75°(2θ).

RESULTS AND DISCUSSION

The Góry Sowie Mts pegmatites are rather enriched in both dioctahedral and trioctahedral micas. The pegmatites, exhibiting non-complex mineral composition, consist mainly of feldspars, quartz, biotite, muscovite, hornblende, chlorite, titanite and opaque minerals. Zircon, apatite, cordierite, epidote, orthite, beryl and garnet occur in traces.

The microscope investigations of thin sections revealed that the muscovites are fresh while some biotites reveal chloritization. Strong, greenish-brown pleochroism of the biotites (GS/1B, GS/7) is probably associated with a considerable amount of Fe in the micas. Orange-brown pleochroism in some biotites (GS/10, GS/11B) is characteristic of micas rich in Ti (Deer et al. 1992).

In the X-ray patterns all basal reflections of dark micas correspond to 1M biotite and $2M_1$ phlogopite (GS/4B, GS/11B, GS/13B, GS/14B). The reflections of biotite--phlogopite solid solution almost completely coincide. In some X-ray patterns (GS/1B, GS/4B, GS/11B) also less intensive chlorite reflections are present (Fig. 2).

Both microscope and X-ray investigations confirm, therefore, the presence of chlorite in biotites samples.

In the IR absorption spectra of the micas there are strong bands of the Si-O and Al-O at 400–1200 cm^{-1}. However, particular attention was paid to the OH-stretching region at 3400–3700 cm^{-1}, because the location of the bands depend on chemical composition of micas (Vedder 1964).

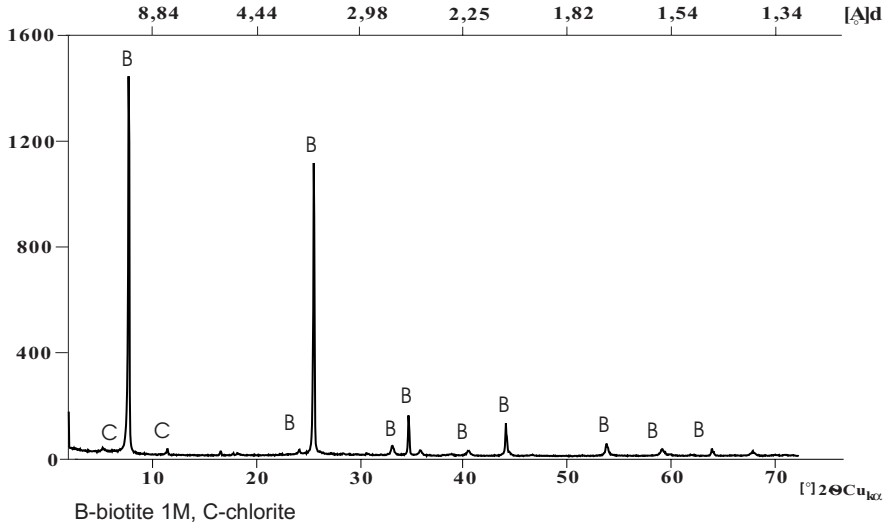


Fig. 2. X-ray pattern of trioctahedral mica from the Zagórze Śląskie pegmatite GS/11

In the IR spectrum of the muscovite from Michałkowa (GS/14M) the band of OH stretching vibrations is located at 3635 cm^{-1} (Fig. 3). The position of this band is caused by higher than average amount of Al at the octahedral sites. The band at 3312 cm^{-1} corresponds to the N-H stretching vibrations, while N-H bending vibrations are responsible for the location of the band at 1427 cm^{-1} (Bastoul et al. 1993). It indicates the presence of some ammonium ions in the muscovite structure, where NH_4^+ ion replaces K^+. The band at 1633 cm^{-1} is connected with the presence of molecular water (Fig. 4). Two weak bands of the biotite (GS/14B) at 1428 and 3267 cm^{-1} are caused by N-H

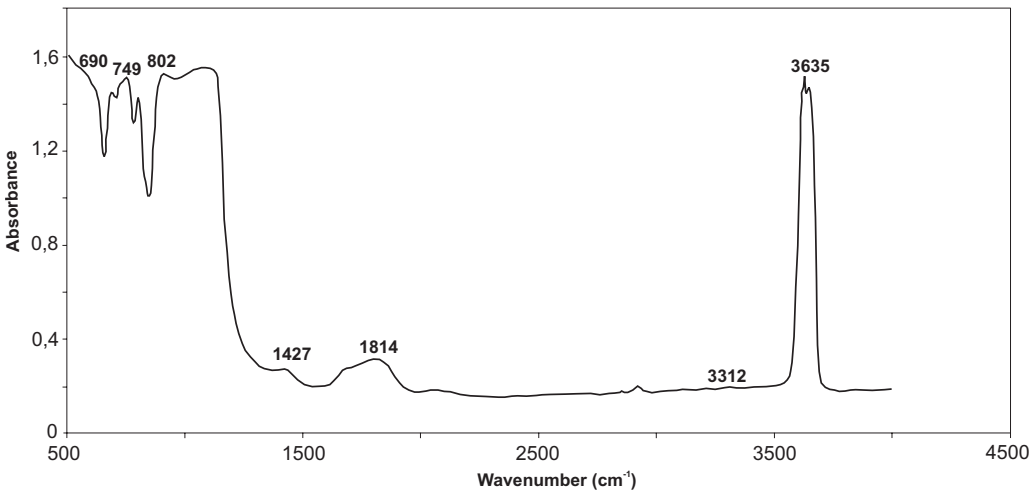


Fig. 3. The IR spectrum of muscovite from the Michałkowa pegmatite GS/14M

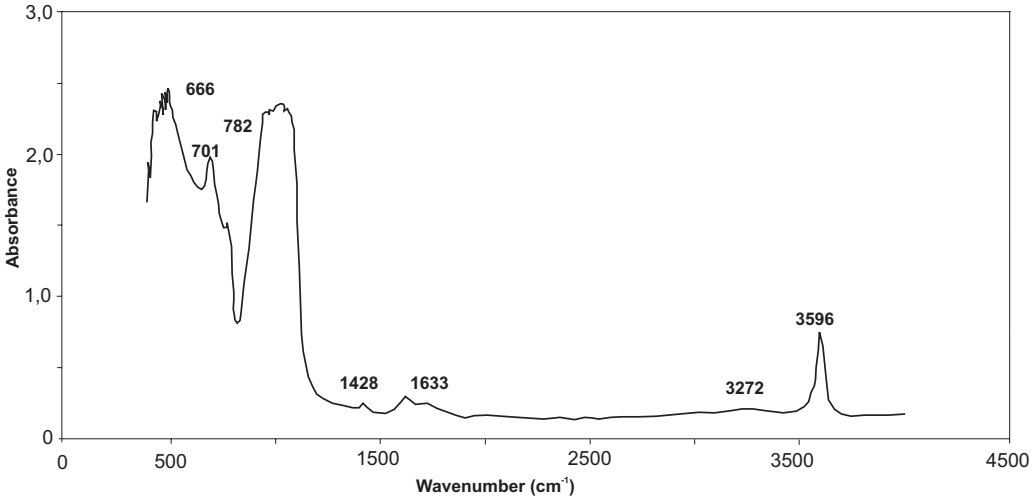


Fig. 4. The IR spectrum of biotite from the Michałkowa pegmatite GS/14B

vibrations. At 3596 cm^{-1} there is a sharp peak associated with OH stretching vibrations (Fig. 4). Location of this band points to the significant content of Fe at octahedral sites, as the higher Mg content of biotite, the higher is the position of the OH stretching band (Vedder 1964).

The main stress of the study put on geochemical analyses of muscovites and biotites from the Góry Sowie Mts pegmatites.

In the **dioctahedral micas** tetrahedral sites are occupied by Si and Al, while in the octahedral positions Al, Fe, Mg, Ti and Mn occur. The muscovite from Lutomia has the most significant amount of Al in the octahedral layer. Relatively high amount of K (1.5–1.7 atoms per formula unit) and traces of Na, Rb, Ba, Ca occur at the interlayer sites (Table 1).

Be accounts on average for 36 ppm in the muscovites from the Góry Sowie Mts pegmatites. Low concentrations of Cr and V are noted in these micas: up to 5 ppm of Cr and 10 ppm of V (Table 3). Similarly the muscovites are depleted of Ni, with the exception of the muscovite from Lutomia (GS/1) which possesses 23 ppm of this element. Co is other element rarely adopted by the muscovites.

Rb and Cs concentration increase with advancing crystallization of magmas. Moreover, Cs rapidly increases in good correlation with Li and F (Černy et al. 1985). An accumulation of these elements in the muscovites investigated is very low: Li content ranges from 9 ppm for GS/6M to 19 ppm for GS/1M, Rb from 96 ppm to 453 ppm, Cs from 4 ppm to 22 ppm and F from 0,08% to 0,19%.

The concentration of Sr in the muscovites ranges from 2 to 19 ppm. On the other hand, the white micas are relatively enriched in Ba, from 28 ppm (GS/14M) up to 1123 (GS/3M), 325 ppm on average. Ba in micas spans from extensive ranges in muscovites of the primitive pegmatites to very low amounts in lepidolite of complex pegmatites (Černy et al. 1985). It follows that the more Cs and Li the less Ba occurs in micas.

TABLE 1

Chemical formulae of the micas from the Góry Sowie Mts

Sample	Mica	Formula
GS/1M Lutomia	muscovite	$(K_{1.770}Na_{0.225}Ca_{0.003})(Al_{3.622}Fe^{3+}_{0.213}Mg_{0.139}Ti_{0.025}Mn_{0.002})$ $[Si_{6.098}Al_{1.899}P_{0.003}O_{20}]\ (OH)_2$
GS/2M Jedlinka G.	muscovite	$(K_{1.404}Na_{0.185}Rb_{0.004}Ca_{0.002})(Fe_{0.139}Mg_{0.094}Mn_{0.002})(Al_{2.539}Ti_{0.017})$ $[Al_{2.216}P_{0.002}Si_{5.782}O_{20}](OH)_2$
GS/3M Kolce	muscovite	$(K_{1.487}Na_{0.164}Ca_{0.008}Ba_{0.006}Rb_{0.002})(Fe_{0.172}Mg_{0.148}Mn_{0.003})$ $(Al_{2.278}Ti_{0.034})\ [Al_{2.572}P_{0.001}Si_{5.427}O_{20}](OH)_2$
GS/4M Osówka	muscovite	$(K_{1.481}Na_{0.156}Rb_{0.003}Ba_{0.002}Ca_{0.003})(Fe_{0.209}Mg_{0.161}Mn_{0.004})$ $(Al_{2.249}Ti_{0.03})\ [Al_{2.542}Si_{5.458}O_{20}](OH)_2$
GS/7M Sokolec	muscovite	$(K_{1.518}Na_{0.178}Ca_{0.009}Rb_{0.003}Ba_{0.001})(Fe_{0.134}Mg_{0.117}Mn_{0.003})$ $(Al_{2.36}Ti_{0.037})\ [Al_{2.578}P_{0.002}Si_{5.42}O_{20}](OH)_2$
GS/14M Michałkowa	muscovite	$(K_{1.552}Na_{0.2}Rb_{0.002})(Fe_{0.142}Mg_{0.097}Mn_{0.001})(Al_{2.403}Ti_{0.026})$ $[Al_{2.604}P_{0.004}Si_{5.392}O_{20}]\ (OH)_2$
GS/13B Bystrzyckie lake	biotite	$(K_{1.477}Ca_{0.118}Na_{0.113}Ba_{0.008}Rb_{0.003})(Fe_{2.073}Mg_{1.998}Mn_{0.02}Zn_{0.004})$ $(Al_{0.233}Ti_{0.35}Cr_{0.008}V_{0.06})\ [Al_{2.831}P_{0.02}Si_{5.149}O_{20}]\ (OH)_2$
GS/14B Michałkowa	biotite	$(K_{1.607}Na_{0.068}Ca_{0.012}Rb_{0.004}Ba_{0.005})(Fe_{2.62}Mg_{1.43}Mn_{0.035}Zn_{0.009})$ $(Al_{0.119}Ti_{0.838}\ V_{0.004}Cr_{0.002})\ [Al_{3.132}P_{0.002}Si_{4.866}O_{20}]\ (OH)_2$
GS/1B Lutomia	biotite	Due to the alteration process it was impossible to calculate the formula

The muscovites from Kolce-Walim (GS/3M) and Sokolec (GS/7M) pegmatites can be a good example of it.

Ti content in the muscovite ranges from 0.18 wt.% to 0.41 wt.%. The maximum TiO_2 contents are contained in Mg and Fe biotites, lowest TiO_2 is shown by the most Li-rich micas. It is generally known that TiO_2 content decreases with advancing crystallization. According to Puziewicz (1987) muscovite containing less than 0.30 wt.% of Ti was formed during the post-magmatic stage of crystallization. Hence, muscovites (GS/1M, GS/2M and GS/14M) probably crystallized later than the muscovites (GS/3M, GS/4M, GS/7M) which host a little higher concentration of TiO_2 (Table 2).

Tetrahedral sites of **trioctahedral micas** are mainly filled by Si and Al, P appears in traces. Fe, Mg, Ti, Al and Mn are largely dominant in the octahedral sites, while V, Cr and Zn show typically low concentrations. Interlayer sites are mainly filled with K and minor amounts of Na, Ca, Rb and Ba (Table 1).

Using molecular proportions, the chemical indices of alteration (CIA) (Nesbitt, Young 1982, *fide* Mongelli et al. 1996) were calculated for the biotites to be 70 (GS/1B),

TABLE 2

The content of major elements in the micas from pegmatites of the Góry Sowie Mts

Main elements [wt. %]	GS/1M	GS/1B	GS/2M	GS/3M	GS/4M	GS/7M	GS/13B	GS/14M	GS/14/B
SiO_2	45.23	33.62	47.91	44.88	45.5	44.95	36.34	44.93	33.48
Al_2O_3	34.77	19.07	33.43	34.03	33.89	34.75	18.35	35.4	18.98
TiO_2	0.24	4.02	0.18	0.37	0.33	0.41	3.28	0.28	3.51
Fe_2O_3	2.1	5.17	1.53	1.89	2.31	1.48	19.44	1.54	23.96
FeO		15.59							
MnO	0.01	0.32	0.02	0.025	0.03	0.03	0.16	0.01	0.28
MgO	0.69	8.36	0.52	0.82	0.9	0.65	9.46	0.54	6.6
CaO	0.02	1.72	0.18	0.06	0.02	0.07	0.78	*	0.08
Na_2O	0.86	0.23	0.79	0.7	0.67	0.76	0.41	0.86	0.24
K_2O	10.29	6.3	9.12	9.64	9.68	9.87	8.17	10.14	8.67
P_2O_5	0.03	0.03	0.02	0.01	*	0.02	0.17	0.04	0.02
H_2O^+	5.64	4.31	5.54	6.54	6.6	6.37	2.77	6.31	3.41
F	*	*	*	0.19	0.19	*	*	0.08	0.27
Total	99.90	100.45	99.24	99.15	100.13	99.36	99.34	100.12	99.51

* Not determined.

68 (GS/14B) and 66 (GS/13). The biotite from Lutomia (GS/1B) is slightly or moderately weathered, while the biotite from the Bystrzyckie lake (GS/13) is relatively fresh. It corresponds well to X-ray investigations. X-ray patterns of the biotites from Michałkowa (GS/14B) and the Bystrzyckie lake (GS/13B) have no chlorite reflections.

The biotite (GS/13B) hosts rather high content of Co (Table 3). Cobalt enrichment may be observed in micas formed during interaction of granitic/pegmatitic melt and metamorphic country rock (Tischendorf et al. 2001). The more Cr is present the more V occurs (Zawidzki 1971). The low concentration of Cr in biotite is associated with magmatic genesis of granitoid rocks, while the significant amount of this element shows metamorphic and metasomatic origin of the host rocks (Fröhlich 1960; *fide* Zawidzki 1971). Fairly high concentrations of V and Cr were detected in the biotites, the highest in the biotite (GS/13B): V-356 ppm, Cr-489 ppm.

There is very low content of Be in the biotites (1–3 ppm). Sachanbiński (1971) detected on average 5.5 ppm in biotites from the Góry Sowie Mts pegmatites.

TABLE 3

The content of trace elements in the micas from pegmatites of the Góry Sowie Mts

Trace elements [ppm]	GS/1M	GS/1B	GS/2M	GS/3M	GS/4M	GS/6M	GS/7M	GS/11B	GS/13B	GS/14M	GS/14/B
As	**	3	**	2	16	0.5	12	84	2	6	6
B	*	*	*	*	*	14	*	2	*	*	*
Ba	86	876	64	1123	434	27	217	1350	1350	28	718
Be	5	1	8	4	9	3	7	1	1	2	3
Bi	*	*	**	16	**	1.5	**	0.2	**	**	5
Cd	**	1.9	**	**	**	**	**	0.2	0.4	**	**
Ce	**	14	2	2	1	1	2	14.2	5	**	2
Co	2	28	1	3	4	0.2	2	39.5	62	3	42
Cr	**	120	3.5	4.5	1.5	1	**	134	489	5	138
Cs	7.5	19.5	11	4.5	11.7	22.6	13.5	22	21	9.2	47
Cu	4	**	33	30	144	5.5	16	9.6	130	30	35
Ga	*	*	*	*	*	21.5	*	24.4	*	*	*
Hf	1	1.5	0.5	**	0.5	**	**	0.2	1.1	**	0.8
La	**	5.5	1	1	0.5	**	0.8	6	2	0.5	1.6
Li	19	116	*	*	*	9	*	129	*	*	*
Lu	**	0.5	0.1	0.02	0.2	**	0.1	0.2	0.06	0.03	0.1
Nb	*	*	*	*	*	2	*	4.6	*	*	*
Nd	*	*	**	**	**	0.1	**	10	3	**	1
Ni	23	30	**	**	4	0.5	**	78.4	161	3	57
Pb	*	*	**	11	17	4.5	3	7.2	18	11	59
Rb	453	335	429	223	305	96.5	306	326	344	273	400
S	*	*	10	10	10	30	**	60	180	20	230
Sc	55	83	9.5	32.5	23.5	*	35	*	39	79	54
Sm	**	1.1	0.2	0.2	0.2	**	0.2	3	0.8	0.2	0.4
Sn	*	*	*	*	*	31.4	*	11	*	*	*
Sr	5	14	6	19	9	1	10	2	21	2	4
Ta	4	7	5	2	4.5	0.05	4.4	**	3.6	4.2	9
Th	0.5	1.5	0.5	0.1	0.2	**	0.1	0.5	**	0.6	**
Tl	*	*	*	*	*	0.5	*	2.5	*	*	*
U	**	5	0.5	**	1.5	**	2	1.5	0.6	0.6	1
V	5	312	**	10	9	2	11	232	356	**	233
W	40	**	14	25	12	3	27	1	3	33	4
Y	3	14	2	**	22	0.1	3	16.4	11	1	5
Zn	79	524	53	39	58	14	37	369	326	43	666
Zr	21	33	13	11	18	0.4	1	5	49	5	14

GS/6. GS/11 — semi-quantitative analysis;
* Not determined;
** Not detected.

The relatively high content of Na is observed in the biotite from Lutomia (GS/1B). Chloritized biotite is enriched in Na and depleted of LREE and Th (Mongelli et al. 1996). The biotites are rather depleted of Th and LREE.

Strontium is enriched in late fractions relative to Ca, although the concentrations of both elements decrease. The biotites possess rather low content of Sr.

The biotites host low concentrations of Li, Cs and F which indicate these minerals were formed probably in early stage of post-magmatic crystallization.

Generally, dioctahedral micas show lower content of trace elements than coexisting biotites. Sn and W are the exception of this rule (Neves 1997). Here, W also shows clear preference for the muscovites. This element ranges from 12 ppm to 40 ppm in the muscovites and from 1 ppm to 4 ppm in the biotites.

According to Zawidzki (1971), Cr and V generally show preference for muscovite. Here, the biotites (GS/1B, GS/14B) host more content of these elements than coexisting muscovites (GS/1M, GS/14M).

The K/Rb ratio increases in the sequence biotite-muscovite (Černy et al. 1985). It is consistent with authors' observations (GS/1M = 213, GS/1B = 174, GS/14M = 280 and GS/14B = 180).

Sr and Ba show preference for muscovite (Zawidzki 1971). However these elements, especially Ba, are highly concentrated in the biotites than in the coexisting muscovites from the Góry Sowie Mts pegmatites (Table 3).

Ta-bearing complexes are stable at low temperature (Černy et al. 1985), accordingly the micas of the Góry Sowie Mts pegmatites host only traces of Ta.

Not all detected trace elements were used for mica genesis interpretation. However, it is scientific documentation and can be used by other authors concerned with similar problems. Trace elements: Eu, In, Sb, Se, Tb, Te, Yb were detected, but their concentration is below 1 ppm, therefore they were not included in the Table 3.

CONCLUSIONS

The micas from the Góry Sowie Mts pegmatites host very low concentration of F, Rb, Cs, Li, Sn, REE and Ta. The impoverishment in these elements indicate early post--magmatic crystallization. High-temperature genesis of the micas may also be confirmed by a high content of Ba. The Sr/Ba ratio increases with advancing crystallization. The low Sr/Ba ratio in the biotites (0.01–0.001) also indicates early crystallization of the micas. High concentrations of Cr in the biotites may confirm anatectic genesis of the Góry Sowie Mts pegmatites. Pegmatitic veins occur within metamorphic rocks. The biotites depleted of REE are characteristic of primitive pegmatites. Mineralogical and geochemical investigations of the micas from the Góry Sowie Mts confirm that the minerals represent an early stage of post-magmatic crystallization.

Concentration of Ti in the muscovites confirms the post-magmatic genesis of the host rocks (pegmatite). Relatively simple mineral composition, characteristic of primitive pegmatites, may confirm relatively high-temperature crystallization of the rocks.

Acknowledgements. Prof. Witold Żabiński is thanked for his support and valuable comments on a previous version of the paper. I also acknowledge the help of dr Andrzej Skowroński in final preparation of the manuscript.

REFERENCES

BASTOUL A.M., PIRONON J., MOSBAH M., DUBOIS M., CUNEY M., 1993: In–situ analysis of nitrogen in minerals. *Eur. J. Miner*. 5, 233–243.

ČERNY P., MEINTZER R.E., ANDERSON A.J., 1985: Extreme fractionation in rare-element granitic pegmatites: selected examples of data and mechanisms. *Canad. Miner*. 23, 381–421.

DEER W.A., HOWIE R.A., ZUSSMAN J., 1992: An introduction to the rock forming minerals. Longman.

KRYZA R., 1977: Pegmatyt z kordierytem w serpentynitach okolic Lubachowa (Góry Sowie) (in Polish, English summary). *Rocznik PTG* 47, 2, 247–263.

MONGELLI G., DINELLI E., TETEO F., ACQUAFREDDA P., ROTTURA A., 1996: Weathered biotites from granitoids: the fractionation of REE, Th and transition elements and the role of accessory and secondary phases. *Miner. Petrogr. Acta*. 39. 77–93.

NEVES L.J.P.F. 1997: Trace element content and partitioning between biotite and muscovite of granitic rocks: a study in the Viseu region (Central Portugal). *Eur. J. Miner*. 9, 849–857.

PIECZKA A., 2000: A rare mineral-bearing pegmatite from the Szklary serpentinite massif, the Fore–Sudetic block, SW Poland. *Geol. Sudet*. 33, 23–31.

PUZIEWICZ J., 1987: Geneza muskowitu w granicie dwułyszczykowym z Siedlimowic i jego enklawach (in Polish, English summary). *Arch. Miner*. 43, 1, 81–85.

SACHANBIŃSKI M., 1971: Geochemia berylu w skałach krystalicznych Gór Sowich (in Polish). *Prace Nauk. Inst. Chemii Nieorganicznej i Metalurgii Pierwiastków Rzadkich Politechniki Wrocławskiej*. 3, 177–187.

SMULIKOWSKI K., 1953: Uwagi o starokrystalicznych formacjach Sudetów (in Polish). *Rocznik PTG* 21,1.

TISCHENDORF G., FÖRSTER H-J., GOTTESMANN B., 2001: Minor- and trace-element composition of trioctahedral micas: a review. *Miner. Mag*. 65, 2, 249– 276.

VAN BREEMEN O., BOWES D. R., AFTALION M., ŻELAŹNIEWICZ A., 1988: Devonian tectonothermal activity in the Sowie Góry gneissic block, Sudetes, southwestern Poland: evidence from Rb-Sr and U-Pb isotopic studies. *Ann. Soc. Geol. Pol*. 58, 3–19.

VEDDER W., 1964: Correlations between infrared spectrum and chemical compositions of micas. *Amer. Miner*. 49, 736–768.

ZAWIDZKI P., 1971: Pierwiastki śladowe w łyszczykach gnejsów Gór Sowich. (in Polish, English summary). *Arch. Miner*. 29, 1–2.

Magdalena DUMAŃSKA-SŁOWIK

BADANIA MINERALOGICZNE I GEOCHEMICZNE MIK Z PEGMATYTÓW GÓR SOWICH

Streszczenie

Minerały grupy mik pochodzące z pegmatytów Gór Sowich zostały poddane badaniom mikroskopowym, rentgenowskim, spektroskopowym w podczerwieni i chemicznym. Określono zawartości w nich pierwiastków głównych, pobocznych i śladowych. Miki są bardzo czułymi wskaźnikami procesów petrogenetycznych, dlatego też analiza składu chemicznego tych minerałów pozwala przybliżyć warunki fizykochemiczne środowiska powstania skały macierzystej. Zubożenie mik w pierwiastki takie jak F, Rb, Cs, Li, Sn i REE, a wzbogacenie w Ba przemawia za wczesną, wysokotemperaturową krystalizacją pomagmową. Podwyższona koncentracja Cr w biotytach sowiogórskich może być związana z metamorficznym otoczeniem pegmatytów z Gór Sowich.

MINERALOGIA POLONICA
Vol. 35, No 2, 2004
PL ISSN 0032-6267

Bartosz BUDZYŃ[1], *Maciej MANECKI*[2], *David A. SCHNEIDER*[3]

CONSTRAINTS ON P-T CONDITIONS OF HIGH-GRADE METAMORPHISM IN THE GÓRY SOWIE MTS, WEST SUDETES

A b s t r a c t . P-T conditions of metamorphism that affected the Góry Sowie Mts gneisses (West Sudetes, SW Poland) were determined with use of garnet-biotite (GB) and muscovite-biotite (MB) geothermometry, and muscovite geobarometry on selected rocks. Granulite and sillimanite-bearing layered gneiss from the Bystrzyckie Lake region (northern part of the Góry Sowie Mts) revealed GB temperatures 652 ± 35°C. To the south, layered gneiss and metapegmatite from the Przygórze area yielded similar GB temperatures (660 ± 28°C), lower MB temperatures (613 ± 25°C) and pressures 6.4 ± 1.4 kbar. In the central part of the massif, finely laminated gneiss and diatexite from the Potoczek region revealed MB temperatures 596 ± 24°C and pressures 5.2 ± 0.7 kbar. A similar temperature (600 ± 25°C) was obtained out of a flaser gneiss from the Kietlice region in the Fore-Sudetic part of the Góry Sowie Block. Differences between GB and MB results might be related to different speed of ion diffusion between coexisting minerals. We suggest that reported data are related to initial midcrustal exhumation and coeval amphibolite facies metamorphism.

Key-words: geothermobarometry, gneisses, granulites, Góry Sowie Mts, Bohemian Massif, West Sudetes

INTRODUCTION

The Góry Sowie Block, located in SW Poland, is an allochtonous terrane that underwent a polyphase thermal evolution (e.g. Żelaźniewicz 1987, 1990). Metamorphic assemblages preserved within the massif include granulite and metabasite units enveloped by a widespread amphibolite-facies matrix. Previous authors have described thermal and barometric histories of the Góry Sowie; however estimates of the conditions of metamorphism that affected main rock types — gneisses and migmatites — were based mainly on the presence of mineral paragenesis in these rocks and structural investigations (e.g. Kryza 1981; Żelaźniewicz 1987, 1990). Quantitative methods were

[1] Jagiellonian University, Institute of Geological Sciences, ul. Oleandry 2a, 30-063 Kraków, Poland; e-mail: budzyn@geos.ing.uj.edu.pl

[2] AGH, University of Science and Technology, Faculty of Geology, Geophysics and Environment Protection, al. Mickiewicza 30, 30-059 Kraków, Poland; e-mail: gpmmanec@cyf-kr.edu.pl

[3] Ohio University, Department of Geological Sciences, Clippinger Laboratories 316, Athens, OH, U.S.A.; e-mail: schneidd@ohio.edu

selectively used mainly to determine metamorphic conditions of metabasites and granulites (e.g. Kryza et al. 1996; O'Brien et al. 1997). Geothermobarometry (e.g. garnet--biotite geothermometry and garnet — Al_2SiO_5 — plagioclase geobarometry) was also used to determine P-T conditions of metamorphism that affected migmatitic gneisses, which enclose metabasites (e.g. Kryza, Pin 1998, 2002). These results indicate that migmatitic gneisses were metamorphosed in peak of metamorphism conditions of 825–875°C and 9.5–11 kbar (Kryza, Pin 1998, 2002). In this paper we report new results from thermobarometric analyses on selected rocks from the Góry Sowie, obtained with use of garnet-biotite and muscovite-biotite geothermometry, and muscovite geobarometry.

GEOLOGICAL BACKGROUND

The Góry Sowie Block — located in West Sudetes, SW Poland — is divided by NW-SE trending Sudetic Marginal Fault into two portions: the Góry Sowie Mts. and the Fore-Sudetic Block (Fig. 1). Paragneisses and migmatites are dominant rock types within this metamorphic complex, with minor amounts of granulites, metabasites, eclogites, peridotites and calc-silicate rocks (e.g. Kryza 1981; Żelaźniewicz 1987, 1990).

The typical composition of gneisses and migmatites is quartz, oligoclase and biotite, with additional sillimanite, muscovite, K-feldspar or cordierite occurring as index minerals. Secondary minerals distinguished are: garnet, kyanite, apatite, zircon, monazite and iron oxides. Most gneisses are interpreted as metamorphosed greywackes and various pelitic-psamitic rocks (e.g. Kryza 1981; Żelaźniewicz 1987). As an alternative, Kröner and Hegner (1998) proposed that many gneisses have a magmatic protolith, as illustrated by zircon geochronology.

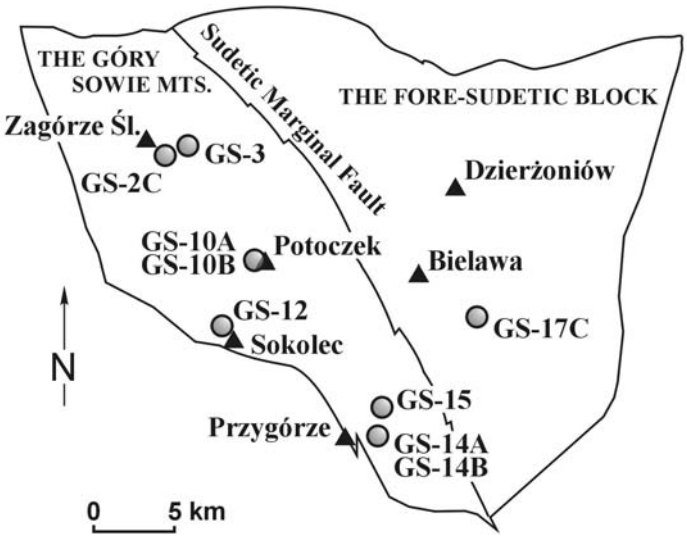


Fig. 1. Sketch of the Góry Sowie Block with sampling locations (modified after Budzyń et al. 2004)

Granulites occur in three close locations in the Bystrzyca Górna–Zagórze Śląskie region (N part of the massif) and are associated with mantle-derived peridotites. A fourth location of granulite occurrence is in the Sieniawka area (NE part of the Góry Sowie Block). Granulites are composed of quartz, plagioclase, garnet, kyanite, rutile and retrogressed micas (biotite and muscovite). Present position of granulites and peridotites is interpreted as a result of tectonic movements that incorporated these rocks into the Góry Sowie gneisses during initial exhumation into the midcrust (e.g. Żelaźniewicz 1985).

Amphibolites usually occur as fine and thin lenses within gneisses (e.g. Żelaźniewicz 1995) and are distinguished by a mineral composition of: hornblende, biotite, plagioclase (andesine-labradore), garnet, pyroxene and — rarely — quartz (Żelaźniewicz 1987). Less common amphibolites with quartz are likely metamorphosed tuffs (Żelaźniewicz 1995). The remaining amphibolite varieties represents mafic rocks and their origin might be related to fractionation of mantle material, which intruded during midcrustal (10–12 km) deformation (Dziedzicowa 1994; *fide* Żelaźniewicz 1995).

SAMPLE SELECTION AND METHODS OF INVESTIGATION

During standard petrographic investigations the suitability of 31 collected samples for geothermobarometric analyses was determined. The highest priority during sample selection was the presence of non-retrogressed garnet-biotite and/or muscovite-biotite pairs, which could register maximum temperatures and/or pressures of metamorphism during amphibolite-facies conditions. As a result of these restrictions eight samples from four regions within the Góry Sowie were selected. Additionally, one sample from the Kietlice region (Fore-Sudetic part of the Góry Sowie Block) was chosen.

Chemical determinations and XRD analyses

Mineral chemistry analyses were performed on a JEOL JXA-50A electron microprobe at the Department of Mineralogy, Petrography and Geochemistry, AGH, Kraków, using silicate and oxide mineral standards. Operating conditions were as follows: accelerating voltage 15 kV, beam current 20 nA, counting time 40 seconds and the beam diameter of 2–5 μm focused on the polished thin section coated with carbon. Twenty--five mineral grains from 9 samples were analysed in 44 spots.

Back-scattered electron images, as well as EDS analyses along garnet traverses, were obtained in the Laboratory of Field Emission Scanning Electron Microscopy and Microanalysis at the Institute of Geological Sciences of the Jagiellonian University, Kraków.

Four samples were chosen for geobarometric XRD analyses using the methodology suggested by Sassi and Scolari (1974). Each rock slice remaining from thin section preparation was polished to obtain a smooth surface perpendicular to the foliation. The $d_{060,\ 33\bar{1}}$ muscovite spacing was measured with use of a Phillips X'Pert diffractometer. A pattern was recorded in the range of 59–63° 2Θ (CuK_α radiation). Quartz present in the rock matrix was used as an internal standard.

Geothermobarometric methods

Three quantitative methods were chosen to determine P-T conditions of metamorphism: garnet-biotite and muscovite-biotite geothermometers, and muscovite geobarometer.

Garnet-biotite geothermometer

Garnet-biotite Fe-Mg exchange geothermometer is one of the most widely used methods for middle-upper amphibolite-facies rocks. This method is based on the reaction:

$$Fe_3Al_2[SiO_4]_3 + KMg_3[(F,OH)_2 \mid AlSi_3O_{10}] = Mg_3Al_2[SiO_4]_3 + KFe_3[(OH)_2 \mid AlSi_3O_{10}]$$

almandine phlogopite pyrope annite

Various calibrations of garnet-biotite geothermometer were tested, including Ferry and Spear (1978), Hodges and Spear (1982), Perchuk and Lavrent'eva (1983), Dasgupta et al. (1991), Bhattacharya et al. (1992) and Holdaway (2000). Maximum differences between temperatures obtained for one sample with use of these calibrations were up to ca. 220°C. Previously (e.g. Gordon et al. 2003; Budzyń et al. 2004) we reported data determined using Bhattacharya's et al. (1992) garnet-biotite geothermometer with Hackler and Wood's (1989) mixing parameters. In this paper we propose use of Holdaway's (2000) garnet-biotite geothermometer, which also takes into account assumed Fe^{3+} values of biotite (11.6%) and garnet (3%) based on the Mössbauer analyses of Dyar (1990) and Guidotti and Dyar (1991). This calibration of garnet-biotite geothermometer is probably the best one currently available (for more details see Holdaway 2000, 2004). A program (GB, the Garnet-Biotite Geothermometer by Holdaway) was used to calculate temperatures of garnet-biotite pairs from their chemical analyses. Average volume Margules parameters of Ganguly et al. (1996), Berman and Aranovich (1996), and Mudhopadhyay et al. (1997) for garnet were used. Taking into consideration ferric iron in the structure of minerals we obtained lower garnet-biotite temperatures by about 10–15°C.

During selection of garnet-biotite pairs for analyses crystallographic orientation of biotite was considered. As a result of that, coexisting minerals with low Θ (the angle between the normal to biotite (001) plane and the interface with garnet) were selected. Chosen analyzed spots in garnet-biotite pairs were close to mineral contact (spot distance within the range 60–120 μm). Temperatures were calculated in combination with muscovite geobarometer, with three exceptions (samples GS-2C, GS-3 and GS-17C), where temperatures were calculated for P = 5 kbar.

Muscovite-biotite geothermometer

The second method chosen for temperature estimations is muscovite-biotite geothermometer (Hoisch 1989) based on exchange reaction:

$$KMg_3[(F,OH)_2 \mid AlSi_3O_{10}] + KAl_2[(OH,F)_2 \mid AlSi_3O_{10}] =$$

phlogopite muscovite

$$= K(MgAl)[(OH)_2 \mid Si_4O_{10}] + K(Mg_2Al)[(OH)_2 \mid Al_2Si_2O_{10}]$$

celadonite eastonite

Analytical spots were located close to contact between minerals (spot distance within the range 60–100 μm). Temperatures were calculated in combination with muscovite geobarometer, except samples GS-12 and GS-15, where temperatures were calculated for P = 5 kbar.

Muscovite geobarometer

Ramírez and Sassi's (2001) muscovite geobarometer was chosen to determine maximum pressures of metamorphism. This method is based on changes of the muscovite $d_{060,33\bar{1}}$ cell dimension, which monitors the baric conditions of metamorphism. These changes are result of the increasing celadonite substitution related to a pressure increase. During XRD analyses, analytical procedure was repeated five times for GS-14A and three times for GS-14B to estimate analytical error.

RESULTS

Mineral chemistry and XRD results

Microanalyses were concentrated on rim values of minerals chosen for geothermometric calculations. In four selected samples (sillimanite-bearing layered gneiss GS-2C; layered gneiss GS-14A; metapegmatite GS-14B; flaser gneiss GS-17C) garnets form subhedral to anhedral blasts, up to *ca* 2 mm in diameter. Some of them contain biotite or quartz inclusions. These garnets — in which crystallization took place during progressive, amphibolite-facies metamorphism — are represented by almandine (Table 1). They have composition of $Alm_{0.61–0.76}Spess_{0.05–0.22}Py_{0.08–0.17}Gross_{0.03–0.10}$. In contrast, one sample (granulite GS-3) contains garnets with retrogressive features. Some of these grains have reaction coronas that emerged during retrogression in the contact with rutile, plagioclase or micas. Quartz, plagioclase, biotite and rutile occur as inclusions. Garnet rim and core compositions in this sample are $Alm_{0.49–0.55}$ $Spess_{0.02}Py_{0.31–0.39}Gross_{0.08–0.12}$ and $Alm_{0.48–0.53}Spess_{0.02}$ $Py_{0.30–0.36}Gross_{0.11–0.15}$ respectively.

A biotite population that should achieve chemical composition in equilibrium with garnets during maximum temperatures of metamorphism was chosen for analyses. Chemical compositions in mica grains free of chlorite or muscovite interlayers were analysed. Biotite has an Fe/(Fe+Mg) ratio of 0.52–0.66 with two values out of this range:

TABLE 1

Selected analyses of garnets

Component [wt. %]	GS-2C Grt 2	GS-2C Grt 3	GS-2C Grt 7	GS-2C Grt 8	GS-3 Grt 1	GS-14A	GS-14B	GS-17C
SiO_2	39.36	39.67	38.12	39.40	41.47	38.46	37.88	39.64
Al_2O_3	21.39	20.63	20.75	20.88	23.17	20.59	20.32	21.71
TiO_2	0.22	0.22	0.23	0.22	0.24	0.27	0.25	0.24
FeO	32.81	32.15	32.71	32.11	24.13	29.90	26.64	30.40
MgO	2.42	2.75	2.50	2.78	7.55	2.11	2.26	4.36
MnO	4.59	4.66	4.97	4.61	1.05	7.78	9.35	2.05
CaO	1.61	1.96	1.14	0.91	4.10	2.84	2.61	3.40
Total	102.40	102.04	100.41	100.90	101.71	101.96	99.32	101.80
Number of cations*								
Si	3.08	3.11	3.05	3.11	3.09	3.05	3.06	3.06
Al	1.97	1.91	1.96	1.94	2.04	1.92	1.90	1.98
Ti	0.01	0.01	0.01	0.01	0.01	0.02	0.02	0.01
Fe	2.15	2.11	2.19	2.12	1.50	1.98	1.80	1.96
Mg	0.28	0.32	0.30	0.33	0.84	0.25	0.27	0.50
Mn	0.30	0.31	0.34	0.31	0.07	0.52	0.64	0.13
Ca	0.13	0.16	0.10	0.08	0.33	0.24	0.23	0.28
Total	7.93	7.93	7.95	7.90	7.88	7.98	7.95	7.94
Fe/(Fe+Mg)	0.88	0.87	0.88	0.87	0.64	0.89	0.87	0.80
Content of end members								
X_{Py}	0.10	0.11	0.10	0.12	0.31	0.08	0.09	0.17
X_{Alm}	0.75	0.73	0.75	0.75	0.55	0.66	0.61	0.68
X_{Gross}	0.05	0.06	0.03	0.03	0.12	0.08	0.08	0.10
X_{Spess}	0.11	0.11	0.12	0.11	0.02	0.17	0.22	0.05

* Number of cations on the basis of 12 oxygen atoms; total Fe = Fe^{2+}.

0.28 (sample GS-3) and 0.39 (sample GS-17C) (Table 2). Mica compositions for muscovite-biotite geothermometry are presented in Table 3. Analytical XRD results document muscovite b_0 values within the range 8.9988–8.9994 Å (Table 4).

TABLE 2

Selected analyses of selected biotites (Bt) and muscovites (Mu)

Composition [wt. %]	GS-2C Bt 2	GS-3 Bt	GS-10A Bt	GS-10A Mu	GS-14A Bt 1	GS-14A Bt 2	GS-14A Mu	GS-14B Bt 1
SiO_2	37.06	38.51	38.11	46.91	37.60	38.65	46.27	37.99
Al_2O_3	20.81	19.14	19.74	38.64	17.04	18.29	35.34	18.35
TiO_2	2.92	4.67	3.40	0.19	3.17	2.80	1.36	2.09
FeO	19.55	9.55	19.89	1.44	22.77	20.20	2.12	19.28
MgO	7.04	13.75	8.17	0.66	7.67	8.60	0.75	7.57
K_2O	9.14	9.20	9.11	9.18	10.31	10.66	11.04	9.60
Na_2O	n.a.	n.a.	n.a.	0.64	n.a.	n.a.	1.96	n.a.
Total	96.53	94.82	98.44	97.65	98.57	99.21	98.85	94.87
Number of cations*								
Si	2.76	2.78	2.78	3.02	2.81	2.83	3.01	2.88
Al	1.82	1.63	1.70	2.93	1.50	1.58	2.71	1.64
Ti	0.16	0.25	0.19	0.01	0.18	0.15	0.07	0.12
Fe	1.22	0.58	1.21	0.08	1.42	1.24	0.12	1.22
Mg	0.78	1.48	0.89	0.06	0.86	0.94	0.07	0.86
K	0.87	0.85	0.85	0.75	0.98	1.00	0.92	0.93
Na	n.a.	n.a.	n.a.	0.08	n.a.	n.a.	0.25	n.a.
Total	7.60	7.57	7.61	6.93	7.75	7.73	7.15	7.65
Fe/(Fe+Mg)	0.61	0.28	0.58	0.55	0.62	0.57	0.61	0.59

* Number of cations on the basis of 11 oxygen atoms; total Fe = Fe^{2+}; n.a. — not analyzed.

TABLE 3

Compositions of analyzed micas for muscovite-biotite geothermometry

Sample symbol	K^{ideal}_{R1}	$X^B_{Mg} - X^B_{[6]Al}$	X^B_{Mg}	$X^B_{[6]Al}$	X^B_{Ti}	X^B_{Fe}	X^M_{Mg}
GS-10A	0.474 ↑	0.138 ↓	0.296 ↓	0.158	0.062	0.404	0.032
GS-10B	0.436	0.152 ↓	0.287 ↓	0.135	0.068	0.436	0.032
GS-12	0.624 ↑	0.122 ↓	0.257 ↓	0.135	0.044	0.495 ↑	0.040
ght GS-14A	0.499 ↑	0.178	0.313 ↓	0.135	0.051	0.412	0.037
GS-14B	0.400	0.238	0.362	0.124	0.049	0.393	0.040
GS-15	0.695 ↑	0.151 ↓	0.259 ↓	0.108	0.073	0.470 ↑	0.054 ↑

Explanations of symbols: $K^{ideal}_{R1} = X_{cel}X_{eas} / X_{phl}X_{ms}$; $X^M_{Mg} = Mg/2$;

$X^M_{[6]Al} = (Al + Si - 4)/2$; $X^B_{Mg} = Mg/3$; $X^B_{[6]Al} = (Al + Si - 4)/3$; $X^B_{Fe} = Fe/3$; $X^B_{Ti} = Ti/3$ (for more details see Hoisch 1989); ↑ — data higher than range given by Hoisch (1989);

↓ — data lower than range given by Hoisch (1989).

TABLE 4

X-ray diffractometry results

Sample symbol	GS-10A	GS-10B	GS-14A (1)	GS-14A (2)	GS-14A (3)
$d_{060,33\bar{1}}$ [Å]	1.4991	1.4990	1.4999	1.4999	1.4998
$b_0 = 6 \cdot d_{060,33\bar{1}}$ [Å]	8.9946	8.9940	8.9994	8.9994	8.9988
Sample symbol	GS-14A (4)	GS-14A (5)	GS-14B (1)	GS-14B (2)	GS-14B (3)
$d_{060,33\bar{1}}$ [Å]	1.4991	1.4994	1.4994	1.4991	1.4988
$b_0 = 6 \cdot d_{060,33\bar{1}}$ [Å]	8.9946	8.9964	8.9964	8.9946	8.9928

Geothermobarometry results

In the northern part of the Góry Sowie Mts, samples (GS-2C and GS-3) revealed temperatures of ca. 652 ± 35°C (Table 5; Fig. 2). Point analyses along traverse in garnet from granulite (GS-3) allowed us to ascertain slight zonation with a retrogressive rim (Fig. 3 and 4). However, this zonation is probably related to ion diffusion between the garnet and inclusions. Two samples (GS-14A and GS-14B) from the Przygórze area yielded

TABLE 5

Temperatures and pressures yielded by analyzed samples

Sample symbol	Rock type	Method		
		Grt-Bt	Mu-Bt	Mu
		T [°C]	T [°C]	P [kbar]
GS-2C	sillimanite-bearing layered gneiss	652 ± 35	—	—
GS-3	granulite	646 ± 25	—	—
GS-10A	diatexite	—	594 ± 22	5.2 ± 0.7
GS-10B	finely laminated gneiss	—	597 ± 22	5.2 ± 0.7
GS-12	flaser gneiss	—	*635 ± 22*	—
GS-14A	layered gneiss	657 ± 25	610 ± 22	6.6 ± 1.2
GS-14B	metapegmatite	662 ± 25	615 ± 22	6.2 ± 1.2
GS-15	flaser gneiss	—	*712 ± 22*	—
GS-17C	flaser gneiss	600 ± 25	—	—

Grt-Bt — garnet-biotite geothermometer (Holdaway 2000); Mu-Bt — muscovite-biotite geothermometer (Hoisch 1989); Mu — muscovite geobarometer (Ramírez and Sassi 2001); *Italic* — data with questioned reliability (explanation in text).

similar results of garnet-biotite geothermometry (660 ± 28°C) and pressures 6.4 ± 1.4 kbar. These samples revealed lower temperatures (613 ± 25°C) with use of muscovite-biotite geothermometry. In the central part of the Góry Sowie temperatures of 596 ± 24°C and

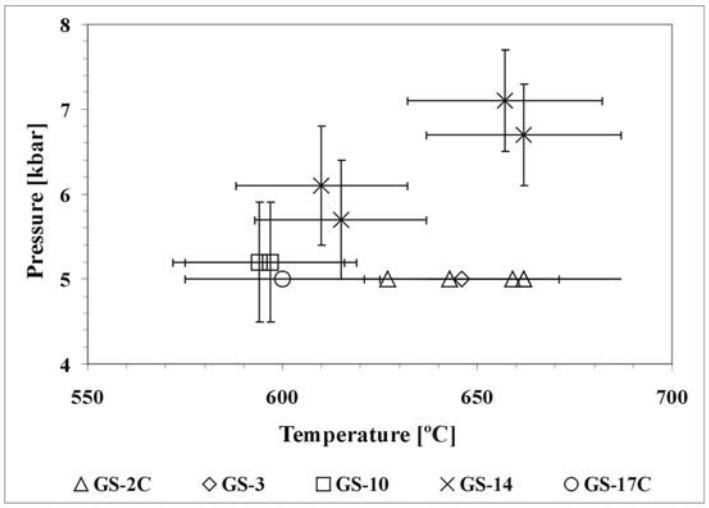


Fig. 2. Results of P-T determinations obtained with use of garnet-biotite geothermometry, muscovite-biotite geothermometry and muscovite geobarometry

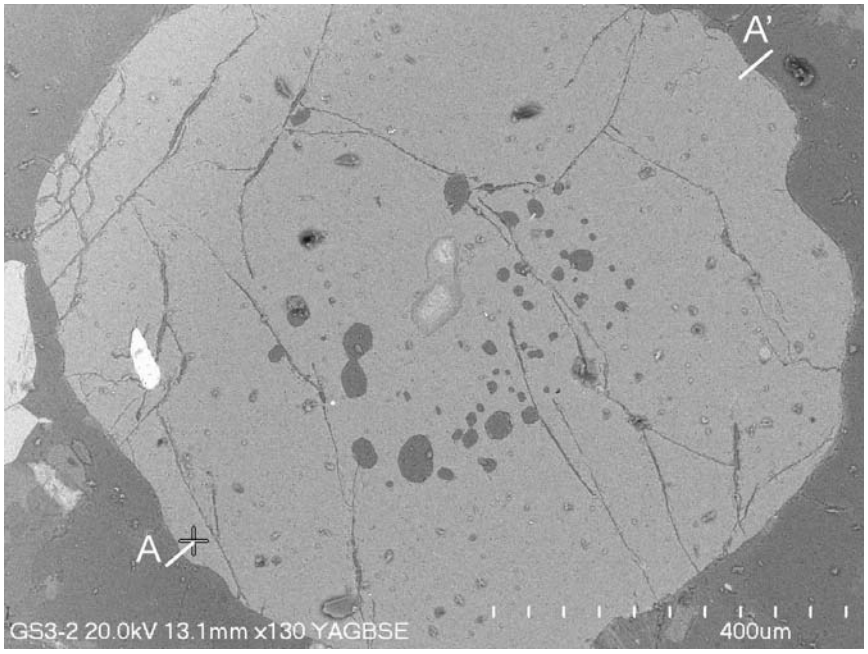


Fig. 3. Backscattered electron image showing garnet from the granulite (GS-3). Profile along traverse A-A′ is shown at Fig. 4

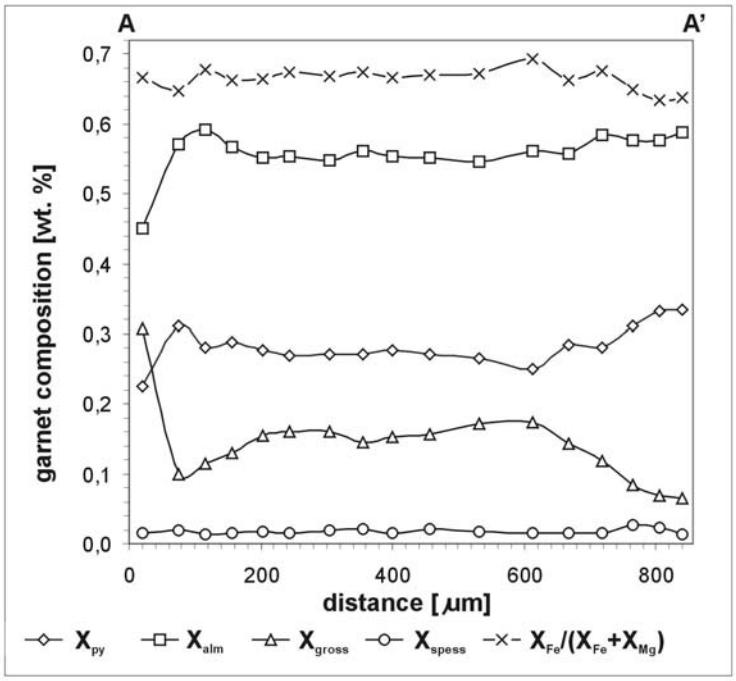


Fig. 4. Plots of garnet composition along A-A′ traverse (as shown in Fig. 3)

pressures 5.2 ± 0.7 kbar were determined. Additionally one sample (GS-17C) from the Kietlice region (the Fore-Sudetic Block) yielded temperatures of 600 ± 25°C.

The disparity determined between mica compositions in four analysed samples (GS-10A, GS-10B, GS-14A and GS-14B; Table 3) and the elemental range in the calibration data set (Hoisch 1989) probably do not influence our geothermometry data. Larger differences in case of two samples (GS-12 and GS-15) cause us to question the reliability of temperatures obtained from both samples (Table 5, in italics); these results will not be consider in further discussion.

DISCUSSION

Analytical differences between the results of the geothermometers might be interpreted as a result of different speeds of ion diffusion between coexisting minerals (especially in case of GS-14A and GS-14B). Temperatures obtained with use of muscovite-biotite geothermometer are probably lower than maximum temperatures of metamorphism. According to Spear (1991), fast cooling ratio affirmed with use of thermochronological investigations (e.g. Oliver, Kelley 1993; Bröcker et al. 1998; Marheine et al. 2002; Zahniser et al. 2003) may be conducive to the preservation of equilibrium between garnet and biotite achieved at maximum temperatures of metamorphism. Moreover, garnet rim with smaller Θ biotite shows higher Mg/(Mg+Fe) values,

which leads to higher temperature estimation (Usuki 2002). Therefore, even if the chemical composition changed during cooling, maximum temperatures should be within the range of calibration error of our results.

Geothermobarometry results have revealed that selected rocks from the Góry Sowie Mts were metamorphosed under middle-upper amphibolite facies conditions. Conditions of peak of metamorphism that affected selected Góry Sowie gneisses were up to *ca* 687°C and *ca* 7.8 kbar (including calibration error value). These data are consistent with, if not slightly higher-temperature than previously published P-T estimations for the peak regional metamorphic event in the massif (e.g. Kryza 1981; Żelaźniewicz 1987, 1990, 2003). Similar P-T values — based on garnet-aluminosilicate-plagioclase and garnet-biotite equilibria — were registered previously in migmatitic gneisses by Kryza and Pin (1998, 2002): 670–750°C at 4.8–6.8 kbar for the mineral rim compositions. Slight inconsistence of our data with these results might be related to metabasites that are enclosed within migmatitic gneisses investigated by the mentioned authors.

Temperatures and pressures obtained out of two samples (GS-14A and GS-14B) from the same outcrop revealed that pegmatites intruded into the gneissic complex before peak of metamorphism. Both rocks registered conditions of later metamorphic events.

We suggest that these P-T constraints are related to the beginning of the midcrustal exhumational stage of the granulite assemblages, coeval with widespread regional metamorphism (Fig. 5). Isothermal decompression of the terrane, and initial exhumation of the gneisses and migmatites — which enclose granulites and metabasites — to mid-crustal depths most likely took place *ca* 380–370 Ma (e.g. Van Breemen et al. 1988; Bröcker et al. 1998; Timmermann et al. 2000; Gordon et al. 2003; Zahniser et al.

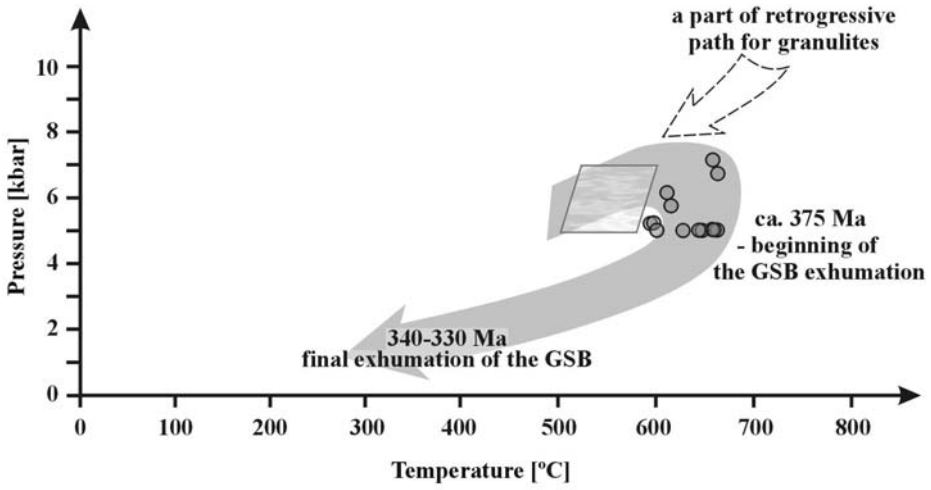


Fig. 5. P-T-t path for gneisses and migmatites determined using data presented in this paper (filled circles). P-T conditions of earlier metamorphic event (M_1) according to Żelaźniewicz (1990) are shown as the box. Dating after Van Breemen et al. (1988), Oliver and Kelley (1993), Bröcker et al. (1998), Timmermann et al. (2000), Gordon et al. (2003) and Zahniser et al. (2003). A part of retrogressive path for granulites determined using data from Żelaźniewicz (1990), Kryza et al. (1996) and O'Brien et al. (1997)
GSB — the Góry Sowie Block

2003). Later, probably weaker Variscan tectonometamorphic events resulted in final exhumation of the Góry Sowie Block at 340–330 Ma (e.g. Oliver, Kelley 1993; Zahniser et al. 2003).

CONCLUSIONS

1. We interpret analytical differences between the data obtained with use of garnet--biotite geothermometer and muscovite-biotite geothermometer as a result of different speeds of ion diffusion within mineral pairs.

2. Geothermobarometry results, presented in this paper, revealed that selected rocks from the Góry Sowie Mts were metamorphosed at middle-upper amphibolite facies conditions.

3. P-T constraints are related to the beginning of the midcrustal exhumational stage of the granulite assemblages coeval with widespread regional metamorphism, which most likely took place *ca* 380–370 Ma.

Acknowledgements. The authors are grateful to Dr. Jerzy Czerny, Dr. Tomasz Bajda, Adam Gaweł M. Sc., Stephan Zahniser M. Sc., Stacia Gordon M. Sc. and Jacob Glascock M. Sc. for their contribution to this work. This research was partly founded by the AGH — UST research grant 11.11.140.158.

REFERENCES

BERMAN R. G., ARANOVICH L. Y., 1996: Optimized standard state and solution properties of minerals. I. Model calibration for olivine, orthopyroxene, cordierite, garnet, and ilmenite in the system FeO-MgO--CaO-Al_2O_3-TiO_2-SiO_2. *Contrib. Mineral. Petrol.* 126, 1–24.

BHATTACHARYA A., MOHANTY L., MAJI A., SEN S. K., RAITH M., 1992: Non-ideal mixing in the phlogopite-annite binary: constraints from experimental data on Fe-Mg partitioning and a reformulation of the biotite-garnet geothermometer. *Contrib. Mineral. Petrol.* 111, 87–93.

BRÖCKER M., ŻELAŹNIEWICZ A., ENDERS M., 1998: Rb-Sr and U-Pb geochronology of migmatitic gneisses from the Góry Sowie (West Sudetes, Poland): the importance of Mid-Late Devonian metamorphism. *J. Geol. Soc. Lond.* 155, 1025–1036.

BUDZYŃ B., MANECKI M., SCHNEIDER D. A., 2004: Geothermobarometry of selected metapelites from the Góry Sowie, Sudetes. *Pol. Tow. Mineral. Prace Spec.* 24, 103–106.

DASGUPTA S., SENGUPTA P., GUHA D., FUKUOKA M., 1991: A refined garnet-biotite Fe-Mg exchange geothermometer and its implication in amphibolites and granulites. *Contrib. Mineral. Petrol.* 109, 130–137.

DYAR M. D., 1990: Mössbauer spectra of biotite from metapelites. *Amer. Miner.* 75, 656–666.

DZIEDZICOWA H., 1994: LP hornblende granulite facies within the Góry Sowie gneisses of the Fore-Sudetic Block. In: Kryza R. (ed.), Igneous activity and metamorphic evolution of the Sudetes area, Abstracts. Wrocław, pp. 43.

FERRY J. M., SPEAR F. S., 1978: Experimental calibration of the partitioning of Fe and Mg between biotite and garnet. *Contrib. Mineral. Petrol.* 66, 113–117.

GANGULY J., CHENG W., TIRONE M., 1996: Thermodynamics of aluminosilicate garnet solid solution: new experimental data, an optimized model, and thermometric applications. *Contrib. Mineral. Petrol.* 66, 271–299.

GORDON S., SCHNEIDER D. A., BUDZYN B., MANECKI M., 2003: Timing constraints on the metamorphism and exhumation of ultra high-grade terranes, Sudete Mountains, NE Bohemian Massif. *GSA Annual Meeting — Abstracts with Programs* 35, 6, 638.

GUIDOTTI C. V., DYAR M. D., 1991: Ferric iron in metamorphic biotite and its petrologic and crystallochemical implications. *Amer. Miner.* 76, 161–175.

HACKLER R. T., WOOD B. J., 1989: Experimental determination of Fe and Mg exchange between garnet and olivine and estimation of Fe-Mg mixing properties in garnet. *Amer. Miner.* 74, 994–999.

HODGES K. V., SPEAR F. S., 1982: Geothermometry, geobarometry and the Al_2SiO_5 triple point at Mt. Moosilauke, New Hampshire. *Amer. Miner.* 67, 1118–1134.

HOISCH T. D., 1989: A muscovite — biotite geothermometer. *Amer. Miner.* 74, 565–572.

HOLDAWAY M. J., 2000: Application of new experimental and garnet Margules data to the garnet-biotite geothermometer. *Amer. Miner.* 85, 881–892.

HOLDAWAY M. J., 2004: Optimization of some key geothermobarometers for pelitic metamorphic rocks. *Mineral. Mag.* 68, 1, 1–14.

KRÖNER A., HEGNER E., 1998: Geochemistry, single zircon ages and Sm-Nd systematics of granitoid rocks from the Góry Sowie (Owl Mts), Polish West Sudetes: evidence for early Palaeozoic arc-related plutonism. *J. Geol. Soc. Lond.* 155, 711–724.

KRYZA R., 1981: Migmatization in gneisses of northern part of the Sowie Góry, Sudetes. *Geol. Sudetica* 14, 7–100.

KRYZA R., PIN C., VIELZEUF D., 1996: High-pressure granulites from the Sudetes (south-west Poland): evidence of crustal subduction and collision thickening in the Variscan Belt. *J. Metamorphic Geol.* 14, 531–546.

KRYZA R., PIN C., 1998: Koronitowe metagabra i amfibolity Gór Sowich: zapis magmatyzmu wewnątrzpłytowego i polimetamorfizmu. [In Polish]. *Pol. Tow. Mineral. Prace Spec.* 10, 125–128.

KRYZA R., PIN C., 2002: Mafic rocks in a deep-crustal segment of the Variscides (the Góry Sowie, SW Poland): evidence for crustal contamination in an extensional setting. *Int. J. Earth Sci. (Geol. Rundsch.)* 91, 1017–1029.

MARHEINE D., KACHLIK V., MALUSKI H., PATOČKA F., ŻELAŹNIEWICZ A., 2002: The $^{40}Ar/^{39}Ar$ ages from the West Sudetes (NE Bohemian Massif): constraints on the Variscan polyphase tectonothermal development. In: Winchester J. A., Pharaon T. C., Verniers J., 2002: Palaeozoic Amalganation of Central Europe. *Geol. Soc. London, Spec. Publ.* 201, 133–155.

MUDHOPADHYAY B., HOLDAWAY M. J., KOZIOŁ A. M., 1997: A statistical model of thermodynamic mixing properties of Ca-Mg-Fe^{2+} garnets. *Amer. Miner.* 82, 165–181.

O'BRIEN P. J., KRÖNER A., JAECKEL P., HEGENER E., ŻELAŹNIEWICZ A., KRYZA R., 1997: Petrological and isotope studies on Palaeozoic high-pressure granulites. Góry Sowie Mts, Polish Sudetes. *J. Petrol.* 38, 433–456.

OLIVER G. J. A., KELLEY S., 1993: $^{40}Ar/^{39}Ar$ fusion ages from the Polish Sudetes: Variscan tectonothermal reworking of Caledonian protoliths. *N. Jb. Geol. Paläont. Mh.* 21, 321–344.

PERCHUK L. L., LAVRENT'EVA I. V., 1983: Experimental investigation of exchange equilibria in the system cordierite-garnet-biotite. In: Saxena S. K. (ed.): Kinetics and equilibrium in mineral reactions. Springer, Berlin, Heidelberg, New York, Tokio, pp. 199–239.

RAMÍREZ E., SASSI R., 2001: The baric character of the Patagonian basement as deduced from the muscovite $d_{060,33\bar{1}}$ spacing: a first contribution from Eastern Andean Metamorphic Complex (Andes, Chile). *Eur. J. Mineral.* 13, 1119–1126.

SASSI F. P., SCOLARI A., 1974: The b_0 value of the potassic white micas as a barometric indicator in low-grade metamorphism of pelitic schists. *Contrib. Mineral. Petrol.* 45, 143–152.

SPEAR F. S., 1991: On the interpretation of peak metamorphic temperatures in light of garnet diffusion during cooling. *J. Metamorphic Geol.* 9, 379–388.

TIMMERMANN H., PARRISH R. R., NOBLE S. R., KRYZA R., 2000: New U-Pb monazite and zircon data from the Sudetes Mountains in SW Poland: evidence for a single-cycle Variscan orogeny. *J. Geol. Soc. Lond.* 157, 265–268.

USUKI T., 2002: Anisotropic Fe-Mg diffusion in biotite. *Amer. Miner.* 87, 1014–1017.

VAN BREEMEN O., BOWES D. R., AFTALION M., ŻELAŹNIEWICZ A., 1988: Devonian tectonothermal activity in the Sowie Góry Gneissic Block, Sudetes, Southwestern Poland: evidence from Rb-Sr and U-Pb isotopic studies. *Ann. Soc. Geol. Polon.* 58, 3–19.

ZAHNISER S. J., SCHNEIDER D. A., MANECKI M., 2003: Exhumation history of the Gory Sowie (Bohemian Massif) revealed through Ar-Ar thermochronometry. *GSA Annual Meeting — Abstracts with Programs* 35, 6, 638.

ŻELAŹNIEWICZ A., 1985: Granulitic inliers amidst a gneissic/migmatitic complex of the Owl Mts, Sudetes. *Acta Geol. Polon.* 35, 157–171.

ŻELAŹNIEWICZ A., 1987: Tektoniczna i metamorficzna ewolucja Gór Sowich. [In Polish]. *Ann. Soc. Geol. Polon.* 57, 203–348.

ŻELAŹNIEWICZ A., 1990: Deformation and metamorphism in the Góry Sowie gneiss complex, Sudetes, SW Poland. *N. Jb. Paläont. Abh.* 179, 129–157.

ŻELAŹNIEWICZ A., 1995: Fore-Sudetic part of the Góry Sowie Block, SW Poland. Przewodnik LXVI Zjazdu PTG. Wrocław. pp. 85–109 (in Polish with English summary).

ŻELAŹNIEWICZ A., 2003: Developments in the geology of the crystalline basement of the West Sudetes in 1990–2003. In: Ciężkowski A., Wojewoda J., Żelaźniewicz A. (ed.) — Sudety Zachodnie: od wendu do czwartorzędu, 7–16, WIND, Wrocław (in Polish).

Bartosz BUDZYŃ, Maciej MANECKI, David A. SCHNEIDER

WARUNKI CIŚNIEŃ I TEMPERATUR METAMORFIZMU WYSOKIEGO STOPNIA W GÓRACH SOWICH, SUDETY ZACHODNIE

Streszczenie

Warunki temperatur i ciśnień metamorfizmu wybranych skał z Gór Sowich (Sudety Zachodnie, SW Polska) zostały określone przy zastosowaniu geotermometrów granat-biotyt (GB) i muskowit-biotyt (MB) oraz geobarometru muskowitowego. Gnejs warstewkowy z sillimanitem i granulit z rejonu jeziora Bystrzyckiego (północna część Gór Sowich) wykazały temperatury 652 ± 35°C (GB). W przypadku gnejsu warstewkowego i metapegmatytu z rejonu Przygórza (południowa część masywu) otrzymano temperatury 660 ± 28°C (GB) i 613 ± 25°C (MB) oraz ciśnienia 6,4 ± 1,4 kbar. Zarejestrowane warunki metamorfizmu gnejsu cienkolaminowanego i diateksytu z okolic Potoczka wyniosły 596 ± 24°C (MB) i 5.2 ± 0,7 kbar. Do badań wybrano ponadto jedną próbkę z przedgórskiej części bloku sowiogórskiego — otrzymane temperatury metamorfizmu gnejsu smużystego z rejonu Kietlic wyniosły 600 ± 25°C (GB).

Różnice pomiędzy otrzymanymi danymi przy użyciu dwóch geotermometrów — co ma miejsce np. dla próbek z centralnej części Gór Sowich — mogą być wynikiem różnic w szybkości dyfuzji jonów pomiędzy minerałami. Otrzymane dane są najprawdopodobniej związane z początkową ekshumacją bloku sowiogórskiego i towarzyszącym metamorfizmem regionalnym w warunkach facji amfibolitowej.

MINERALOGIA POLONICA
Vol. 35, No 2, 2004
PL ISSN 0032-6267

Wojciech FRANUS[1,2], *Jerzy KLINIK*[3], *Małgorzata FRANUS*[1]

MINERALOGICAL CHARACTERISTICS AND TEXTURAL PROPERTIES OF ACID-ACTIVATED GLAUCONITE

A b s t r a c t . The authors activated glauconite from the Lubartowska Lowland (E Poland) in 3M HCl for 1, 3, 4 and 7h at 100°C and studied impact of the activation on mineralogical and textural features (specific surface area, porosity and microporosity) of the mineral. Acid activation does not destroy the glauconite: its layer structure has been preserved despite leaching a considerable number (about 60%) of octahedral cations. The activation has significantly increased major textural parameters of the glauconite, i.e. its specific surface, porosity and microporosity.

Key-words: glauconite, acid activation, surface area, microporosity

INTRODUCTION

Acid activation of clay minerals has been a subject of many papers. The process has been studied mainly on the minerals of the smectite group as potential mineral materials for manufacturing of bleaching earths (e.g. Fijał et al. 1975a, b; Kheok et al. 1982; Christidis et al. 1997). Much less such data have been published for glauconite.

Glauconite is a common mineral in widespread clayey-sandy rocks in the vicinity of Lubartów (Krzowski 1995; Gazda et al. 2001), so the authors carried out basic investigations aimed at testing of the effects of acid activation on the structure and textural parameters of the glauconite as a possible mineral raw material in environmental engineering technologies. This mineral, with many applications outside our country (Smith et al. 1996; Baker, Uwins 1997; Kuusik, Viisimaa 1999; Stefanova 1999; Srasra, Trabelsi-Ayedi 2000; Griffioen 2001), in Poland has not been frequently utilized so far. As glauconites are strongly diversified in their mineral and chemical com-

[1] Lublin University of Technology, Faculty of Civil and Sanitary Engineering, Department of Geotechnics, ul. Nadbystrzycka 40, 20-618 Lublin, Poland; e-mail: wfranus@akropolis.pol.lublin.pl

[2] A scholarship holder of the Foundation Supporting Polish Science, the program Domestic Outgoing Scholarship.

[3] AGH, University of Science and Technology, Faculty of Fuels and Energy, al. Mickiewicza 30, 30-059 Kraków, Poland.

positions, the results obtained by different authors are not directly comparable. The investigations presented here were to determine industrial potential of the Tertiary glauconite from the vicinity of Nowodwór.

MATERIALS AND METHODS

Glauconite

The glauconite studied was collected from Tertiary sands of the Lubartowska Lowland near Nowodwór. Its average content in these sediments varies between 20 and 30% (Gazda et al. 2001). The sands were washed on the 63 μm sieve; then, from the glauconite-quartz concentrate left on the sieve the glauconite was magnetically separated.

Acid activation

Activation was carried out using 3M HCl for 1, 3, 4 and 7h, boiling samples of the glauconite concentrate on the water bath at 100°C. The glauconite samples were also activated at 60°C in 3M HCl for 3h using a magnetic stirrer. After acid treatment, the samples were washed with distilled water until the Cl^- ion disappeared, and dried at 80°C.

Methods of mineralogical and chemical investigations

The mode of the glauconite occurrence was studied using a JEOL 5200 scanning electron microscope with an EDS attachment for chemical analyses in microareas. Samples were covered with graphite.

A mineralogical type of the glauconite was determined using the X-ray method with a TUR-M62 diffractometer (CoK_α radiation).

The composition of the natural glauconite as well as the degree of degradation of its octahedral layer due to acid activation were analysed using a Perkin-Elmer Plasma 40 ICP–AES analyser.

Methods of textural investigations

Sorption and desorption isotherms were determined using a sorption manostate (Ciembroniewicz, Lasoń 1972) with argon vapours at a temperature of liquid nitrogen (–195.5°C) after degassing of the samples to the pressure around 10^{-5} mm Hg. The specific surface was calculated applying the theory of multilayer vapour adsorption of Brunauer, Emmett and Teller (BET) (Brunauer et al. 1938; Ościk 1979; Klinik 2000). The specific volume of micropores was determined with Dubinin-Radushkievitch equation (Ościk 1979). The specific surface of mesopores and their specific volume were calculated applying the II variant of Dubinin method (Dubinin 1956; Ościk 1979; Klinik 2000).

RESULTS OF MINERALOGICAL AND CHEMICAL ANALYSES

The glauconite separated from the glauconite sands of the Nowodwór area is developed as spherical, loaf-like or ellipsoidal, grass green aggregates (pellets) characteristic of this mineral, with prevalent diameters between 0.12 and 0.25 mm (Fig. 1). A heterogeneous nature of platy glauconite accumulations can be seen under the scanning microscope in the fractures of its grains (Phot. 2). Acid activation affects only the outermost glauconite surfaces, resulting in distinct corrosion along these fractures (Phot. 3).

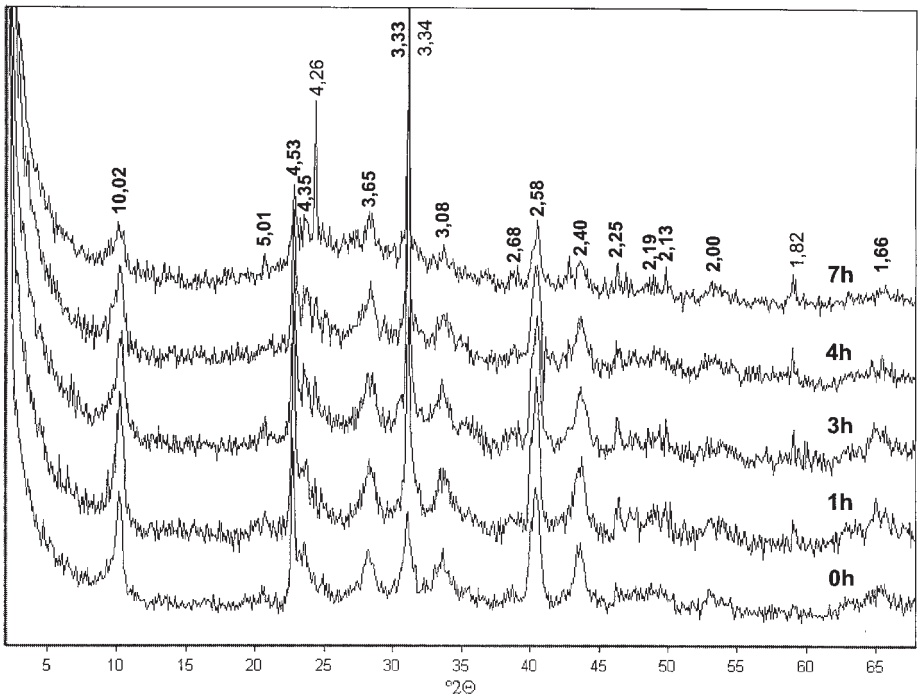


Fig. 1. X-ray patterns of the glauconite samples

The results of XRD investigations provide an almost complete set of d_{hkl} reflections, characteristic of the 1M-glauconite polytype (Fig. 1, sample 0h). The X-ray patterns of the oriented, air-dry samples and the samples saturated with ethylene glycol indicate that the glauconite studied contains about 10% of smectite layers, possessing thus the structure with an ordered arrangement of interstratifications of the IISI type (Środoń, Gaweł 1988).

After activation in 3M HCl the structure of the glauconite remains generally unchanged. In all X-ray patterns the major reflections of glauconite have the same *d* values (10.02; 5.53; 3.33; 2.58 Å). The time of activation affects, however, the intensity of the glauconite reflections: in the sample activated for 7h it is two times lower than in

the sample not activated. It can be explained by formation of amorphous reaction products when the structure of glauconite is leached of some elements but does not collapse. The presence of the amorphous substance also explains a distinctly elevated background of the X-ray pattern in the range 20–40°(2Θ) in the sample activated for 7h.

TABLE 1

Chemical composition of the glauconite (sample hand-picked under the binocular)

Component [wt.%]	SiO_2	Al_2O_3	Fe_2O_3	MgO	CaO	Na_2O	K_2O	H_2O
	49.70	5.36	24.44	4.06	0.36	0.08	7.83	8.39

The chemical composition of the glauconite studied (Table 1), and particularly its Fe_2O_3>Al_2O_3 ratio, classifies it as a ferruginous glauconite (Krzowski 1995). Recalculation of the chemical composition into the formal unit according to the respective crystallochemical rule (22 charges of anions in a half of the formal unit) gives the following formula:

$$(K_{0.74}Na_{0.01}Ca_{0.03})[(Fe^{3}_{1.37}Al_{0.16}Mg_{0.45})(Al_{0.31}Si_{3.69}O_{10})(OH)_2]$$

Acid activation affects mainly chemical composition of the octahedral layer, while the tetrahedral layer is less prone to it because of strong bonds among silicon and oxygen ions. The amount of major ions of the octahedral layer removed is presented in Table 2 and Figure 2, while Figure 3 shows the range of damage of this layer. This damage increases with activation time and after 7 h reaches 63%.

TABLE 2

Content [wt.%] of the main octahedral cations of the glauconite samples (bulk samples after magnetic separation)

Activation time	Fe_2O_3	Al_2O_3	MgO
0 h	22.67	4.34	4.25
1 h	19.73	3.97	3.68
3 h	18.57	3.02	3.43
4 h	11.99	2.16	2.33
7 h	7.98	1.61	1.68

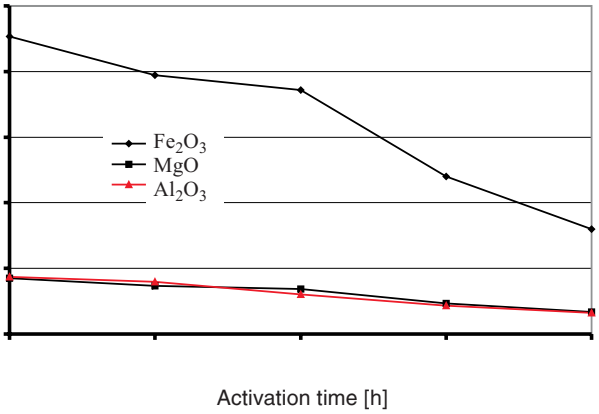


Fig. 2. Change of the amount of main octahedral cations of the glauconite samples due to acid activation

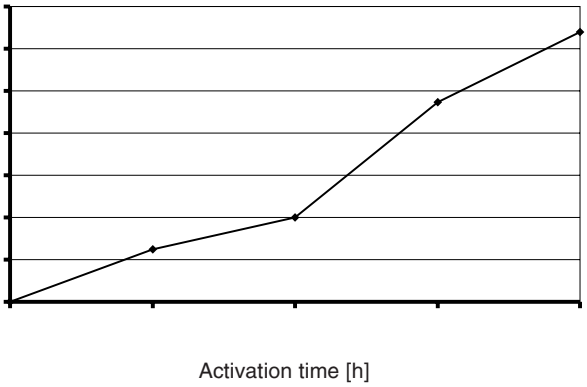


Fig. 3. The total of the main octahedral cations removed from the glauconite samples during acid activation

RESULTS OF TEXTURAL ANALYSES

Isotherms of argon sorption and desorption at the temperature of liquid nitrogen prior and after activation are presented in Figure 4. The activation does not change their character and the curves correspond to the type I of the BET isotherm (Brunauer et al. 1938; Ościk 1979; Klinik 2000), being equivalent of the type I according to the IUPC classification (Gregg, Sing 1982; Sing et al. 1985). The hysteresis loop corresponds to the loop H4 in the IUPC classification and indicates that the pores in the material studied are developed as narrow slits between two surfaces (in the case of clay minerals these are interlayers).

Textural parameters of the natural and activated glauconite are shown in Table 3 and Figure 5. All these parameters increase with the activation time: for instance the specific surface from 78 m^2/g in natural glauconite to 329 m^2/g after 7-hour activation

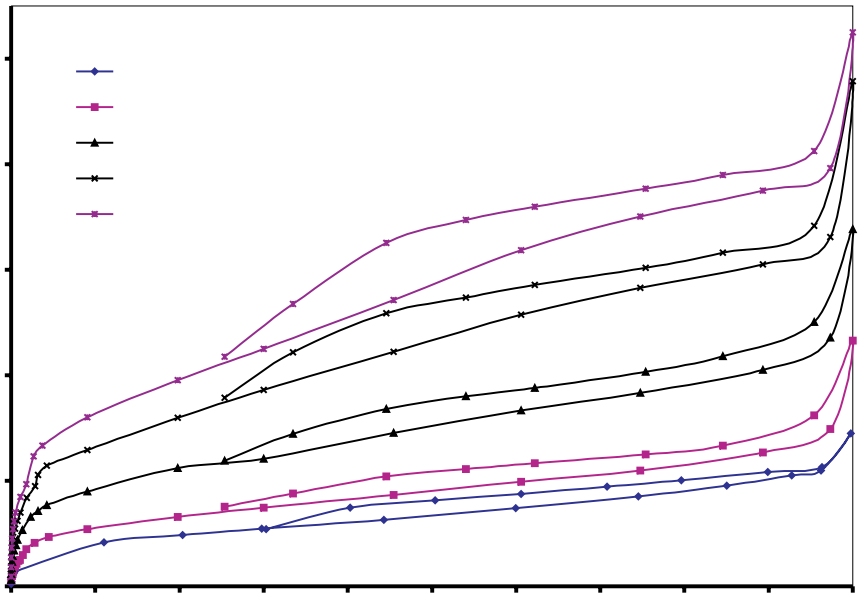


Fig. 4. Isotherms of sorption and desorption of argon on the natural and activated glauconite samples

TABLE 3

Textural properties of the glauconite

Time and temperature of activation	S_{BET} [m^2/g]	V_{mic} [mm^3/g]	S_{mes} [m^2/g]	V_{mes} [mm^3/g]
0h	78.0	21	33.1	44
1 h — 100°C	106.1	25	35.3	63
3 h — 60°C	131.0	27	46.1	77
3 h — 100°C	186.7	40	53.6	90
4 h — 100°C	269.8	58	73.6	104
7 h — 100°C	324.1	72	104.0	128

S_{BET} — specific surface [m^2/g],
V_{mic} — specific volume of micropores [mm^3/g] calculated from Dubinin- Radushkievitch equation,
S_{mes} — specific surface of mesopores [m^2/g] calculated according to variant II of Dubinin method,
V_{mes} — specific volume of mesopores [m^2/g] calculated according to variant II of Dubinin method.

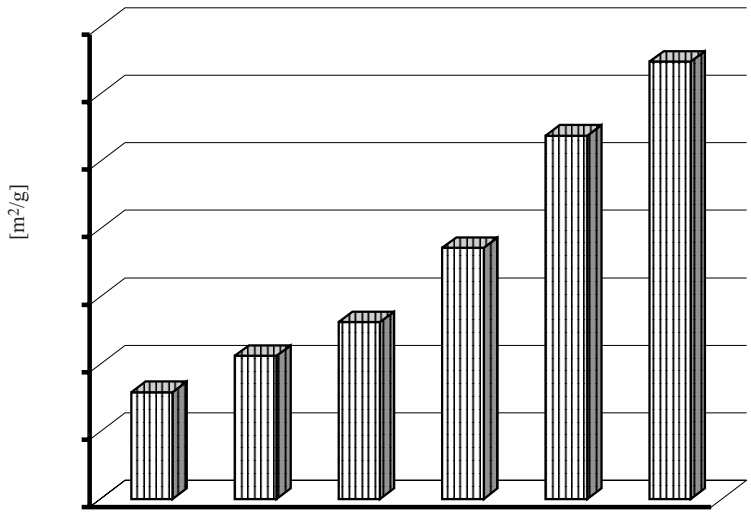


Fig. 5. Specific surface area of the natural and activated glauconite samples

in 3M HCl. Specific surface of activated glauconite depends also on activation temperature, being 131 m^2/g after 3-hour activation at 60°C and 186 m^2/g after 3-hour activation at 100°C. The volume of micropores and mesopores as well as the surface of the latter also follow this trend.

SUMMARY

Activation of the glauconite separated from Tertiary sands of the Lubartowska Lowland was carried out in 3M HCl for 1, 3, 4 and 7 h at 100°C. The investigations have shown that after the acid activation the mineral phase still represents glauconite despite a strong damage of its structure resulting from leaching of major elements of the octahedral layer. Almost all the X-ray reflections from the interplanar surfaces of the mineral have been recorded after acid activation, although of considerable lower intensity. It can be explained as an effect of formation of amorphous reaction products of the silica gel type (the same process also takes place in the case of acid activation of montmorillonite) and has been proved particularly by increases in the volume and specific surface of mesopores. The structure of these products assumes most probably a globular character, and micropores must be developed as empty spaces among the newly formed, gel-type silica molecules.

Applying chemical treatment it is possible to change the mineralogical character and textural properties of glauconite, so these procedures are perspective in utilization of glauconite as a bleaching agent.

Acknowledgements. The study was supported by KBN (Warsaw), Grant no. 4 T09D 029 22; and AGH — University of Science and Technology (Cracow), Faculty of Fuels and Energy, Scientific Project No. 10.10.210.52.

REFERENCES

BAKER J.C., UWINS P.J.R. 1997: Freshwater sensitivity of glauconitic hydrocarbon reservoirs. *J. Petrol. Sci. Eng*. 18, 83–91.

BRUNAUER. S., EMMETT P.H., TELLER E. 1938: Adsorption of gases in multimolecular layers. *Jour. Am. Chem. Soc*. 60, 309–319.

CHRISTIDIS G.E., SCOTT P.W., DURHAM A.C. 1997: Acid activation and bleaching capacity of bentonites from the islands of Milos and Chios, Aegean, Greece. *Appl. Clay Sci*. 12, 329–347.

CIEMBRONIEWICZ A., LASOŃ M. 1972: Manostat sorpcyjny — półautomatyczny aparat do badań sorpcyjnych. *Roczn. Chemii* 46, 703 (in Polish).

DUBININ M.M. 1956: Issliedowanije poristoj struktury twierdych tieł sorbcjonnymi mietodami. *Zh. Fiz. Khim*. 30. 1652 (in Russian).

FIJAŁ J., KŁAPYTA Z., ZIĘTKIEWICZ J., ŻYŁA M. 1975a: On the mechanism of the montmorillonite acid activation. Part I. Degradation of Ca-montmorillonite structure. *Miner. Polon*. 6, 1, 29–43.

FIJAŁ J., KŁAPYTA Z., KWIECIŃSKA B., ZIĘTKIEWICZ J., ŻYŁA M. 1975b: On mechanism of acid activation of montmorillonite. Part II. Changes in the morphology and porosity in the light of electron microscopic and adsorption investigations. *Miner. Polon*. 6, 2, 49–57.

GAZDA L., FRANUS M., FRANUS W., KRZOWSKI Z. 2001: Mineralogical and crystallochemical characteristic of glauconite from Gawłówka (Lublin Upland, Poland). *Miner. Slov*. 33, 2, 16.

GRIFFIOEN J. 2001: Potassium adsorption ratios as an indicator for the fate of agricultural potassium in groundwater. *J. Hydrogeol*. 254, 244–254.

GREGG S.J., SING K.S.W. 1982: Adsorption, surface area and porosity (2nd ed.). Academic Press, London.

KHEOK S.C., LIM E.E. 1982: Mechanism of palm oil bleaching by montmorillonite clay activated at various acid concentrations. *J. Am. Oil Chem. Soc*. 59, 129–131.

KLINIK J. 2000: Tekstura porowatych ciał stałych. Wyd. AGH, Kraków, 125 pp. (in Polish).

KRZOWSKI Z. 1995: Glaukonit z osadów trzeciorzędowych regionu lubelskiego i możliwości jego wykorzystania do analiz geochronologicznych. *Prace Nauk. Polit. Lub*. (rozpr. habilit.), 9–133 (in Polish).

KUUSIK R., VIISIMAA L. 1999: A new dual coagulant for water purification. *Wat. Res*. 33/9, 2075–2082.

OŚCIK J. 1979: Adsorpcja. PWN, Warszawa (in Polish).

SING K.S.W., EVERETT D.H., HAUL R.A.W., MOSCOU L., PIEROTTI R.A., ROUQUÉROL J., SIEMIENIEWSKA T. 1985: Reporting physisorption data for gas/solid systems with special reference to the determination of surface area and porosity. *Pure Appl. Chem*. 57, 4, 603–619.

SMITH E.H., LU W., VENGRIS T., BINKIENE R. 1996: Sorption of heavy metals on Lithuanian glauconite. *Water Res*. 12, 2883–2892.

SRASRA E., TRABELSI-AYEDI M. 2000: Textural properties of activated glauconite. *Appl. Clay Sci*. 17, 71–84.

STEFANOVA I.G. 1999: Natural sorbents as barriers against migration of radionuclides from radioactive waste repositories. In: P. Misaelides et al. (eds.) *Natural Microporous Materials in Environ. Techn., Ser. E — Applied Sci*. 362, 371–379.

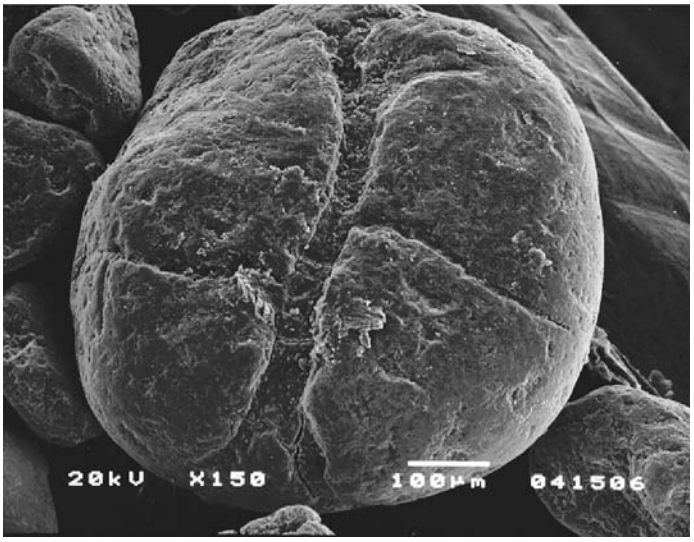
ŚRODOŃ J., GAWEŁ A. 1988: Identyfikacja rentgenowska mieszanopakietowych krzemianów warstwowych. In: A. Bolewski. W. Żabiński (eds.) Metody badań minerałów i skał, 290–307 (in Polish).

Wojciech FRANUS, Jerzy KLINIK, Małgorzata FRANUS

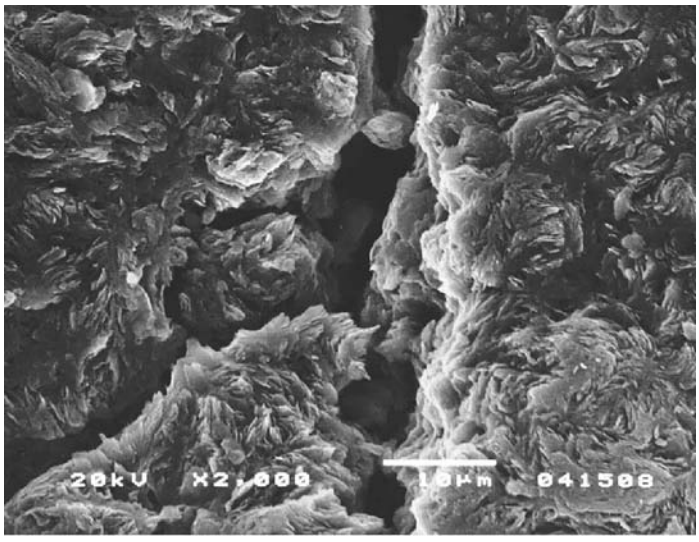
CHARAKTERYSTYKA MINERALOGICZNA I WŁAŚCIWOŚCI TEKSTURALNE AKTYWOWANEGO KWASOWO GLAUKONITU

Streszczenie

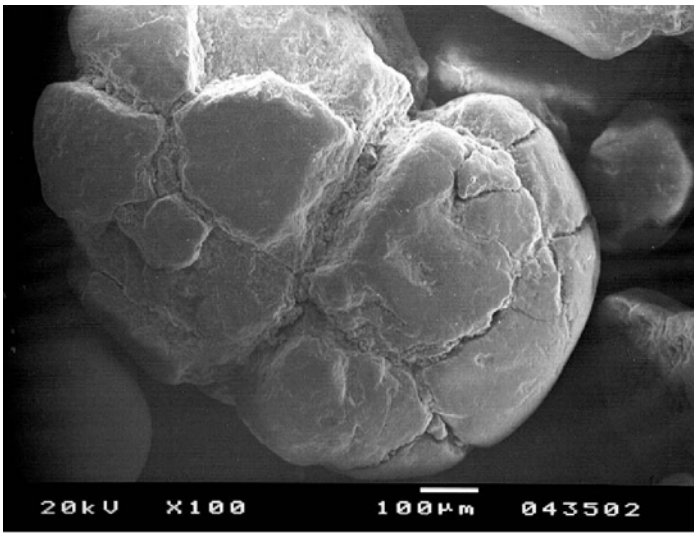
Badaniom poddano próbki glaukonitów aktywowanych 3M HCl przez okres 1, 3, 4 i 7 godzin w temperaturze 100°C. Studiowano wpływ aktywacji na zmianę charakteru mineralogicznego, jak również właściwości teksturalne glaukonitu (powierzchnia właściwa, porowatość i mikroporowatość). Badania mineralogiczne wykazały, że aktywacja kwasowa nie wpłynęła w sposób znaczący na strukturę glaukonitu (budowa pakietowa została zachowana) pomimo wyługowania z warstwy oktaedrycznej znacznej ilości (nieco ponad 60%) kationów ją budujących. Wyraźnie zaznaczyła się także tendencja wzrostowa głównych parametrów teksturalnych badanych glaukonitów, tj.: powierzchni właściwej (4-krotnie), porowatości (3-krotnie) i mikroporowatości (3,5-krotnie).



Phot. 1. Glauconite. A SEM image



Phot. 2. A close-up of the Photo 1



Phot. 3. Glauconite activated for 7h. A SEM image

MINERALOGIA POLONICA
Vol. 35, No 2, 2004
PL ISSN 0032-6267

Krzysztof DUDEK[1], *Krzysztof BUKOWSKI*[1], *Wiesław HEFLIK*[1]

MINERALOGICAL CHARACTERISTICS OF THE BOCHNIA TUFF FROM THE CHODENICE BEDS (CARPATHIAN FOREDEEP, S POLAND)

Abstract. The tuff from the Chodenice Beds, sampled in a natural outcrop in Chodenice, was subjected to mineralogical and geochemical analyses. Main components of the rock proved to be glass shards, quartz and feldspar crystals, as well as mixed-layered Ca-Na-smectite, formed by alteration of volcanic glass. The distinguished heavy fraction consists of ilmenite (predominating component), zircon, secondary iron oxides and scarce crystals (or crushed fragments) of apatite, tourmaline, rutile, monazite, garnet and staurolite. SEM/EDS analyses revealed crypto-inclusions of a metallic, Ni-Fe-rich phase, presumably of cosmic origin.

Key-words: tuff, Chodenice Beds, smectite, zircon, taenite

GEOLOGICAL BACKGROUND

Chodenice, once a village near Bochnia, presently within the borders of the town (Fig. 1), is the type locality for the Chodenice Beds (Niedźwiedzki 1883, *fide* Alexandrowicz 1961). In the general stratigraphic column of Middle Miocene (Badenian) in the Wieliczka-Bochnia area they overlie the evaporites of the Wieliczka Formation and marly and clastic sediments of the Skawina Beds (Fig. 2), all these units belonging to the so-called folded Miocene. The Chodenice Beds, up to 350 metres in thickness, consist of dark-grey or brownish marly clays, fine-grained sandstones and sands, and several intercalations of pyroclastic sediments, mostly in the upper part of the profile (Porębski 1999). The Bochnia Tuff (TB), occurring 200–250 metres above the bottom of the Chodenice Beds, is one of the most broadly extended pyroclastic horizons in the whole Carpathian Foredeep (Alexandrowicz 1997). In the area between Wieliczka and Bochnia it was encountered in several natural outcrops (Chodenice, Chełm upon Raba, Moszczenica, Sułków), in the Bochnia Salt Mine as well as in numerous drillholes. In other parts of the Carpathian Foredeep this horizon was reported from the Upper

[1] AGH, University of Science and Technology, Faculty of Geology, Geophysics and Environment Protection, al. Mickiewicza 30, 30-059 Kraków, Poland; e-mail: kadudek@uci.agh.edu.pl, buk@geolog.geol.agh.edu.pl

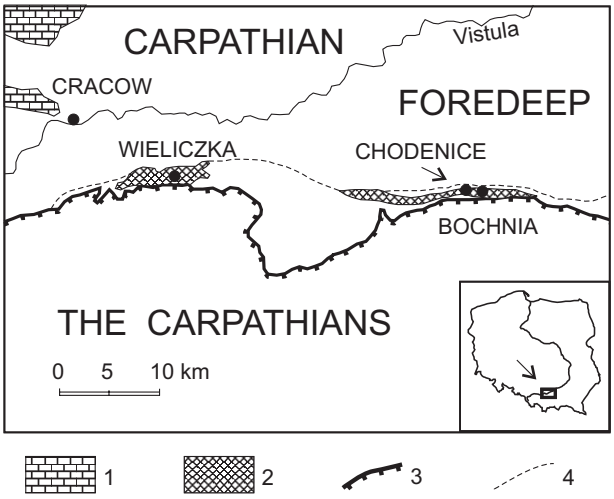


Fig. 1. Geological sketch of the Wieliczka-Bochnia area
1 — platform Mesozoic sediments, 2 — Miocene salt deposits, 3 — Flysch Carpathians border, 4 — extent of folded Miocene sediments

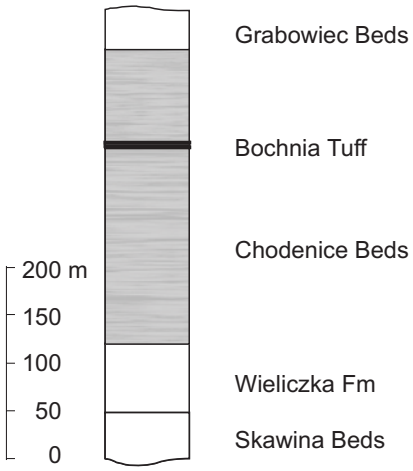


Fig. 2. Position of the Bochnia Tuff and Chodenice Beds in the generalized profile of Middle Miocene (Badenian) for the Wieliczka-Bochnia area

Silesia (Alexandrowicz, Pawlikowski 1980) and from drillholes near Mielec and Przemyśl (Parachoniak 1962).

SAMPLES

A natural outcrop of the Bochnia Tuff, situated on the high, left bank of the Grabowiec creek in Chodenice, was investigated as far as 50 years ago (Parachoniak 1954).

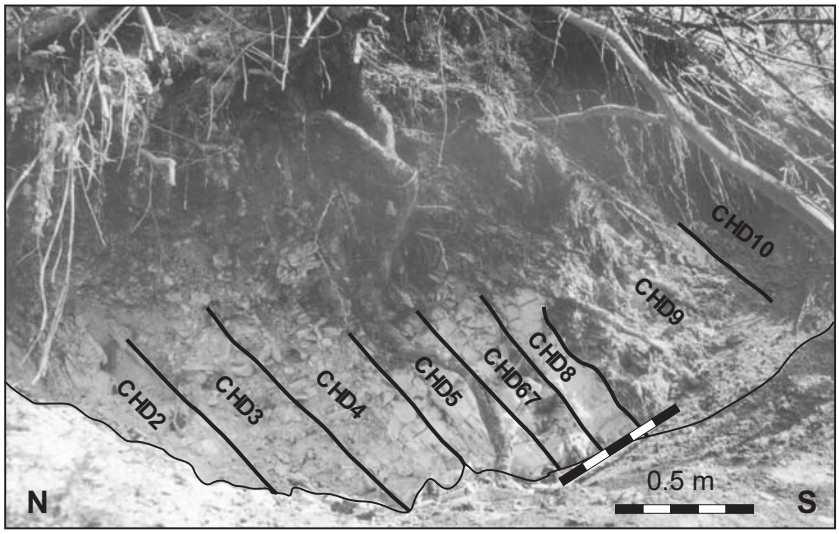


Fig. 3. The investigated outcrop in Chodenice with the distinguished tuff (CHD2–CHD8) and marly (CHD9, CHD10) layers

Presently the outcrop is significantly smaller, not more than three metres in length and around one metre in height (Fig. 3). Field work resulted in distinguishing several layers of pyroclastic sediments (CHD1–CHD8) and two adjacent layers of marly clays (CHD9 and CHD10) at the southern edge of the outcrop, all of them dipping to the south at steep angles of about 60–70°. The layers CHD2, CHD4 and CHD8 represent hell-grey or even whitish, medium-grained tuff, the layers CHD1, CHD3, and CHD67 — fine--grained, and the layer CHD5 — very fine-grained material. The layers of coarser (medium-grained) tuff are somewhat thicker (up to 30 cm), devoid of lamination, and easily weather into loose debris and mineral grains. The fine-grained varieties are slightly darker and distinctly laminated, splitting into thin, relatively hard plates. All the layers distinguished were sampled for laboratory analyses.

METHODS

Samples of the tuff and adjacent marls were subjected to microscope observations in thin sections. Then, clay and heavy fractions were separated. The distinguished heavy fractions as well as coarser grains were examined under a binocular microscope, heavy minerals having been determined in grain mounts with a polarizing microscope. Polished thin sections and selected grains of main and accessory minerals were observed and analysed with the SEM/EDS apparatus.

Clay fractions (below 2 μm) were separated from coarser components of mechanically disintegrated rocks as relevant-size particles suspended in distilled water, thereafter sedimented and dried in evaporating dishes. Samples prepared in this way were subjected to X-ray powder diffraction, IR spectroscopy, DTA, SEM/EDS analyses,

and ICP chemical analyses for major and trace elements. ICP chemical analyses were also carried out for selected whole-rock samples.

Microscope observations were made with the Olympus BJ51 polarizing microscope, microphotographs were taken with a digital camera and processed with the AnalySIS computer program. Heavy minerals were separated in tetrabromoethane ($C_2H_2Br_4$, d = 2.97 $g \cdot cm^{-3}$) from the coarser grain fractions (> 0.0625 mm) of disintegrated samples.

X-ray analyses were made with a Philips X'pert APD PW 3020 diffractometer, using CuK_α radiation, and a graphite reflexion monochromator. The clay fractions were analysed in the form of powdered samples with randomly oriented grains as well as parallel oriented grains, sedimented from suspension on glass slides. The latter were also analysed after saturation with ethylene glycol and after heating to 500°C.

IR spectra were registered with a Bio-Rad FTS 165 Fourier Transform Infrared spectrometer. The clay fractions were prepared in the form of discs (1 mg of a sample pressed with 300 mg KBr) and self-supporting films, produced on Mylar foil, from several drops of a clay sample, earlier dispersed in distilled water with an ultrasonic disintegrator. After evaporation of water at a room temperature, thin layers of dried clay were separated out of the Mylar substratum. Self-supporting smectite films were placed in a FTIR gas cell, the spectra were registered during 60 seconds.

Differential thermal analysis was made with a Hungarian MOM Derivatograph-C; samples weighting 200 mg were heated in the temperature range 20–1000°C.

SEM/EDS analyses were made in the FESEM Laboratory of the Institute of Geological Sciences, Jagiellonian University, using a NORAN Vantage spectrometer coupled to a HITACHI S-4700 scanning electron microscope operating at 15 kV. Chemical analyses with the ICP method were made by the Activation Laboratory, Ancaster, Canada.

RESULTS

Microscope analysis revealed that the non-laminated, medium-grained tuff is composed of glass shards, crystals, and sparse rock fragments disseminated in clay matrix (Phot. 1). The main component of the clay matrix, displaying dark-brownish interference colours, is apparently smectite formed through alteration of the volcanic glass. The pumice- and obsidian-type shards are of dimensions of tiny ash and volcanic dust, generally below 0.2 mm. The obsidian shards often display characteristic parallel cleavage and fan-like bending. Feldspars and quartz, prevailing among the crystal components of the tuff analysed, usually occur as euhedral or subhedral tablets (feldspars) or sharp-edged, wedge-shaped broken fragments (quartz), up to 0.3–0.5 mm. The feldspars are sanidine, Na-Ca plagioclases as well as high-temperature anorthoclase, relatively rich in both Na and K (Table 1). Observations of disintegrated rock under binocular microscope revealed octahedral crystals of pyrogenic quartz, up to 0.5 mm (Phot. 2). Less frequent crystal components are colourless flakes of muscovite and/or hydromuscovite, and pale-brown ones of weathered biotite, with adjacent aggregates

TABLE 1

EDS analyses of glass, feldspars and biotite from medium-grained tuff, sample CHD8. Total iron as Fe_2O_3 in glass and feldspars, as FeO in biotite. Cations normalized to 24 oxygens in glass and feldspars and to 22 oxygens in biotite

Component	Glass 87-6-1	Feldspar 87-2-1	Feldspar 87-4-7	Biotite 8H-28-1	Biotite 8H-28-2	Biotite 8H-28-3
SiO_2	80.34	78.71	80.78	30.49	32.32	31.28
TiO_2				6.52	6.05	6.22
Al_2O_3	12.15	11.50	12.10	11.75	12.65	12.11
Fe_2O_3/FeO	1.63	3.45	1.50	36.81	34.58	35.65
MgO		0.35		4.05	4.54	4.41
CaO	0.98	1.18	0.78			
CuO				1.02	0.86	1.26
K_2O	2.89	3.13	2.85	9.01	8.75	8.87
Na_2O	2.01	1.46	1.99			
Cl		0.22		0.35	0.25	0.20
Total	**100.00**	**100.00**	**100.00**	**100.00**	**100.00**	**100.00**
Cations						
Si	10.211	10.110	10.247	5.425	5.620	5.507
Ti				0.872	0.791	0.823
Al	1.820	1.741	1.808	2.464	2.592	2.513
Fe	0.156	0.334	0.143	5.477	5.028	5.250
Mg		0.067		1.075	1.178	1.156
Ca	0.133	0.162	0.106			
Cu				0.137	0.114	0.168
K	0.468	0.513	0.461	2.045	1.940	1.992
Na	0.496	0.364	0.488			
Total	**13.284**	**13.291**	**13.253**	**17.495**	**17.263**	**17.409**

of dark-brown or opaque iron oxides. Accessory components are sparsely distributed green aggregates of glauconite and isometric, opaque crystals of ilmenite, in thin sections below 0.1 mm. Transparent heavy minerals are very rare and in thin sections practically indistinguishable.

Fine-grained tuff varieties, displaying distinct lamination on microscopic scale, are mostly composed of clay matrix and glass shards. Minor components are tiny flakes of micas and sparse, isolated crystals of quartz and feldspars, less abundant and smaller (0.1–0.2 mm) than in the medium-grained tuff.

The adjacent marls are yellow-brown, soft and plastic, with weak (CHD9) and more intensive (CHD10) reaction with diluted HCl. The sample CHD9 consists of clay minerals with sparse, tiny quartz grains (below 0.1 mm) and flakes of hydromuscovite. The second layer (CHD10) is mostly composed of microcrystalline carbonate mineral (proved to be dolomite in the X-ray analysis) with pale interference colours. Minor components are sharp-edged quartz grains, iron-oxide aggregates and bioclasts in the form of shell fragments.

The clay particles (below 2 μm), ubiquitous in all the tuff and marl samples examined, were analysed after having been separated from coarser components. The distinguished clay fraction accounts for 10–12 wt.% of the fine-grained tuff samples (CHD5, CHD67), but only for 2–3 wt.% of the medium-grained ones (CHD1, CHD2, CHD4, CHD8). X-ray diffraction patterns of clay samples demonstrate that the predominating component in all of them is smectite, with the main peak (d_{001}) at 15.44–15.73 Å in cases of randomly arranged crystals, and at 14.44–15.35 Å for oriented samples (Table 2). These differences may result from varying contents of interlayer water molecules, caused by drying of the material analysed. For the oriented samples the d_{001} peak was shifted to 17.17–17.51 Å after treatment with ethylene glycol, and to 9.82–10.05 Å after heating to 500°C. The X-ray patterns represent practically pure, swelling smectite with small admixture of quartz, indicated by a very weak peak at 4.27 Å (Fig. 4).

TABLE 2

Values of the first-order peak (d_{001}, in Å) in the clay fraction samples distinguished from the analysed tuff

Sample	Random	Oriented	Glycolated	Heated
CHD2cl	15.73	14.44	17.20	10.05
CHD4cl	15.51	15.02	17.51	10.04
CHD5cl	15.44	15.35	17.27	10.02
CHD8cl	15.56	14.99	17.17	9.82

The IR spectra of the clay samples were identified with help of widely known published data (Moenke 1962; Van der Marel, Beutelspacher 1976); the registered absorption bands are listed in Table 3. The spectra of samples dispersed in KBr discs display strong maxima at 470, 525 and 1057 cm^{-1}, related to Si-O and Al-O structural stretching vibrations in tetrahedral layers, and several weak ones in the range 600–940 cm^{-1}. Distinct absorption bands at 1635 and 3400 cm^{-1} indicate the presence of H_2O molecules, whereas a sharp maximum around 3620 cm^{-1} is due to stretching vibrations of the OH groups (Fig. 5). In the self-supporting film spectra the 470, 525 and 1057 cm^{-1} peaks are extremely high, but the remaining ones appear more distinct, enabling their precise determination (Table 3, Fig. 6). The maximum at 800 cm^{-1}, together with slight inflexion of the spectrum around 780 cm^{-1} apparently mark a small admixture of quartz pelite. The absorption bands at 840 and 917 cm^{-1} are related to Mg-OH and Al-OH

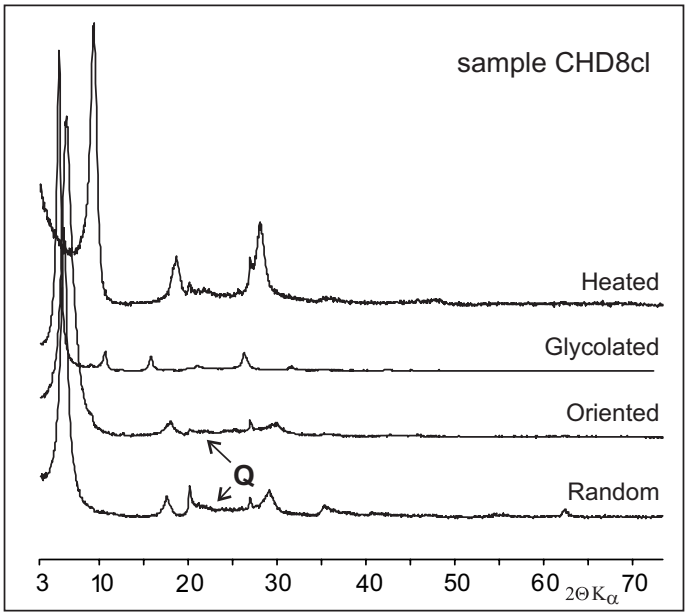


Fig. 4. X-ray patterns of clay fraction (sample CHD8cl) separated from medium-grained tuff

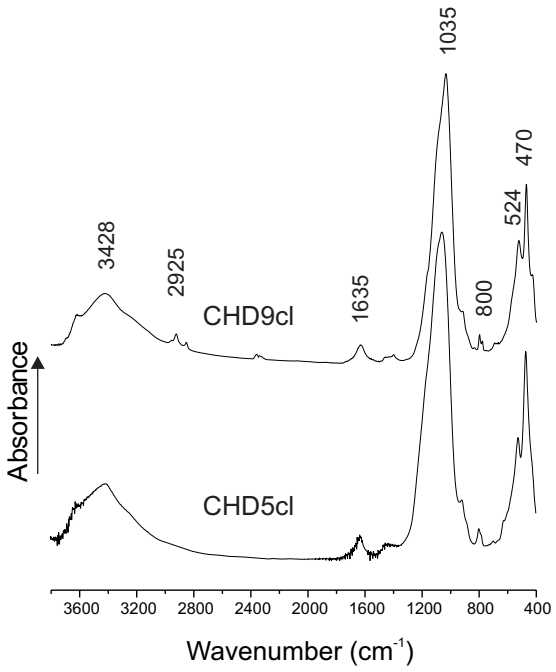


Fig. 5. IR spectra of clay fractions — samples CHD5cl and CHD9cl in KBr discs

TABLE 3

Absorption peaks (in cm^{-1}) in the IR spectra of the clay fractions; information on sample preparation (KBr discs or self-supporting films) in brackets

CHD5cl (KBr)	CHD5cl (film)	CHD67cl (film)	CHD8cl (film)	CHD4cl (film)	CHD2cl (film)	CHD9cl (KBr)	CHD9cl (film)
	405			405	420	431	
470						471	
525						524	
				627			
		692					780
799	800	799	799	800	800	800	800
	844	838	843	844	840		837
911	917	917	917	915	916	911	917
1 057						1 035	
1 630	1 635	1 635	1 635	1 635	1 634	1 635	1 635
3 413	3 400	3 400	3 400	3 400	3 400	3 428	3 400
3 629	3 625	3 622	3 622	3 622	3 622		3 622

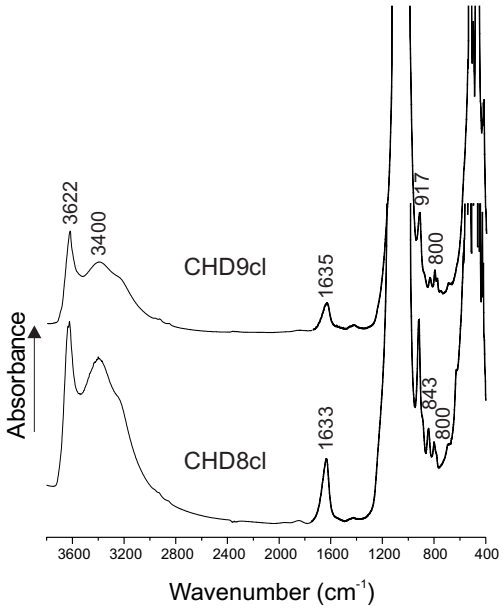


Fig. 6. IR spectra of clay fraction — samples CHD8cl and CHD9cl as self-supporting films

deformation vibrations in octahedral layers. The above listed H_2O and OH vibrations could be precisely ascertained to 1635 (H_2O bending vibrations), 3400, and 3622–3625 cm^{-1}. The whole IR absorption spectra of selected samples are presented in Figs 5 and 6.

DTA patterns of three clay samples analysed indicate strong endogenic effects around 140°C, accompanied by 9% of loss on weight in the temperature range 20–200°C, related to physically adsorbed and interlayer water. Lower, though systematic loss on weight of 4.0–4.5% was registered in the TG curves in the range 200–700°C. Small endogenic effects on the DTA curve around 540 and 685°C are related to dehydroxylation of illite and pure montmorillonite layers, respectively (Wyrwicki 1988). Total loss on weight amounts to 12% in the case of the clay fraction from the CHD9 marl sample and to around 14–15% for the clays from the tuff samples (Fig. 7).

Chemical analyses of clay samples, performed with the ICP method, are presented in Table 4. Normalization of the oxide contents led to a general formula:

$$K_{0.11}Na_{0.04}Ca_{0.09}Mg_{0.23}Fe_{0.16}Al_{1.22}Si_{4.30}O_{10}(OH)_2 \cdot 2.3H_2O$$

Such results indicate a certain excess of SiO_2, accompanied by a deficit of exchangeable cations (K, Na and Ca). The excess of silica is presumably due to admixtures of quartz pelite and acid, silica-rich volcanic glass, whereas the cations could have been partly removed during separating of clay fractions from coarser particles in distilled

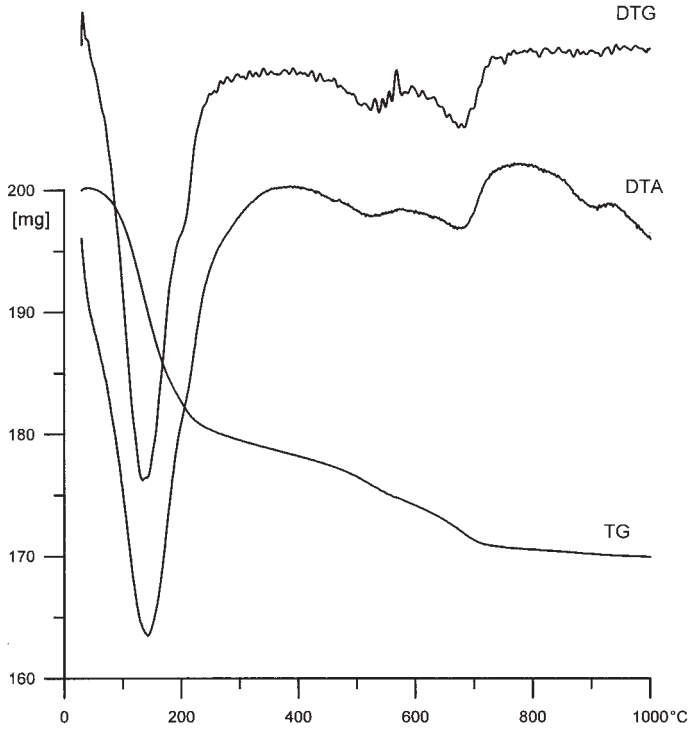


Fig. 7. DTA, DTG and TG curves for clay fraction — sample CHD5cl

TABLE 4

ICP chemical analyses of clay fractions distinguished from the analysed tuff samples.
Total iron as Fe_2O_3, cation contents normalized to 11 oxygens

Component \ Sample	CHD5cl	CHD8cl	CHD67cl	CHD9cl
SiO_2	62.39	55.35	63.50	54.35
Al_2O_3	15.09	16.71	13.99	16.10
Fe_2O_3	3.01	4.31	3.09	7.90
MnO	0.03	0.01	0.01	0.04
MgO	2.21	2.59	2.04	2.45
CaO	1.04	1.51	1.23	1.28
Na_2O	0.34	0.27	0.32	0.26
K_2O	1.31	0.72	1.50	2.68
TiO_2	0.25	0.21	0.28	0.51
P_2O_5	0.04	0.13	0.05	0.22
LOI	14.45	18.39	14.07	14.25
Total	**100.16**	**100.20**	**100.08**	**100.04**
Cations				
Si	4.27	4.01	4.33	3.88
Al	1.22	1.43	1.12	1.35
Fe	0.15	0.24	0.16	0.42
Mn	0.00	0.00	0.00	0.00
Mg	0.23	0.28	0.21	0.26
Ca	0.08	0.12	0.09	0.10
Na	0.05	0.04	0.04	0.04
K	0.11	0.07	0.13	0.24
Ti	0.01	0.01	0.01	0.03
P	0.00	0.01	0.00	0.01
Total	**6.12**	**6.21**	**6.09**	**6.33**

water. Loss on weight of around 15 wt.%, in perfect agreement with the DTA results, accounts for two OH groups and 2.3 H_2O molecules pfu. The EDS data, regardless of non registered water content, indicate similar proportions of major oxides and cations as the chemical analyses.

Accessory heavy minerals proved to be more abundant in the medium-grained tuff layers (CHD2, CHD4, and CHD8) than in the fine-grained ones (CHD5 and CHD67).

The predominating component of the heavy fraction is ilmenite, occurring in form of black, rhombohedral tablets, the largest reaching 0.3 mm (Phot. 3), but most of them being below 0.1 mm. The ilmenite crystals contain small admixtures of MgO, MnO (each around 1.5 wt.%), and V_2O_5 (below 0.8 wt.% — see Table 5). Other opaque

TABLE 5

EDS chemical analyses of heavy minerals from sample CHD8. Total iron as Fe_2O_3 in tourmaline and as FeO in staurolite, garnet, and ilmenite analyses. Cation contents normalized to 24 oxygen atoms

Sample / Component	Tourmaline 8H-11-1	Tourmaline 8H-17-1	Tourmaline 8H-23-1	Staurolite 8H-25-1	Garnet 8H-32-1	Ilmenite 8H-1-1	Ilmenite 8H-4-3
SiO_2	43.47	43.93	42.85	26.31	34.71		
TiO_2	0.73	0.82	0.82	0.91	0.23	48.11	48.38
Al_2O_3	34.05	38.34	34.57	52.12	18.97	0.42	
Fe_2O_3/FeO	7.60	3.77	7.90	16.99	25.98	47.66	48.28
V_2O_5						0.71	0.49
MgO	8.99	8.99	8.20	1.03	1.52	1.76	1.44
MnO				0.84	16.08	1.34	1.41
CaO	0.56	1.02	0.51		1.15		
Na_2O	2.81	2.09	2.93				
CuO	0.98	1.04	1.16	1.80	1.36		
ZnO	0.81		1.06				
Total	**100.00**	**100.00**	**100.00**	**100.00**	**100.00**	**100.00**	**100.00**
Cations							
Si	5.965	5.909	5.903	3.852	5.817		
Ti	0.075	0.083	0.085	0.101	0.030	7.365	7.445
Al	5.507	6.077	5.612	8.992	3.748	0.101	
Fe	0.785	0.381	0.818	2.081	3.642	8.115	8.261
V						0.096	0.066
Mg	1.840	1.802	1.684	0.224	0.380	0.534	0.440
Mn				0.104	2.284	0.230	0.244
Ca	0.083	0.147	0.075		0.207		
Na	0.749	0.546	0.783				
Cu	0.102	0.106	0.121	0.199	0.172		
Zn	0.082		0.108				
Total	**15.188**	**15.051**	**15.189**	**15.553**	**16.280**	**16.441**	**16.456**

components of the heavy fraction are dark-brownish, relatively loose and porous aggregates of secondary iron oxides.

Microscope inspection of grain mounts enabled to identify such transparent minerals as zircon, apatite, tourmaline, rutile, monazite, garnet, staurolite, and biotite. Zircon crystals generally occur as euhedral, elongated prisms up to 0.2 mm in length (Phot. 4), while small (0.05 mm), rounded grains (Phot. 5) are significantly less frequent. Most of the analysed zircons are pure $ZrSiO_4$, only some of the euhedral crystals contain small amounts of HfO_2, up to 2.22 wt.%, i.e. less than 0.02 Hf pfu. Apatite was observed in form of euhedral prisms (Phot. 6), chemically pure. Tourmaline, staurolite, garnet and rutile were observed only as sharp-edged fragments of broken crystals; chemical analyses are presented in Table 5. Monazite, observed only in few grains, displays numerous isomorphic admixtures of REE (Table 6). SEM/EDS analyses of a polished thin section allowed detecting submicroscopic inclusions of Ni-Fe rich phases (Phot. 7). The chemical analyse indicates 95.60% Ni, 2.75% Fe, and 1.65% Si (in wt.%), the last value could have been from the surrounding silicate. Such a Ni/Fe ratio indicates Ni-rich taenite.

TABLE 6

EDS chemical analysis of monazite from sample CHD8 (8H-21-1). Cation contents normalized to 24 oxygen atoms

Component	SiO_2	P_2O_5	ThO_2	CaO	La_2O_3	Ce_2O_3	Nd_2O_3	Sm_2O_3	Gd_2O_3	Pr_2O_3	Total
Oxide content [wt.%]	0.31	36.17	6.01	2.25	10.18	27.94	10.09	2.40	1.16	3.49	100.00
Cation	0.066	6.537	0.292	0.515	0.802	2.184	0.769	0.176	0.082	0.272	11.695

Chemical analyses of whole-rock samples are presented in Table 6. High content of silica (over 70 wt.%) and relatively high amounts of alkalis (over 2.0% Na_2O and over 2.5% K_2O) indicate acid composition of the analysed tuff from Chodenice.

CONCLUDING REMARKS

Mineral and chemical composition of the investigated tuff samples indicate strongly acid character of the parent material. Abundant pyrogenic components, like glass shards, high-temperature alkali feldspars, euhedral, pseudo-hexagonal biotite flakes, and bipyramidal quartz, record its volcanic origin (Fisher, Schmincke 1984). This is also supported by mineral composition of the heavy fractions and euhedral shapes of predominating components (ilmenite, zircon). On the other hand, an admixture of rounded grains of zircon and broken fragments of metamorphic minerals (garnet, staurolite) indicate more complex origin of the sediments analysed. Crypto-inclusions

TABLE 7

Chemical analyses of whole-rock samples of the tuff from Chodenice

Component \ Sample	CHD2r	CHD5r	CGD67r	CHD8r
SiO_2	75.89	70.78	70.55	70.35
Al_2O_3	10.55	12.30	12.46	12.71
Fe_2O_3	1.54	1.63	1.59	1.39
MnO	0.032	0.029	0.026	0.031
MgO	0.36	0.63	0.69	0.53
CaO	0.94	1.01	1.04	1.19
Na_2O	2.31	2.18	2.03	2.62
K_2O	2.52	2.71	2.61	2.64
TiO_2	0.167	0.149	0.133	0.156
P_2O_5	0.04	0.03	0.03	0.04
LOI	5.71	8.13	8.59	7.93
Total	100.06	99.58	99.75	99.59

of a metallic, Ni-Fe-rich phase, presumably of cosmic origin, record a fall of extra--terrestrial matter during the sediment formation. Ubiquitous smectite, practically of the same composition in subsequent tuff layers, points out to advanced alteration of the volcanic glass in rather uniform, sub-marine conditions.

Sequence of the distinguished tuff layers, granularity, size distribution and other textural features indicate that the whole series analysed represents at least three subsequent volcanic events. Direct contact of the medium-grained tuff with the overlying marly clays demonstrates that the whole complex in the area of the discussed outcrop in Chodenice is reversed (Parachoniak 1954; Dudek, Bukowski 2002). Small and relatively uniform dimensions of the sediment components suggest rather a distant eruption source, apparently in the neighbouring Carpathians. As published radiometric datings of zircon and biotite from the Bochnia Tuff from Chodenice give the ages slightly over 12 Ma (Van Couvering et al. 1981; Wieser et al. 2000), these pyroclastic sediments could be related to the Carpathian post-orogenic volcanism.

Acknowledgement. This study was financially supported by the Polish Committee for Scientific Research (KBN), grant no 6 PO4 D 089 21.

REFERENCES

ALEXANDROWICZ S.W., 1961: Stratygrafia warstw chodenickich i grabowieckich w Chełmie nad Rabą. *Kwart. Geol.* 5, 3, 646–668.

ALEXANDROWICZ S.W., PAWLIKOWSKI M., 1980: Policykliczny poziom tufitowy w miocenie okolic Gliwic. *Kwart. Geol.* 24, 663–678.

ALEXANDROWICZ S.W., 1997: Lithostratigraphy of the Miocene deposits in the Gliwice area (Upper Silesia, Poland). *Bul. Pol. Acad. Sc., Earth Sc.* 45, 168–179.

DUDEK K., BUKOWSKI K., 2002: New data on the Bochnia tuff from Chodenice, Forecarpathians, Poland. *Pol. Tow. Mineral. Prace Spec.* 20, 85–87.

FISHER R.V., SCHMINCKE H.-U. 1984: Pyroclastic Rocks. Springer, Berlin.

MOENKE H., 1962: Mineralspektren. Akademie Verlag, Berlin.

PARACHONIAK W., 1954: Tortońska facja tufitowa między Bochnią a Tarnowem. *Acta Geol. Pol.* 4, 67–92.

PARACHONIAK W., 1962: Mioceńskie utwory piroklastyczne przedgórza Karpat Polskich. *Pr. Geol. Kom. Nauk. Geol. PAN Oddz. w Krakowie*. 11, 7–77.

PARACHONIAK W., PAWLIKOWSKI M., 1980: Hornblenda z tufitu andezytowego z Wieliczki. *Spraw. z Pos. Kom. Nauk. PAN Oddz. w Krakowie*. 21, 2, 127–128.

PORĘBSKI S.J., 1999: Środowisko depozycyjne sukcesji nadewaporatowej (górny baden) w rejonie Kraków–Brzesko (zapadlisko przedkarpackie). *Prace PIG* 168, 97–119.

VAN COUVERING I.A., AUBRY M.P., BERGGREN Q.A., BUJAK J.P., NAESER C., WIESER T., 1981: Terminal Eocene event and Polish connections. *Palaeogeography. Palaeoclimatology, Palaeoecology* 36, 321–362.

VAN DER MAREL H.W., BEUTELSPACHER H., 1976: Atlas of infrared spectroscopy of clay minerals and their admixtures. Elsevier, Amsterdam.

WIESER T., BUKOWSKI K., WÓJTOWICZ A., 2000: Korelacja mineralogiczna i wiek radiometryczny tufitu z warstw chodenickich z okolic Bochni. *V Ogólnopolska Sesja Naukowa: Datowanie Minerałów i Skał, Kraków, 11.02.2000*. 50–55.

WYRWICKI R., 1988: Analiza derywatograficzna skał ilastych. Wyd. UW, Warszawa.

Krzysztof DUDEK, Krzysztof BUKOWSKI, Wiesław HEFLIK

CHARAKTERYSTYKA MINERALOGICZNA TUFITU Z BOCHNI Z WARSTW CHODENICKICH (ZAPADLISKO PRZEDKARPACKIE, S POLAND)

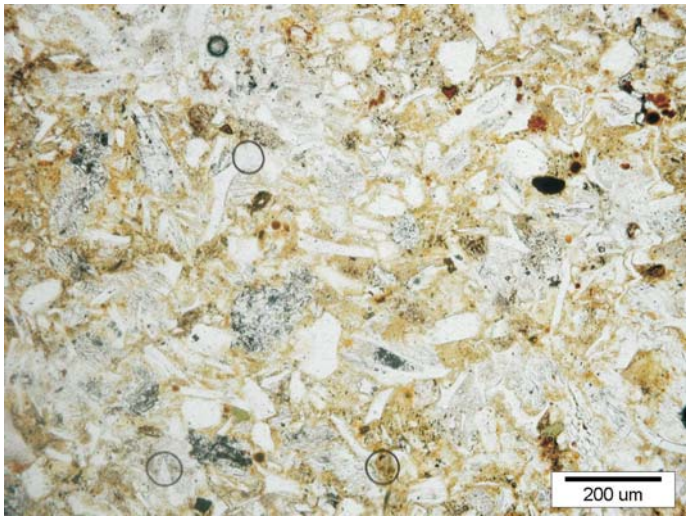
Streszczenie

Analizom mineralogicznym i chemicznym poddano próbki tufitu z Bochni (TB), pobrane z naturalnego odsłonięcia w Chodenicach. Główne składniki tej skały to okruchy szkliwa wulkanicznego, krystaloklasty kwarcu i skaleni oraz mieszanopakietowy Ca-Na-smektyt, będący produktem wietrzenia szkliwa. Wydzielone frakcje ilaste poddano analizie dyfraktometrycznej (wraz z glikolowaniem i prażeniem preparatów orientowanych), spektroskopii absorpcyjnej w podczerwieni, termicznej analizie

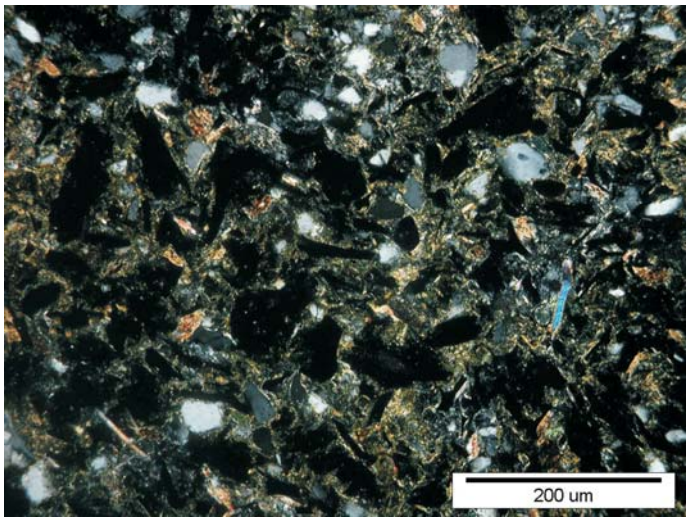
różnicowej, mikroskopii elektronowej (wraz z analizą EDS) oraz analizie chemicznej metodą ICP. W wydzielonej frakcji ciężkiej zidentyfikowano ilmenit (główny składnik), cyrkon, wtórne agregaty wodorotlenków żelaza oraz pojedyncze kryształy (lub ich pokruszone fragmenty) apatytu, turmalinu, rutylu, monacytu, granatu i staurolitu. Analizy SEM/EDS ujawniły krypto-inkluzje metalicznej fazy niklowo-żelazowej, zapewne pochodzenia pozaziemskiego.

Uziarnienie i inne cechy teksturalne analizowanego osadu świadczą o stosunkowo dalekim transporcie drobnego materiału wulkanicznego, zapewne z sąsiednich Karpat. Skład mineralny i chemiczny skał oraz publikowane wyniki datowań radiometrycznych wskazują, że analizowany osad piroklastyczny jest zapewne produktem kwaśnego wulkanizmu postorogenicznego.

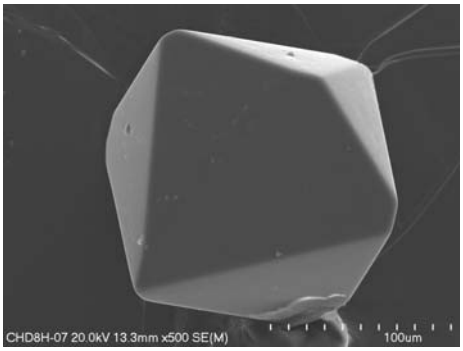
a)



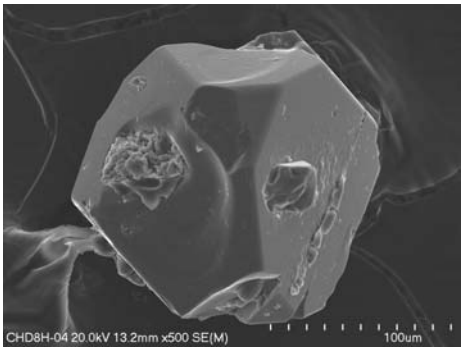
b)



Phot. 1. Microphotograph of medium-grained tuff (sample CHD8)
a — plane polarized light; b — crossed polars



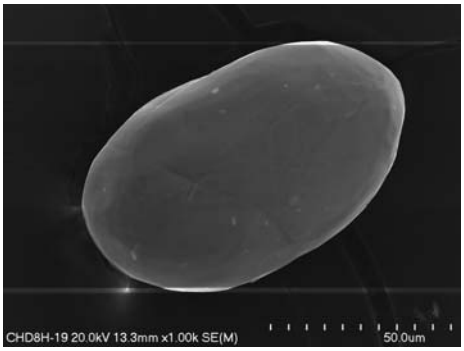
Phot. 2. SEM image of bipyramidal quartz



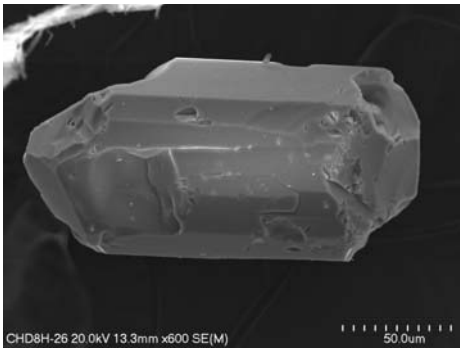
Phot. 3. SEM image of ilmenite euhedral crystal with included apatite (right from the centre)



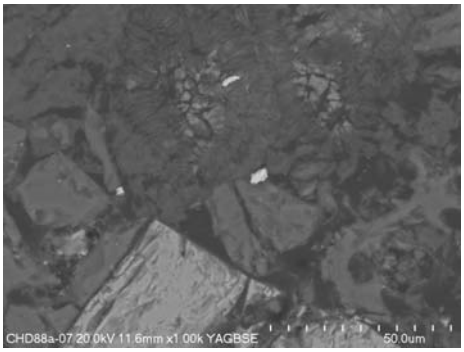
Phot. 4. SEM image of zircon euhedral crystal with apatite overgrown (in lower part of the zircon prism)



Phot. 5. SEM image of rounded zircon grain



Phot. 6. SEM image of apatite broken crystal



Phot. 7. SEM image of metallic Ni-Fe phases (white spots in the centre)

MINERALOGIA POLONICA
Vol. 35, No 2, 2004
PL ISSN 0032-6267

Beata DZIUBIŃSKA[1], *Wojciech NARĘBSKI*[1]

SIDERITE CONCRETIONS IN PALEOCENE SERIES OF POLISH PART OF THE EASTERN FLYSCH CARPATHIANS

A b s t r a c t . The present paper deals with the results of studies of siderite concretions occurring in black Paleocene shales of the Dukla and Silesian Units. The samples were examined using optical and scanning microscopy, X-ray diffraction and chemical analysis (SEM-EDS, INNA, ICP and estimation of TOC). The main diagenetic minerals of these concretions are iron carbonates close to siderite. Less common are dolomite, ferrous dolomite and calcite. The first phases precipitated from pore solutions were carbonates enriched in manganese. The concretions studied contain up to 49.15 wt.% Fe_2O_3, at most 16.46 wt.% CaO and up to 8.49 wt.% MgO, whereas the content of organic carbon (TOC) is at most 1.42 wt.%. Sideritic concretions of Paleocene beds of the eastern part of the Flysch Carpathians represent, in fact, sideroplesites and manganospherites of early diagenetic origin. They are, in general, impoverished in all trace elements, except Sr, when compared with shales embedding them. The siderite-bearing series in question can be assigned to the siderite-pyrite and siderite geochemical facies.

Key-words: siderite concretions, Flysch Carpathians, diagenesis

INTRODUCTION

Siderite concretions are fairly common in the Flysch Carpathians and some their occurrences were reported already by Pusch (1836) in his Atlas. The formation of these concretions was related to specific conditions of sedimentation and diagenesis in geosynclinal basin as noticed by Narębski (1956, 1957), who examined in detail numerous occurrences of carbonate concretions and published pioneer papers on geochemical aspects of their origin in the Outer Carpathians. This problem was also studied by Gucwa and Wieser (1978), Muszyński et al. (1979), Rajchel and Szczepańska (1997) and Szczepańska (1998). These papers were referring mainly to carbonate concretions in the Skole Unit and other local occurrences. Narębski (1956) was the first to indicate ferrous dolomitic nature of concretions from Menilite (near Komańcza) and Transition Beds (near Wetlina) of the Dukla Unit. Thus, the current paper can be considered as supplementary to the mentioned publications.

[1] Jagiellonian University, Institute of Geological Sciences, ul. Oleandry 2a, 30-063 Kraków, Poland.

The present studies refer to the concretions occurring in Paleocene black shales of the Dukla and Silesian Units, called Majdan Beds and Upper Istebna Beds, respectively. These series were examined in detail by Ślączka (1958, 1971).

The concretions in black shales are lenticular in shape or occur as fairly continuous layers, 3–8 cm thick. Because of their hardness they often protrude from parent shales what facilitates their finding.

MATERIALS AND METHODS

The concretions examined show micritic texture and are dark grey with brownish tint on fresh surfaces but yellowish grey on weathered ones. For detailed mineralogical--geochemical studies six samples from three different cross-sections of the Dukla Unit were selected: the Jamista stream from Wisłok, the Roztoka stream from Maniów and the Solinka Górna stream from Wetlina, as well as (for comparison purposes) from one cross-section of southern part of the Silesian Unit: the Jabłonka stream from Bystre. The sampling sites are marked in Figure 1.

The samples selected were examined using optical and scanning microscopy, X-ray diffraction and chemical analyses (SEM-EDS, INNA, ICP and estimation of TOC).

Optical observations of universal thin sections were carried out using a polarizing ECLIPS E600 POL microscope produced by NICON. Morphology and chemical composition of individual grains were studied in the Laboratory of Electron Microscopy of the Jagiellonian University using a Japan JEOL JSM-5410 microscope and applying a NORAN VOYAGER 3100 EDS apparatus at the voltage 20 and 25 kV.

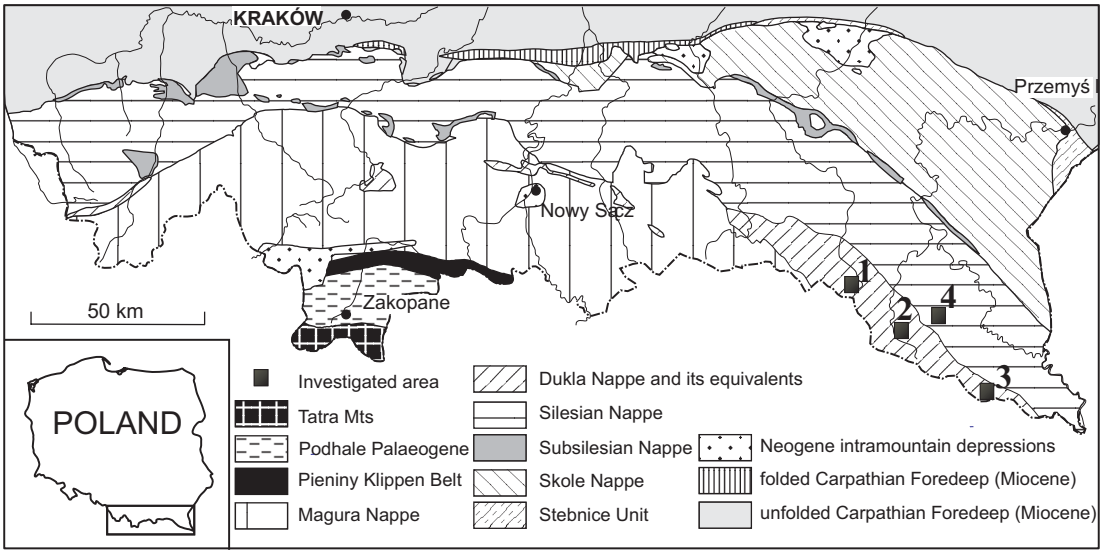


Fig. 1. Simplified geologic map of the Polish Outer Carpathians with marked location of sampling
1 — Wisłok, 2 — Maniów, 3 — Wetlina, 4 — Bystre

X-ray diffraction investigations of powdered samples were carried out using a Philips PW 1730 diffractometer, applying CuKα radiation at accelerating voltage 40 kV and anode current 30 mA.

Instrumental chemical analyses (INNA and ICP) were carried out in the Activation Laboratories Ltd., Ancester in Canada, using a 2MW Pool Type reactor, applying the Ge detectors ORTEC and CANBERRA and ICP spectrometers JARRELL ASH Enviro model and PERKIN ELMER model 6000.

The estimation of total organic carbon (TOC) was carried out using a LECO (USA) instrument after burning samples at 1250°C.

Detailed chemical data were obtained for three samples from the Dukla unit and one sample from the Silesian unit. In two samples (Wisłok and Maniów 2) the chemical data refer both to central and marginal parts of concretions.

RESULTS

Microscope observations have shown that the concretions consist of fine grains of carbonate minerals and clay material dispersed within the whole groundmass. Detrital quartz grains and framboidal pyrite occur in small amounts.

As follows from X-ray data, in three samples (Maniów 1, Maniów 2 and Bystre) siderite is the dominant mineral (Fig. 2a), whereas in two others (Wisłok and Wetlina) it

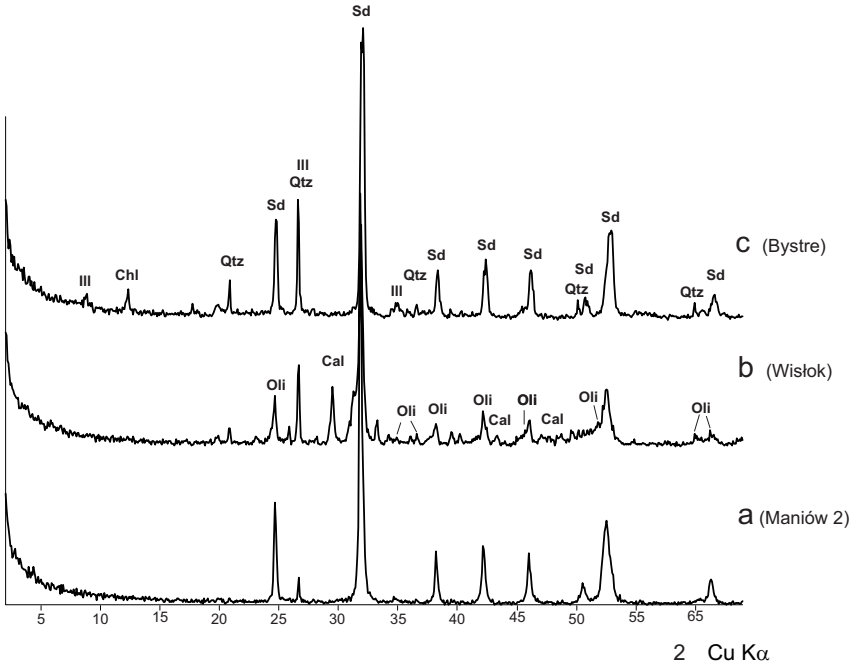


Fig. 2. X-ray powder diffraction patterns of siderite concretions studied
Cal — calcite, Chl — chlorite, Ill — illite, Oli — oligonite, Qtz — quartz, Sd — siderite

is accompanied by calcite. The latter carbonate dominates in the Wisłok sample, containing an oligonite admixture (Fig. 2b). X-ray data have also evidenced the presence of quartz, muscovite (illite) and chlorite admixtures, particularly abundant in the marginal part of the Maniów 2 sample (Fig. 2c).

Important data were obtained by means of observations with a scanning microscope, and particularly, point chemical analyses applying EDS countershaft. They have revealed that the idiomorphic, mainly Fe carbonates with an Mg, Ca and Mn admixture show the composition close to siderite (Phot. 1) and form pseudorhombohedral crystals, often rimming detrital, rounded quartz, calcite and, rarely, albitic feldspar grains (Phot. 2). Common are pyrite grains, forming both idiomorphic crystals and small framboids. Siderite crystals are of variable size (2–30 μm) and the smallest are often grouped in irregular aggregates (Phot. 3).

As follows from SEM-EDS analytical data, iron distinctly dominates among accompanying elements in the sideritic minerals:

$$Fe_{(1.08–1.6)}\,Mg_{(0.22–0.46)}\,Ca_{(0.1–0.27)}\,Mn_{(0.01–0.22)}\,(CO_3)_2 \quad (1)$$

$$Fe_{(0.8–1.3)}\,Mn_{(0.36–0.74)}\,Mg_{(0.17–0.28)}\,Ca_{(0.17–0.26)}\,(CO_3)_2 \quad (2)$$

It was noticed that the carbonates represented by formula (1) occur in outermost parts of individual crystals.

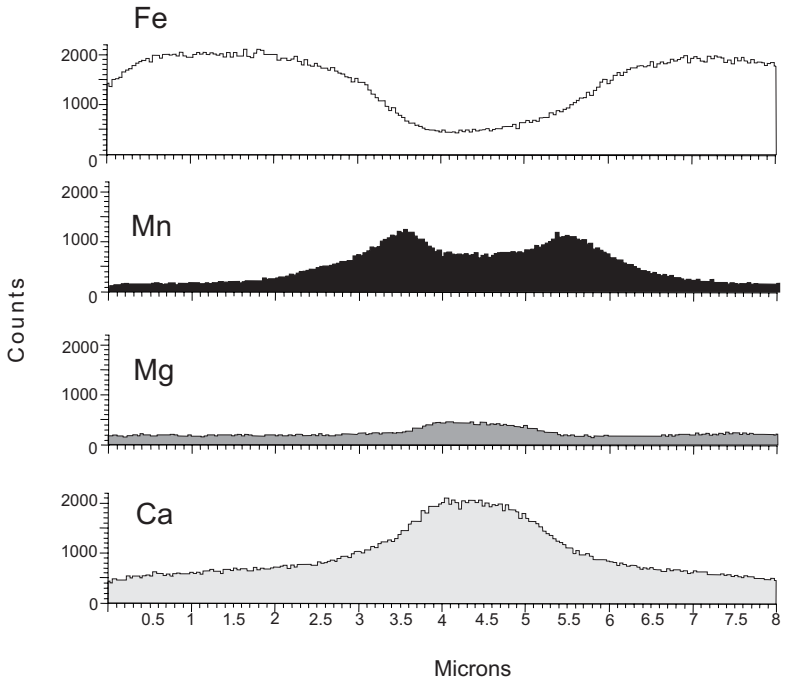


Fig. 3. Variations of Fe, Mn, Mg and Ca contents in a carbonate grain along the line marked in Phot. 4. (SEM-EDS analysis). Maniów 1 sample

In some of the concretions studied there also occur carbonates of different chemical composition, corresponding to dolomites and ferrous dolomites. Their general formula can be presented as follows:

$$Ca_{(0.81–1.11)}\, Mg_{(0.77–0.96)}\, Mn_{(0.02–0.70)}\, Fe_{(0.01–0.75)}\, (CO_3)_2$$

These minerals occur most commonly in the Wetlina sample and form crystallization centres of sideritic substance (Phot. 4).

A characteristic feature of all the samples is the enrichment in Mn of central parts of siderite crystals and at the contact with detrital grains, overgrown by siderite substance. These are the centres of crystallization of carbonates presented best in Figure 3. It was found that the Mn-enriched carbonates occur most abundantly in the Wisłok sample. These carbonates, close to rhodochrosite in composition, can be characterized by the following formula:

$$Mn_{(0.83–1.48)}\, Ca_{(0.31–0.53)}\, Fe_{(0.05–0.68)}\, Mg_{(0.1–0.43)}\, (CO_3)_2$$

Usually they form less regular grains (Phot. 3)

GEOCHEMISTRY

The chemical data of six samples of siderite concretions were correlated to those of the shales embedding them. It is comprehensible that their major elements considerably differ. The concretions are impoverished in SiO_2, Al_2O_3, Na_2O, K_2O and TiO_2 but enriched in Fe_2O_3, MnO, MgO, CaO and P_2O_5 (Table 1).

The content of SiO_2 varies within the limits 4.48–19.05 wt.% and the ranges of other elements are: 1.22–7.22 wt.% Al_2O_3, 012–0.84 wt.% Na_2O, 0.28–2.82 wt.%, K_2O and 0.07–0.35 wt.% TiO_2, whith the highest concentrations of these elements found in the Wetlina and Bystre samples, containing significant admixture of detrital material.

The contents of most abundant elements in the concretions studied vary within the below limits: 24.42–49.15 wt.% Fe_2O_3, 1.85–16.46 wt.% CaO, 0.34–8.49 wt.% MnO, 2.35–5.05 wt.% MgO and 0.08–5.41 wt.% P_2O_5. Some similarity of major element contents is noted between pairs of samples: Maniów 2 (middle part of the Dukla Unit) and Bystre (Silesian Unit) as well as Wetlina (eastern part of the Dukla Unit) and Wisłok (western part of the Dukla Unit). The highest contents of Mn (8.40 wt.% both in central and marginal part of the concretion) was found in the Wisłok sample, enriched in Mn carbonates.

The chemical data were recalculated into molecular percents in order to specify mineralogical character of the concretions studied. It was assumed that all Fe, Mg, Mn and Ca are bound with carbon dioxide in carbonates, although it cannot be quite correct as far as Fe and Mg are concerned, in view of the observed admixture of clay minerals. The results are presented in Table 2. For comparison purposes, the chemical composition and mineralogical character of siderite concretions from the Majdan Beds, analysed by W. Narębski, are detailed in Table 3.

TABLE 1

Chemical composition [wt.%] of siderite concretions and of shales embedding them

Sample	SiO_2	Al_2O_3	Fe_2O_3	MnO	MgO	CaO	Na_2O	K_2O	TiO_2	P_2O_5	LOI	TOTAL	S	TOC
WESTERN PART OF DUKLA UNIT														
Wisłok shale	54.68	19.39	5.84	0.03	2.54	1.04	0.71	3.27	0.82	0.11	11.59	100.02	0.22	0.89
Wisłok-conc-marginal	11.71	3.13	31.18	8.40	3.70	9.85	0.16	0.62	0.14	2.23	28.98	100.09	0.03	0.97
Wisłok-conc-centre	11.94	2.46	24.42	8.49	2.95	16.46	0.19	0.41	0.12	5.41	26.86	99.72	0.04	1.42
MIDDLE PART OF DUKLA UNIT														
Maniów 2-conc-margin.	19.05	4.75	40.23	1.19	4.57	3.11	0.26	0.57	0.32	0.08	25.97	100.10	0.22	0.38
Maniów 2-conc-centre	4.48	1.72	49.15	3.56	4.58	3.86	0.12	0.28	0.07	0.21	32.37	100.40	0.03	1.22
EASTERN PART OF DUKLA UNIT														
Wetlina shale	nd	14.98	9.50	0.06	1.68	8.61	0.57	6.91	0.57	0.16	nd	43.04	0.07	0.73
Wetlina-conc	nd	6.76	29.46	1.28	2.35	15.50	0.84	2.82	0.35	4.30	nd	63.66	0.18	0.26
SILESIAN UNIT														
Bystre-conc	17.08	7.22	40.15	0.34	5.05	1.85	0.13	1.23	0.35	0.17	26.51	100.09	0.21	1.11

nd — not determined.
conc — concretion.

TABLE 2

Molecular contents of individual carbonates and mineralogical nomenclature of the concretions studied

Sample	Lithostratigraphic horizon	$FeCO_3$	$MnCO_3$	$MgCO_3$	$CaCO_3$	Mineralogical name
Wisłok	Majdan Beds	40.31	13.32	6.96	23.49	manganospherite and calcite
Maniów 2	Majdan Beds	64.80	3.75	9.57	6.22	sideroplesite
Wetlina	Majdan Beds	42.72	2.02	4.92	27.68	sideroplesite and calcite
Bystre	Upper Istebna Beds	58.22	0.53	10.56	3.30	sideroplesite

TABLE 3

Chemical composition and mineralogical character of sideritic concretions (analysed by W. Narębski)

Sample	FeO	MnO	MgO	CaO	$FeCO_3$	$MnCO_3$	$MgCO_3$	$CaCO_3$	Mineralogical name
Majdan 1	17.69	0.82	4.36	6.44	28.51	1.33	9.12	11.50	sideroplesite
Majdan 2	15.43	0.56	3.32	5.13	24.86	0.91	6.94	9.16	sideroplesite
Wetlina 1	27.71	0.93	4.85	nd	44.65	1.51	10.15	—	sideroplesite
Wetlina 2	30.41	0.93	5.52	nd	49.00	1.51	11.55	—	sideroplesite

nd — not determined.

Molecular contents of individual carbonates in all the above samples are presented in the classification diagram (Fig. 4). The siderite concretions from the Dukla and Silesian Units studied are mainly sideroplesites from mineralogical viewpoint, except of manganospheritic character of the Wisłok sample. Similarly sideroplesitic in character are concretions from Paleocene beds of the Dukla Unit (Table 3).

The results of estimations of trace elements in siderite concretions and shales embedding them indicate in general that the former are impoverished in the vast majority of them, namely in Ni, V, Rb, Ba, Cu, Cr, Cs, Pb, Sc and Th, except of Sr (Fig. 5). The content of the latter element is at least two times higher in the concretions, which

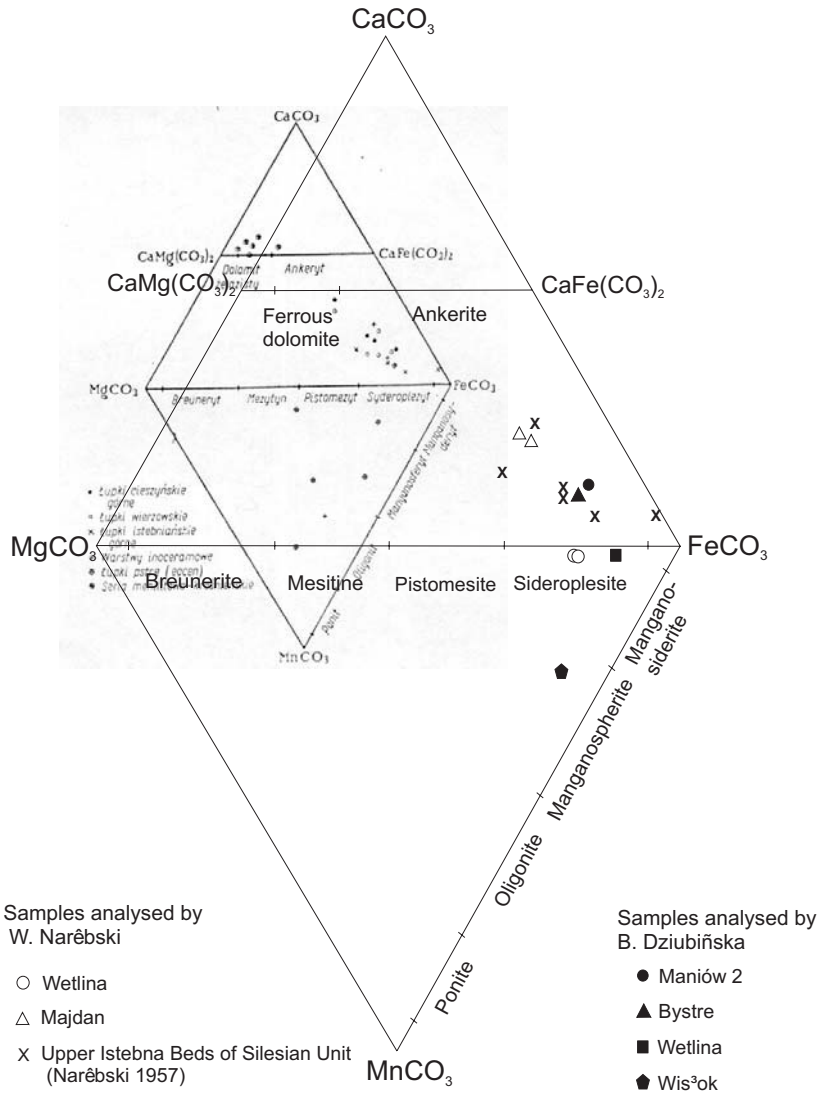


Fig. 4. Concretions from Paleocene series of the Dukla and Silesian Units in classification diagram

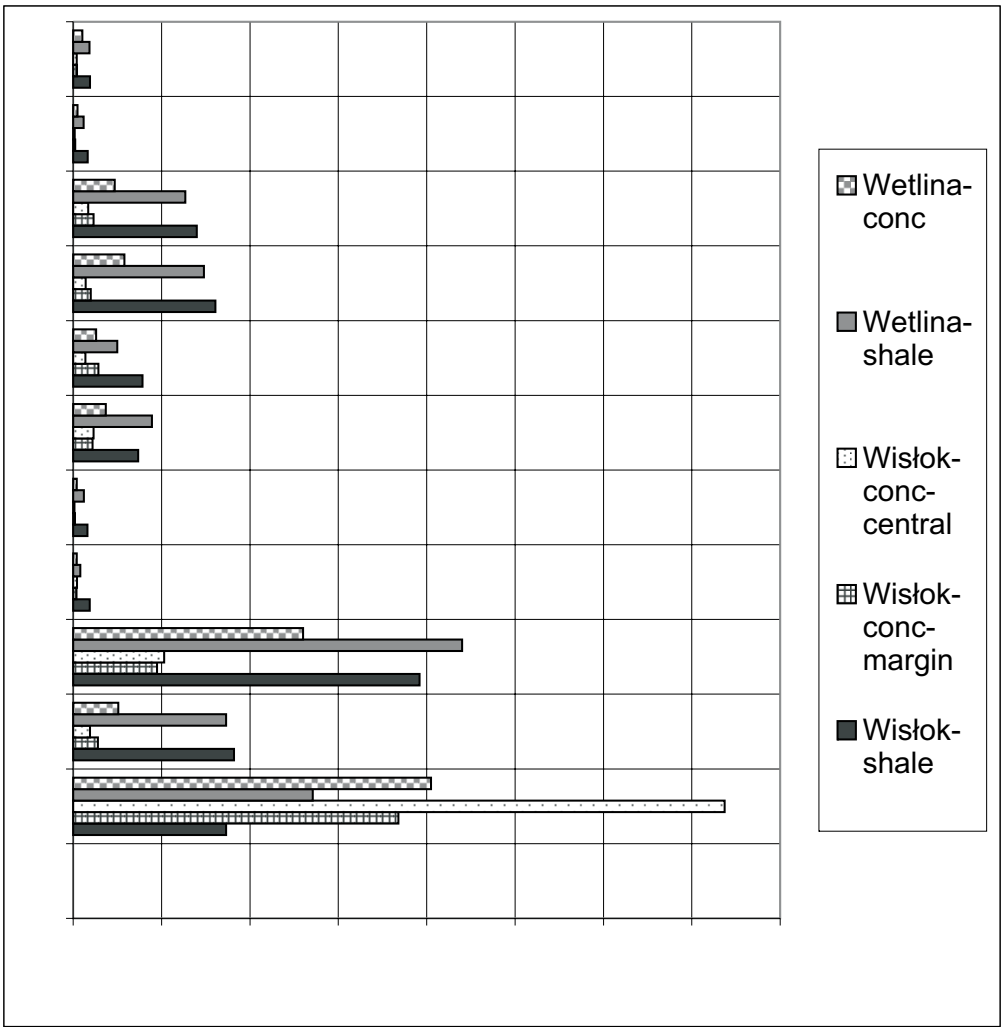


Fig. 5. Trace elements in selected concretions and containing them shales

can be explained by isovalent diadochy of Sr and Ca. Lower contents of trace elements in the concretions studied result from a small admixture of clay minerals, since the latter are usually enriched in them by sorption.

On the other hand, the concentrations of REE (La, Ce, Nd, Sm, Eu, Tb, Yb and Lu) in the concretions studied are higher than in the shales embedding them (Fig. 6). This is rather unexpected phenomenon since carbonate rocks and siderite concretions are, in general, impoverished in rare earth elements (e.g. Zodrow, Cleal 1999).

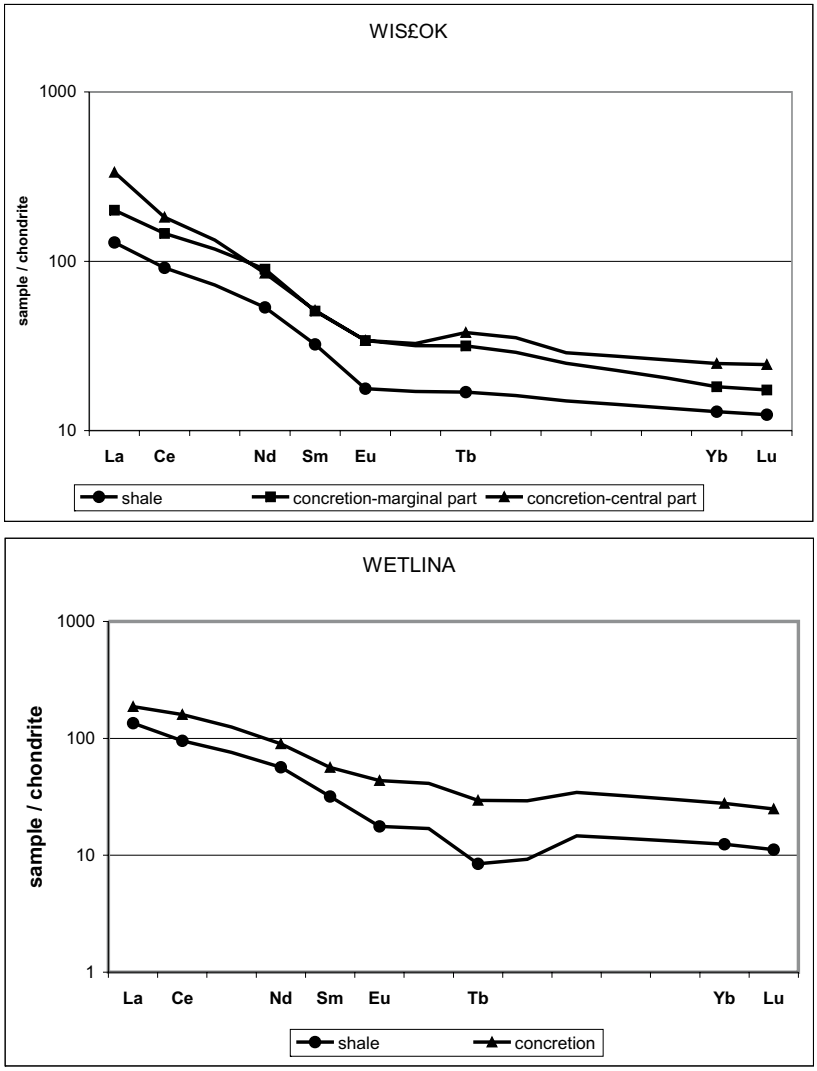


Fig. 6. Chondrite–normalized REE contents in selected concretions and containing them shales

ORIGIN OF SIDERITE CONCRETIONS

Siderites are formed under conditions of negative Eh values and high concentration of ferrous ions in the environment low in sulphate but high in carbonate anions and favouring the mobility of carbon dioxide. Organic matter is generally considered to be the main producer of carbonate ions in clay sediments. On the other hand, the supply of

this matter depends on microbiotic activity (Coleman 1985). Moreover, the amount of organic matter trapped in clay sediment depends also on its exposition to oxidizing sea water. Consequently, rapid sedimentation and short exposition of deposited clay minerals to sea water favour the entrapment of organic matter (Coleman 1993). In slowly accumulating sediments the majority of organic matter is, most probably, consumed at the water-sediment interface by sulphate reducing aerobic bacteria and anaerobic organisms (Gautier 1982). The presence of pyrite in slowly depositing clay sediments suggests, by analogy to recent deposits, that the depth of precipitation of siderite depends on the rate of sedimentation.

The genetic model presented follows the concept of Narębski (1957), described in detail in the monograph on mineralogy and geochemical conditions of origin of the so-called siderites of the Carpathian Flysch. It was based on the idea of sedimentary geochemical facies (Teodorovich 1949) and on the method of their identification by estimation of different forms of iron in pelitic deposits as well as on the character of early diagenetic concretions occurring in them (Strakhov 1953). In the opinion of Teodorovich (1949) geochemical siderite facies are usually related to near-shore or peri-insular zones of not very deep basins.

The dominant chemical elements of the concretions studied are iron and manganese. It is, therefore, necessary to characterise their geochemical behaviour in sedimentary environments.

One of typical features of siderite geochemical facies are slight fluctuations of the oxidation-reduction boundary within sedimentary environment, usually situated at the surface. of deposited material. The separation of iron from sialic part of the weathering material needs a transitional environment between reducing, H_2S-bearing, and oxidizing one. The dissolution of iron from weathering material and from surficial layer of sediments takes place in those benthic zones of basins where, due to poor ventilation and partial decomposition of organic remnants, the environment is distinctly enriched in carbon dioxide (Borchert 1952; Taupitz 1954). Iron — in the mobile form of hydroxide — is most intensely deposited in trough-like depressions of the bottom. Since sedimentation in geosynclinal basins is progressing fairly rapidly, the boundary of oxidizing and reducing zones usually moves quickly upwards. Colloidal concentrations of ferric hydroxide are in reducing environment and in the presence of carbon dioxide easily transformed into soluble ferrous bicarbonate $Fe(HCO_3)_2$. This form of iron, mobile in pore solutions of pelitic sediments, can be — under very variable conditions of flysch sedimentation — easily transformed into insoluble, anhydrous ferrous carbonate (siderite) when carbon dioxide is given off. This process, leading to the formation of siderite and similar concretions, proceeds within the freshly deposited sediments during their early diagenetic transformations, ordering chaotic distribution of their components. It should be emphasized that the main factor of these processes is bacterial decomposition of organic matter, being the source of active carbon dioxide and very effective reducing agent.

Manganese is oxidized at considerably higher redox potential than iron and, consequently, can be much more easily reduced to the divalent form. Therefore, its compounds dissolve more rapidly and can migrate at longer distances both in water

basin and in pore solutions. These geochemical properties of Mn control its often observed separation from iron and more rapid precipitation from solutions what was confirmed by detailed analytical studies of the concretions in question. As already stated, some unquestionably earlier formed central parts of these carbonate concretions are distinctly enriched in manganese.

Moreover, all the carbonate concretions studied are distinctly enriched in magnesium and, therefore, defined as sideroplesites. This is an important geochemical evidence of their marine origin since similar concretions, e.g. from Tertiary lacustrine fresh-water sediments of the Turów brown coal mine, are composed of nearly Mg-free siderites (Narębski 1974).

Summing up it is concluded that the black shales containing the sideroplesitic concretions studied should be generally assigned to marine siderite-pyrite facies, and, partly — due to local occurrence of manganospherite — to siderite facies.

CONCLUSIONS

Siderite concretions of Paleocene series of eastern part of the Flysch Carpathians are sideroplesites and manganospherites of early diagenetic origin. These series composed of black shale deposits should be assigned to siderite-pyrite and siderite facies.

Common occurrence of framboidal pyrite in the Majdan beds suggests more reducing conditions of their early diagenetic changes.

REFERENCS

BORCHERT H., 1952: Die Bildungsbedingungen mariner Eisenerzlagerstätten. *Chemie. d. Erde* 16, 1, 49–74.

COLEMAN M.L., 1985: Geochemistry of diagenetic non-silicate minerals: kinetic considerations. *Philosophical Transactions of the Royal Society of London*. 315 (series A), 39–56.

COLEMAN M.L., 1993: Microbial processes: Controls on the shape and oposition of carbonate concretions. *Marine Geology* 113, 127–140.

GAUTIER, D.L., 1982: Siderite concretions: indicators of early diagenesis in the Gammon shale (cretaceous). *Journal of Sedimentary Petrology* 52, 3, 859–871.

GUCWA I., WIESER T, 1978: Ferromanganese nodules in the Western Carpathian flysch deposits of Poland. *Rocz. Pol. Tow. Geol*. 48, 147–184.

MUSZYŃSKI M., RAJCHEL J., SALAMON W., 1979: Concretionary iron and manganese carbonates in Eocene shales of the environs of Dynów near Przemyśl (Flysch Carpathians). *Miner. Pol*. 9, 1, 111–122.

NARĘBSKI W., 1956: O diagenetycznych dolomitach żelazistych z Karpat fliszowych. *Rocz. Pol. Tow. Geol*. 26, 1, 29–50.

NARĘBSKI W., 1957: Mineralogia i geochemiczne warunki genezy tzw. syderytów fliszu karpackiego. *Arch. Miner*. 21, 5–100.

NARĘBSKI W., 1974: Mineralogia i geneza konkrecji sferosyderytowych północno-wschodniej części niecki żytawskiej. *Prace Muz. Ziemi* 22, 65–77.

PUSCH G. G., 1836: Geognostischer Atlas von Polen. J. G. Cotta Verlag.

RAJCHEL J., SZCZEPAŃSKA M., 1997: Dolomity żelaziste z warstw krośnieńskich jednostki skolskiej okolic Dynowa. *Geologia (Kwart. AGH)* 23, 229–248.

STRAKHOV N.M., 1953: Diagenesis of sediments and its significance for sedimentary ore formation. *Izv. AN SSSR Ser. Geol.* 5, 12–49 (in Russian).
SZCZEPAŃSKA M., 1998: Sferosyderyty z łupków spaskich jednostki skolskiej. *Przegl. Geol.* 46, 4, 342–347.
ŚLĄCZKA A., 1958: O pozycji geologicznej okruszcowania w okolicy Baligrodu. *Kwart. Geol.* 2, 4
ŚLĄCZKA A., 1971: Geologia jednostki dukielskiej. *Prace Inst. Geol.* 63, 1–124.
TAUPITZ K. CH., 1954: Über Sedimentation, Diagenese, Metamorphose, Magmatismus und die Entstehung der Erzlagerstätten. *Chemie. d. Erde* 17, 2*:* 104–164.
TEODOROVICH G.I., 1949: Marine and salt-water siderite geochemical facies as oil-perspective environment. *Doklady AN SSSR* 69, 2, 227–230 (in Russian).
ZODROW E.L., CLEAL CH.J, 1999: Anatomically preserved plants in siderite concretions in the shale split of the Foord Seam: mineralogy, geochemistry, genesis (Upper Carboniferous, Canada). *Intern. J. of Coal Geol.* 41, 371–393.

Beata DZIUBIŃSKA, Wojciech NARĘBSKI

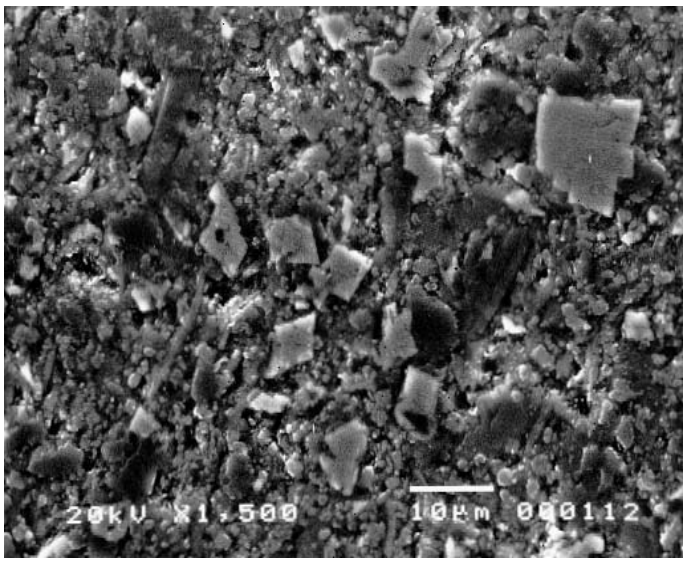
KONKRECJE SYDERYTOWE W WARSTWACH PALEOCEŃSKICH POLSKIEJ CZĘŚCI WSCHODNICH KARPAT FLISZOWYCH

Streszczenie

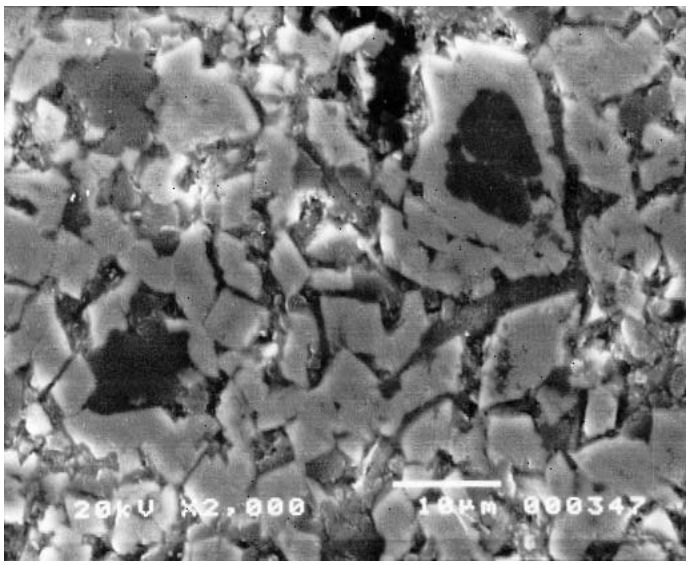
Badaniom poddano konkrecje syderytowe występujące w paleoceńskich czarnych łupkach jednostki dukielskiej i śląskiej — odpowiednio w warstwach z Majdanu i górnych łupkach istebniańskich. Próbki konkrecji poddano obserwacjom mikroskopowym (mikroskop optyczny i skaningowy), badaniom rentgenowskim i analizie chemicznej (SEM-EDS, INNA, ICP i oznaczeniu TOC).

Badania SEM-EDS wykazały, że głównymi minerałami diagenetycznymi są węglany żelaza zbliżone do syderytu, następnie dolomit, dolomit żelazisty i kalcyt. Węglany bogatsze w Mn krystalizują jako pierwsze z roztworów. Badane konkrecje zawierają do 49,15% wag. Fe_2O_3, do 16,46% wag. CaO, do 5,05% wag. MgO i do 8,49% wag. MnO, natomiast zawartość węgla organicznego (TOC) dochodzi do 1,42% wag.

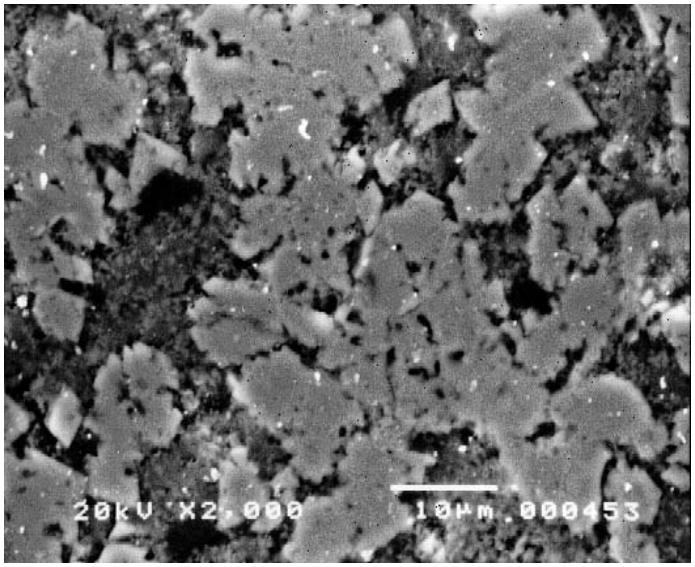
Konkrecje syderytowe warstw paleoceńskich wschodniej części Karpat fliszowych są głównie syderoplezytami i w znacznie mniejszym stopniu manganosferytami pochodzenia wczesnodiagenetycznego. Świadczy o tym m.in. wykazana analizami punktowymi zmienność składu chemicznego konkrecji od środka ku peryferiom, przy wzbogaceniu części centralnej w mangan. Badania geochemiczne wykazały niższe w stosunku do łupków zawartości wszystkich pierwiastków śladowych w konkrecjach z wyjątkiem diadochowego z wapniem strontu. Utwory te wraz z otaczającymi je łupkami można zaliczyć do facji syderytowo-pirytowej i syderytowej.



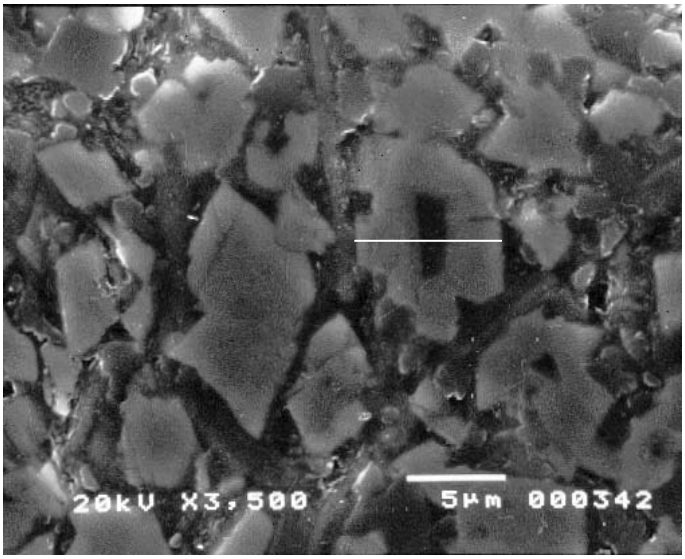
Phot.1. Idiomorphic siderite crystals (Wetlina sample)



Phot. 2. Idiomorphic siderite crystals rimming detrital grains (Maniów 1 sample)



Phot. 3. Idiomorphic siderite crystals, forming irregular aggregates (Wisłok sample)



Phot. 4. Idiomorphic siderite crystals (Maniów 1 sample).
Trace of linear analysis is marked — see Fig. 3

Acknowledgements

We would like to bring to kind notice of our Readers the fact that the two current issues of our journal (*Mineralogia Polonica* 35/1 and 2) have been edited due to the financial help of several institutions, whose sponsorship is duly acknowledged. The support came from:

- Ministry of Scientific Research and Information Technology, Warsaw,
- Faculty of Geology, Geophysics and Environment Protection, AGH University of Science and Technology, Cracow,
- KGHM Polska Miedź S.A., Lubin,
- Laboratory of Scanning Microscopy of Biological and Geological Sciences, Faculty of Biology and Earth Sciences, Jagiellonian University, Cracow,
- PANalytical B.V., Branch Poland, Warsaw,
- Geol-Min Ltd. – Ceramic Raw Materials, Kielce,
- THERMO Electron Corporation, Wien,
- The Stanisław Staszic Scientific Association, Cracow,
- COMEF – Scientific and Research Equipment; Katowice.

KGHM Polska Miedź S.A.

ul. M. Skłodowskiej Curie 48
59-301 Lubin, Poland

We are a company with deep traditions, rich in experience and numerous achievements. It is enough to mention that in 2001 we celebrated the 40th anniversary of the founding of KGHM, and a year later the 45th anniversary of the discovery of the copper deposit. Tradition, remembrance, caring for values – these are the foundations on which our current vision has been based. We shall always express our gratitude and honour the memory of those who discovered the copper deposit, and the pioneers who built KGHM.

The history of KGHM began with the discovery in 1957 by Jan Wyżykowski of a copper ore deposit in the vicinity of Lubin and Sieroszowice, in south-western Poland. Mining of this copper deposit on an industrial scale began in 1968. At that time KGHM functioned as a multi-divisional state-owned enterprise. Besides the mines and smelters it also included several dozen service facilities.

On 12th September, 1991 KGHM was transformed into a state-owned, joint stock company under the name KGHM Polska Miedź S.A. This was the first step in the later privatization of the company. In July 1997 the shares of the company debuted on the Warsaw Stock Exchange, while its GDRs (Global Depositary Receipts) appeared simultaneously on the London Stock Exchange. As at 31st December, 2003 the largest shareholders of KGHM were: the Polish State Treasury, which owned 44.28% of the share capital, the owners of Global Depositary Receipts (GDRs), to whom belonged 5.95% of the shares and PKO Bank Polski S.A., which held 5.38% of the shares of the Company.

The Lubin-Sieroszowice Mining zone is a world-class copper stratabound deposit. It lies near the Lower-Upper Permian boundary. The ore transgresses the geological strata at low angles. The economic deposit is composed of a dolomite type of ore, Kupferschiefer (black shale) ore and sandstone ore. The richest and thickest ore is in the Weissliegendes and occupies the central part of the zone. The deposit currently being mined extends over nearly 400 sq. km, varies in thickness from 0.4 to 26 m, and contains on average above 2.3% Cu, 47 ppm Ag, 0.2% Pb and 0.1% Zn. Anomalous concentrations of Co, Ni, As, Mo, Re, Se, Au and PGMs are also observed. It has been calculated that KGHM Polska Miedź S.A. owns a deposit containing 18 mln Mg of metallic copper and 46,000 Mg of Ag (proven reserves). The total geological copper reserves within the zone, having a potential of about 40 Mt of Cu, ranks as one of the largest ore deposits in the world.

KGHM is the largest copper producer in Europe to possess its own copper deposit and operate under a fully-integrated production structure, from initial mining to the final, high-quality product. The production of non-ferrous metals in KGHM is performed in three mining divisions (ZG Lubin, ZG Polkowice-Sieroszowice and ZG Rudna), two smelting/refining facilities

(HM Legnica and HM Głogów), a copper wire rod plant (HM Cedynia) and a precious metals plant (located within HM Głogów). Silver and other commodities appear in the excavated ore together with copper.

Current mining of this deposit is done at a level of from 650 to 1,150 m. KGHM will be in a position to mine at a level deeper than 1,150 m in a decade or so. Initiating mining at deeper levels requires the solving of problems connected with higher temperatures, which affects mining costs.

KGHM Polska Miedź S.A. is above all one of the largest companies in the world involved in the production of refined copper and silver. In 2003 KGHM produced 529,616 tonnes of copper (3.5% of world production, 7th place globally). This is mainly electrolytic copper, referred to as "four zeros copper" because of its quality (99.99 percent pure copper), and the more highly-processed wire rod, produced in accordance with the ISO 9002 norm. The cathode copper produced by the Company is registered as "Grade A" by the London Metal Exchange.

KGHM Polska Miedź S.A. is also amongst the world's top four silver producers – in 2003 silver production amounted to 1,223 tonnes (2nd place globally) – the silver being recognized as "Good Delivery – Silver" and traded both on the London Bullion Market as well as on the London Metal Exchange (the world's largest market for non-ferrous metals). Silver is the second most important product of the Company. It is sold in the form of granulate and bars. Thanks to this the silver produced by the Company may be used in bank settlements. Other products of KGHM include: gold, lead, sulphuric acid, rock salt, and others.

Copper in KGHM is mainly recovered from primary ore (the copper ore deposit), from which concentrate is obtained (containing app. 27% copper). This concentrate is next processed in the smelter/refineries into anode copper (app. 99% copper), and then undergoes electrolythical treatment to produce refined copper (containing 99.99% copper). This method is applied to produce copper from sulphide copper ores.

The Company has an independent commercial structure. Sales are carried out through the Commercial Department, and are assisted by two subsidiary companies: KGHM Polish Copper LTD in London and Kupferhandelsges. m.b.H. in Vienna (both are 100% owned by KGHM Polska Miedź S.A.). The main export markets include Germany, France, Great Britain, Austria and Belgium.

KGHM exports the majority of its production (with only a third of revenues arising from domestic sales). Despite the fact that KGHM is the main supplier of copper for Polish industry, it is not able to apply monopolistic practices with respect to its products. This is because Polish customers enter into contracts based on copper prices set by global markets.

The financial results of KGHM are dependent on global metals prices, as well as on the currency exchange rate. Nearly all revenues are expressed in foreign currencies, primarily the US dollar. Copper represents around 76% of sales in KGHM, while silver accounts for 18%. Remaining revenues come from the sale of gold, lead and other products. Copper sales are based on average monthly copper prices as set on the London Metal Exchange, plus a defined margin.

KGHM is a company which is continuously pursuing a program for growth and for cutting costs. The deep restructurization of KGHM enabled a reduction in employment from around 42,000 persons in 1992 to 17,994 at the end of 2003. This restructurization has also enabled the

separation from the core business of those activities not directly connected with the production of copper into subsidiaries, which in turn will eventually be disposed of. As a result of the costs cutting program, the total unit copper production cost was reduced from nearly 2,000 USD in 1995 to 1,603 USD in 2003. This fall in the unit cost was impacted by increased effectiveness in the mining of the deposit, a systematic increase in production volume and the rationalization of external costs.

The long term development program of KGHM anticipates a further expansion of current production and the production of other metals. The Company is aiming at optimum exploitation of its production capacity from its own resources, and is also seeking new resources outside of Poland. Normal practice for a company expanding abroad is to form a joint venture with other companies in this sector, although KGHM does not exclude the possibility of independent action in smaller projects. In 1997 a preliminary trial run at mining the rich copper and cobalt Kimpe deposit in the Republic of Congo was launched.

In pursuit of diversification of its activities, the Company invests in areas which have the potential to represent “strategic substitutes”, and which do not include metal production. At the moment the investments in telecommunications (Polkomtel, Telefonia Dialog) serve this purpose. In addition, KGHM is actively engaged in the growth of the local region by exploiting the economic strength of the Company and by supporting local entrepreneurship.

KGHM Polska Miedź S.A. is not only a modern company in the sense of the technology which it employs, but also in its adherence to environmental protection standards. Over the last ten years KGHM has been consistently carrying out a program of environmental protection, with total expenditure in this regard reaching over PLN 500 mln. As a result of investments carried out, the impact of the copper industry with respect to emissions of hazardous substances, waste flows and tailings has been reduced to a level achieved in the most highly-developed countries, with the Company having one of the cleanest industrial operations in Poland. In 2001, in a prestigious competition hosted by the Minister of the Environment, KGHM was honored with the title Leader of Polish Ecology for its project entitled “Protection of the atmosphere as an element of a complex system of environmental policy”. In 2001 KGHM was honoured with the title Environment Friendly Firm by the President of the Republic of Poland and the Minister of the Environment. In 2002 KGHM was honoured with the Gold Card of Work Leader by the Central Institute for Labour Protection, Warsaw.

We believe that we are – and wish to be seen as being – an effective, innovative and communicative European company, aimed at the realization of economic and environmental goals, pursuant with our mission and with the strategic growth of our Company.

PANalytical PANalytical Sp. z o.o. Oddział w Polsce, 02-222 Warszawa, Al.Jerozolimskie 195 B, tel.:(22) 57-10-370 (-371), fax: (22) 57-10-004

Spektrometry i dyfraktometry rtg

Dyfraktometr rentgenowski X'Pert PRO

- Analiza fazowa, krystalografia, tekstura, analiza Rietvelda itp.
- System PreFix - zmiana konfiguracji bez re-justowania
- Super-szybki detektor paskowy RTMS X'Celerator
- Wysokorozdzielczy goniometr
- Kamery temperaturowe i reakcyjne Anton Paar
- Zastosowanie w szerokim zakresie badań dyfrakcyjnych



Spektrometr rentgenowski EDS - Minipal

- Uniwersalny spektrometr do analizy w zakresie Na - U
- Poziomy oznaczalności do 1 ppm dla pierwiastków ciężkich
- Analiza jakościowa, ilościowa i bezwzorcowa
- Próbki lite, proszkowe i ciekłe
- 12-pozycyjny zmieniacz próbek
- Zaskakująco dobre wyniki zwłaszcza dla pierwiastków ciężkich



PANalytical *(dawniej Philips Analytical)*

Kopalnia PAŁĘGI

www.geol-min.pl

Złoże „Pałęgi”, położone w gminie Mniów, w zachodniej części województwa świętokrzyskiego, jest jednym z kilku udokumentowanych w ostatnich latach w tym regionie złóż surowców ilastych. Po czterech latach od rozpoczęcia eksploatacji daje ono największe wydobycie iłów ceramiki budowlanej w województwie, porównywalne z wydobyciem ze wszystkich pozostałych czynnych złóż.



Złoże budują dolnotriasowe (środkowy pstry piaskowiec) iłowce pylaste i mułowce, miejscami piaszczyste, o barwie wiśniowoczerwonej do ciemnobrązowej z plamami i smugami seledynowymi. Wśród nich pojawiają się różnej grubości wkładki piaskowców, którym towarzyszą warstwy iłowców i mułowców żółtoszarych i szaroseledynowych.

Kopalina ze złoża „Pałęgi” ma charakter illitowy z podrzędnym udziałem chlorytu i kaolinitu oraz mieszanopakietowych minerałów ilastych I/S i Ch/S. Minerały nieilaste są reprezentowane przez kwarc i hematyt. Kopalina jest całkowicie wolna od marglu i rozpuszczalnych siarczanów. Pod względem własności ceramicznych surowiec można scharakteryzować jako średnioplastyczny, mało wrażliwy na suszenie. Charakteryzuje się on bardzo korzystnymi właściwościami technologicznymi. Po wypaleniu już w stosunkowo niskich temperaturach, rzędu 1050–1070°C, tworzywo osiąga nasiąkliwość <6%. Dobremu spiekaniu sprzyja wysoka zawartość topników (przede wszystkim Fe_2O_3), jak też bogatych w potas minerałów z grupy mik. Intensywne spieczenie czerepu następuje w zakresie temperatur 1100/1150–1200°C. Uzyskane wyroby są całkowicie mrozoodporne, o dużej wytrzymałości mechanicznej.



Dzięki swoim parametrom jakościowym, iły z kopalni Pałęgi stały się w ostatnich latach jednym z głównych krajowych surowców do produkcji klinkieru budowlanego i dachówki ceramicznej. Zakres możliwości stosowania tego surowca jest bardzo szeroki. *Geol-Min Spółka z o.o.,* eksploatująca złoże, rozpoczyna wytwarzanie na jego bazie mas ceramicznych – plastycznych i lejnych, dla licznych krajowych warsztatów i pracowni ceramicznych.

Laboratory of Scanning Microscopy of Biological and Geological Sciences
Faculty of Biology and Earth Sciences
Jagiellonian University

Division of Field Emission Scanning Electron Microscopy and Microanalysis at the Institute of Geological Sciences

30-063 Kraków, ul. Oleandry 2a; Poland
www.uj.edu.pl/LabFESEM

Division of Field Emission Scanning Electron Microscopy and Microanalysis at the Institute of Geological Sciences is equipped with modern cold field emission scanning electron microscope (FESEM) HITACHI S-4700 and energy dispersive spectrometer (EDS) NORAN Vantage.

Analytical possibilities:

- Magnification up to 500 000x,
- High resolution imaging (1.5 nm at 15 kV or 2.1 nm at 1 kV and 12 mm working distance),
- two SE (secondary electrons) detectors (upper and lower) with energy filter, possibility of mixing of SE and BSE (backscattered electrons) signals,
- Backscattered electrons detector (YAG BSE; TV mode),
- Cathodoluminescence detector,
- EDS system for spot chemical analysis, line scan, and mapping of elements distribution,
- 45° specimen tilt,
- Digital image acquisition (as JPEG, TIFF and BMP files)

FESEM – EDS system can be applied for high magnification observation of various objects and chemical analysis with high spatial resolution, e.g.:

- Morphology and chemical composition of components of rocks, soils, industrial products and wastes, biological materials,
- Observation of structure of rocks, soils and sediments,
- Analysis of morphology and chemical composition of atmospheric dust and aerosols,
- Analysis of chemical composition of archaeological artefacts,
- Analysis of composition of pigments, glasses, tissues, paper, metals in conservation of objects of cultural heritage.

FESEM – EDS system is very efficient; software is user-friendly. Preparation of analytical documentation is very easy. Facilities for samples preparation are also available in the Laboratory.

FESEM – EDS laboratory offers two scholarships for Ph.D. or M.Sc. Students in the field of Earth sciences (10 hours of free access to FESEM-EDS + samples preparation + technical assistance).

For more information, contact please:

Marek Michalik (Institute of Geological Sciences, Jagiellonian University)
+48 12 6334603 or +48 604 147828 or e-mail: michalik@geos.ing.uj.edu.pl
Anna Łatkiewicz (Institute of Geological Sciences, Jagiellonian University)
+48 12 6334603 or +48 693 318544 or e-mail: alatk@geos.ing.uj.edu.pl

Thermo
ELECTRON CORPORATION

ThermoARL to firma szwajcarska produkująca od 70 lat spektrometry emisyjne oraz fluorescencji rentgenowskiej wraz z kanałem dyfrakcyjnym. Posiadamy tysiące użytkowników na całym świecie, głównie w przemyśle metalurgicznym, wapienniczym, cementowym, petrochemicznym oraz w wielu znanych ośrodkach naukowo badawczych. Jednym z naszych nowych produktów jest specjalizowany dyfraktometr proszkowy ARL X'TRA posiadający następujące cechy:

ARL X'TRA



- Detektor półprzewodnikowy chłodzony efektem Peltiera
- Podwójne ramię detektora pozwalające na szybkie przechodzenie z konfiguracji Theta-Theta na wiązkę równoległą
- Rozdzielczość energetyczna pozwalająca na eliminację promieniowania K ß bez stosowania dodatkowych filtrów czy monochromatorów powodujących osłabienie sygnału
- Regulowana średnica goniometru w zakresie 400–520 mm pozwalająca na optymalizację rozdzielczości i czułości systemu
- Szczeliny na wiązce padającej i odbitej regulowane w sposób ciągły śrubą mikrometryczną
- Łatwo usuwalne, wymienne szczeliny Sollera
- Doskonała praca w zakresie niskich kątów bez dodatkowych przystawek
- Zasilacz 4 kW
- Dodatkowe opcje pozwalające na pracę w zmiennej temperaturze, w otoczeniu gazu inertnego, wielopozycyjny podajnik próbek, przystawka do badań naprężeń i wiele innych
- Wszystkie przystawki typu „plug and play"

Polskie przedstawicielstwo zapewniające instalację, szkolenia i serwis:

Spekom Sp. z o.o.
ul. Sowińskiego 33
40-272 Katowice
tel. 032-2555372
fax 032-2561037
e-mail spekom@spekom.pl

Stowarzyszenie Naukowe im. Stanisława Staszica

Adres: 31-124 Kraków, ul. Dolnych Młynów 7/1
Tel./Fax (12) 632-76-93, E-mail: geo-staszic@wp.pl
Godziny pracy: od 8.00 do 15.30 od poniedziałku do piątku

Główne cele Stowarzyszenia

1. Promocja nauki, techniki, kultury i sztuki szczególnie propagowanie i upowszechnianie myśli technicznej.
2. Wykonywanie prac naukowych, badawczych i innych, prowadzonych samodzielnie lub we współpracy z wyższymi uczelniami i innymi jednostkami badawczymi oraz podmiotami gospodarczymi.
3. Reprezentowanie interesów ludzi nauki, techniki, kultury i sztuki przed władzami państwowymi i innymi.
4. Podejmowanie wszelkich inicjatyw, mających na względzie dobro ludzi nauki, techniki, kultury i sztuki. Pomoc i wsparcie dla twórców, będących w trudnej sytuacji życiowej oraz dla dzieci i młodzieży o szczególnych uzdolnieniach, lub z rodzin zagrożonych.
5. Dotowanie prac naukowych i popularno-naukowych (książki, skrypty, podręczniki, albumy itp.).
6. Inicjowanie, popieranie i prowadzenie międzynarodowej wymiany technicznej.
7. Wspieranie wszelkich akcji dobroczynnych i charytatywnych, zaproponowanych przez członków Stowarzyszenia.

Zakres prac

- *Górnictwo:*
  - Badania własności geomechanicznych skał i węgla.
  - Prace badawcze i ekspertyzy w zakresie doboru obudowy wyrobisk korytarzowych.
  - Oceny stateczności oraz prognozowania przemieszczeń górotworu pod wpływem eksploatacji.
- *Ceramika:*
  - Analizy chemiczne szkieł przemysłowych i specjalnych wraz z analizą pierwiastków akcesorycznych i śladowych.
  - Badanie właściwości fizykochemicznych szkieł.
  - Opinie w zakresie szkła budowlanego, technicznego, gospodarczego, opakowaniowego i innych asortymentów.
  - Projektowanie syntez szkieł o żądanych własciwościach.
- *Ochrona terenów górniczych:*
  - Pomiary deformacji powierzchni terenu w rejonach eksploatacji górniczej wraz z analizą wpływów eksploatacji na obiekty budowlane i inżynierskie.
  - Prognozowanie deformacji górotworu i powierzchni w rejonach eksploatacji głębinowej złóż rud miedzi, węgla kamiennego, soli, gazu ziemnego i ropy naftowej.

- Analizy wpływu eksploatacji na wyrobiska kopalniane (przekopy, szyby) i ocena zagrożenia tych obiektów.
- Ocena zagrożenia obiektów na terenach podlegających wpływom eksploatacji górniczej.
- Oprogramowanie komputerowe dla celów prognoz deformacji na terenach górniczych, analiz wyników pomiarów deformacji i oceny zagrożeń.
- Opracowywanie i budowa systemów informacji o terenie górniczym (GIS).
- Analiza zagrożeń w rejonach likwidowanych obiektów górniczych oraz na terenach dawnej eksploatacji górniczej.

➢ *Wycena nieruchomości:*

- Wycena podmiotów gospodarczych, nieruchomości, znaków firmowych – pełny pakiet usług.
- Organizowanie warsztatów szkoleniowych dla rzeczoznawców.

➢ *Organizacja seminariów, konferencji itp.*

Kontrahenci Stowarzyszenia

- KGHM Polska Miedź,
- KWB „Bełchatów”,
- KWK „Staszic”,
- KWK „Pniówek”,
- Luboń S.A.
- ZG „Centrum”,
- PAN,
- AGH,
- Centrum Badawczo-Projektowe Miedzi CUPRUM,
- Ceramika „Tubądzin”,
- KW „Czatkowice”,
- ERGO HESTIA,
- „Orzeł Biały” S.A.,
- Pilkington Automotive Poland,
- ZG „Trzebionka”

Zapraszamy do współpracy i korzystania z naszych usług.

The Stanisław Staszic Scientific Association

Some of the aims of the Association:

- Promotion of science and technologies,
- Research – also in co-operation with universities and R&D departments,
- Editioral activities,
- Organization of conferences, seminars, etc.

Research concentrates on mining (geomechanics, underground lining and roof support), ceramics (particularly glass problems), protection of mining areas (underground and surface deformations), real estate evaluation.

COMEF

APARATURA NAUKOWO-BADAWCZA



Firma COMEF reprezentuje w Polsce
czołowych producentów aparatury
naukowo-badawczej oraz kontrolno-pomiarowej

Prowadzimy pełny serwis oferowanych przez
nas urz□dze□ oraz szkolenia w zakresie ich obsługi

ALCATEL
ANTON PAAR
CAMECA
DANSENSOR
HITACHI
GORATEC
GV INSTRUMENTS
HORIBA
JOBIN YVON
NORAN INSTRUMENTS
RIBER
QUESANT
SECOMAM
SETARAM
SPEX
SPECTRA PHYSICS
THERMAL TECHNOLOGY INC
VG SCIENTIFIC
WALTER-BAI

COMEF Aparatura Naukowo-Badawcza, ul. Topolowa 21/2, 40-163 Katowice
tel.: (032) 203 41 49, tel./fax: (032) 203 58 23, e-mail: **comef@comef.com.pl** , **www.comef.com.pl**
Oddzia³ w Warszawie ul. I. Krasickiego 18/4, 02-611 Warszawa
tel.: (022) 844 32 11, fax: (022) 844 08 49, e-mail: **maria@comef.com.pl**

Oferta wg firm

Proponujemy Państwu wysokiej jakości urządzenia renomowanych firm:

ALCATEL www.alcatel.fr	helowe detektory nieszczelności, pompy próżniowe, mierniki próżni, akcesoria próżniowe
ANTON PARR www.anton-paar.com	wysokowydajne mineralizatory mikrofalowe
CAMECA www.cameca.fr	urządzenia do badań w technice EPMA, SIMS i TAP
DANSENSOR www.pbi-dansensor.com	analizatory gazów, miksery gazów, wykrywacze nieszczelności, kontrolery gazów
HITACHI www.hitachi.co.jp	mikroskopy elektronowe
GORATEC www.goratec.de	pomiar i analiza promieniowania podczerwonego, kamery termowizyjne
GV-INSTRUMENTS www.gvinstruments.co.uk	analiza ICP-MS, pomiar gazów szlachetnych, pomiar proporcji izotopów (również izotopów stabilnych)
HORIBA, **JOBIN YVON** www.horiba.com	mierniki wielkości cząstek, jakości wody, analizatory zawartości niektórych pierwiastków w metalach i produktów ropopochodnych w wodzie
JOBIN YVON, **HORIBA,** **SPEX** www.jyhoriba.com	spektrometry, spektrofluorometry, kryminalistyka, siatki dyfrakcyjne oraz spektrografy dla producentów aparatury, systemy ramanowskie, monochromatory, detektory CCD i ICCD, badanie warstw cienkich oraz kontrola procesów ich tworzenia.
NORAN INSTRUMENTS www.noran.com	detektory rentgenowskie, spektrometry z dyspersją długością fali, mikroazalizatory
RIBER www.riber.com	systemy MBE (Molecular Beam Epitaxy) służące do nanoszenia warstw epitaksjalnych
QUESANT www.quesant.com	mikroskopy sił atomowych
SECOMAM www.secomam.fr	spektrofotometry i analizatory UV-VIS, analizatory wody i ścieków oraz analizatory biochemiczne
SETARAM www.setaram.com	zestaw urządzeń do wszystkich technik analizy termicznej
SPECTRA - PHYSICS www.splasers.com	lasery
THERMAL TECHNOLOGY INC www.thermaltechnologyinc.com	piece: wysokotemperaturowe, próżniowe, ciśnieniowe, laboratoryjne
VG SCIENTIFIC www.vgscientific.com	zestaw urządzeń do mikroanalizy powierzchni
WALTER-BAI www.walterbai.com	uniwersalne maszyny wytrzymałościowe (statyczne i dynamiczne)

INSTRUCTIONS FOR THE AUTHORS

Mineralogia Polonica publishes original papers in the scope of mineralogical sciences (mineralogy, petrography, geochemistry). All papers are reviewed and the author is obliged to make corrections suggested by a referee, or give, in the written form, ones reasons for not doing so. Additionally, the Editorial Board reserves the right of selecting the submitted materials and — after contacting the author — introducing all necessary changes and shortenings of the text.

Papers should be arranged exactly in the manner used in current issues of *Mineralogia Polonica,* i.e. applying the same layout, spacings, font characters, style of references and their punctuation, etc. The following updated remarks may be of some help to the authors.

1. Papers are accepted in **English** only. Be sure to use the standard of English acceptable in a journal of international circulation. Attach also a full Polish version of the paper (does not apply to foreign authors).

2. **The length** of each paper is limited to 20 normalized pages (1,800 characters per page), including references, figures, tables and the Polish summary. Two copies of manuscripts should be standard, one-sided printouts (size A-4, Times New Roman or Times New Roman CE, font 12), accompanied by an electronic version (3.5" disk), written preferably in MS-Word 97 or any older version (WordPerfect 6.0 or older is also acceptable). In the case of any differences, the printed version is treated as the decisive one.

3. **The first page** starts with *the Name(s) and SURNAME(S) of the author(s)* and is followed by **THE TITLE IN CAPITALS** (bold, centred). On the same page is the Abstract that should give as much hard data as possible, without vague general statements (not what was being done but what results have been obtained). The Abstract is followed by Key-words (up to seven entries), arranged in a hierarchic manner, from specific to general information. Then, the main body of the text starts if there is enough space. A footnote on page 1 gives affiliation(s) of the author(s), i.e. institution, postal address, e-mail etc.

4. **The main body of the text** is divided into unnumbered chapters, whose hierarchy is: 1st grade — centreed, in capitals, 2nd grade — centreed, in italics, 3rd grade — left-hand side, indented, in italics.

5. **Illustrations —** numbered consecutively, submitted on separate sheets, marked with pencil on their opposite sides with the respective number and the name(s) of the author(s). Each of the illustriation requires a caption and, if necessary, explanations. These must not be entered in the illustration, but should be listed on a separate sheet. The maximum size of the illustration (A-4) is subject to reducing (down to 25% of the original), so be sure that the size of descriptions is large enough. An electronic version of figures in a widely-used graphic program is welcome but not necessary. Keep the number of figures as low as possible. Refer to the illustrations as, e.g., Figure 1 in the text and (Fig. 1) when in parentheses.

6. **Tables** — submitted on separate sheets. Please avoid long listings and select appropriate data to visualize your research but not to make a full documentation.

7. **Photographs** — numbered consecutively, glossy, black-and-white, preferably 10 × 15 cm in size, marked with pencil on their opposite sides with the respective number and the name(s) of the author(s). Each of the photographs requires a caption and, if necessary, explanations. These must not be entered in the photograph, but should be listed on a separate sheet. An extra charge will be levied if the author wishes to have colour photographs printed.

8. **References** — set in alphabetical order, must follow exactly the pattern used throughout in the journal. List all authors, even if more than three.

Articles. ŻABIŃSKI W., 1975: Stilbite from Strzegom (Lower Silesia). *Miner. Polon.* 6, 2, 93—98. (6 = volume number, 2 = issue number — if necessary, 93—98 = pages)

Books. WILLIAMS W., TURNER F.J., GILBERT C.M., 1982: Petrography — an introduction to the study of rocks in thin sections, 2nd edn. W.H. Freeman and Co., San Francisco, 626 pp.

Chapters in a collective book. RUB M.G., PAVLOV V.A., 1978: Geochemical and petrographical features of ... In: M. Stemprok, L. Burnol, G. Tischendorf (eds), Metallization associated with acid magmatism, 3, 267-277, Rumcajs Ed., Praha. (3 = volume number)

Papers in conference materials. USUI A., IIZASA K., 1995: Deep-sea mineral resources in the northwestern Pacific Ocean: geology, geochemistry, origin and exploration. Proc. of the First ISOPE Ocean Mining Symp., 131—137. Tsukuba, Japan.

Others. NOWAK A., 1998: Okruszcowanie miedzią w ... M.Sc. thesis (manuscript), University of Silesia, Sosnowiec (in Polish).

WIESER T., 1998: Spoiwa piaskowców karpackich. Raport No 234 (manuscript), Polish Geol. Inst., Cracow (in Polish).

BAHRANOWSKI K., in press: Sorption by clays. J. of Catalysis.

Cite: Nowak (1960), Nowak and Smith (1960), Nowak et al. (1960) in the text, while (Nowak 1960) or (Nowak, Smith 1960) or (Nowak et al. 1960) in parentheses (et al. = three or more authors). Note semi-colon in parentheses: (Nowak 1960; Werner 1965). Use 1960a,b when there is more than one paper of the same author(s) in one year.

References in Russian should be transliterated.

9. After References there is a **Polish summary** that can be more extended than the English abstract. The layout is: *the Name(s) and SURNAME(S) of the author(s)*, **THE TITLE IN POLISH** (centred, bold, next line), Streszczenie (centred, next line), one line blank and then the text of Streszczenie follows.

10. Give at the very end of the paper (not necesserily on the special page) information concerning addresse(s), telephone number(s), e-mail address(s) of the author(s), and indicate to whom all correspondence should be directed.

11. **Spelling:** Oxford English. Use -ize not -ise, but remember about common exceptions: advise, analyse, catalyse, devise, emphasise, exercise, synthesise.

Units and numbers: use generally SI units. There is always a space between a number and a unit: 10 mg, 2.76 mm. Degrees and percentages are exceptions: 10°C, 25.67%. Numbers from one to ten in the text are in the written form, then quoted in digits: 11, 12, etc. Therefore: twofold, but 20-fold. Contributions: 5 l per hour or 5l h^{-1}. Note the use of a decimal point, not a comma: 2.76 mm. A comma separates off thousands: 12,000.

Abreviations: 15 s (not sec), 5 min (not min.), 1980s, 1999/2000 (e.g. for an academic year), 1998—1999 (not 1998—99), Mts, *ca* (circa).

Acronyms (especially those not commonly used): spell name out in full and follow with the acronym in parentheses when used for the first time.

12. Please, comply with the above mentioned requirements to save paper and avoid additional work, delays and extra costs of technical redaction.

CONTENTS

PIECZKA A., ŁOBOS K., SACHANBIŃSKI M.: The first occurrence of elbaite in Poland 3
SZUSZKIEWICZ A., ŁOBOS K.: Gahnite from Siedlimowice, Strzegom-Sobótka granitic massif, SW Poland 15
ŁATKIEWICZ A., ŻABIŃSKI W.: Greenockite CdS from the Silesia-Cracow Zn-Pb ore deposits 23
DUMAŃSKA-SŁOWIK M.: Mineralogical and geochemical investigation of micas from the Góry Sowie Mts pegmatites 27
BUDZYŃ B., MANECKI M., SCHNEIDER D.A.: Constraints on P-T conditions of high-grade metamorphism in the Góry Sowie Mts, West Sudetes 39
FRANUS W., KLINIK J., FRANUS M.: Mineralogical characteristics and textural properties of acid-activated glauconite 53
DUDEK K., BUKOWSKI K., HEFLIK W.: Mineralogical characteristics of the Bochnia tuff from the Chodenice beds (Carpathian Foredeep, S Poland) 63
DZIUBIŃSKA B., NARĘBSKI W.: Siderite concretions in Paleocene series of Polish part of the Eastern Flysch Carpathians 79